AN EVALUATION OF THE TRANSPORT REACTOR

by

Andrew Duncan Robertson, M.A.

October, 1977.

A thesis submitted for the Degree
of Doctor of Philosophy of the
University of London and for the
Diploma of Imperial College.

Department of Chemical Engineering
and Chemical Technology,
Imperial College,
LONDON, S.W.7.

ABSTRACT

The present state of knowledge regarding Transport Reactors has been examined and found to indicate a lack of information. Relevant works from the pneumatic conveying and suspension flow literature have also been discussed.

Mathematical models for the transport reactor have been developed, leading to both analytical and numerical solutions for reactant conversions. The result of the analysis for typical values of the system parameters has shown that often a simplication of the models can be made by the assumption of a steady state effectiveness factor for the catalyst particles. The effects of film heat and mass transfer resistance have been discussed and expressions have been given for estimating their magnitude. With the object of maximizing the production of the intermediate in a set of two, consecutive first order reactions, optimization of the axial profile of an imposed wall heat flux has been considered and it has been found that isothermal conditions are desirable.

An experimental system, involving the oxidation of a 1% carbon monoxide in air mixture at atmospheric pressure and 350°C using 155 μm diameter particles of a palladium on alumina catalyst, was studied. Operation at a low solids to gas mass flow ratio (< 0.2) made clear the difficulties of obtaining sufficient conversion of reactant under such conditions. Electrostatic charging of the catalyst particles was found to be a major problem requiring careful consideration. Adhesion of catalyst particles to the reactor walls prevented an accurate picture of the suspension from being obtained. The value of the determination of radial concentration profiles for furthering the understanding of the transport reactor and for the diagnosis of unusual behaviour has been shown.

ACKNOWLEDGEMENTS

I wish to thank my Supervisor, Dr. K. C. Pratt, for the continued interest he has shown in this work and for the many valuable suggestions he has made.

Thanks are also due to the Department of Chemical Engineering and Chemical Technology of Imperial College for the use of its facilities. In particular I should like to express my appreciation to the staff of the Engineering and the Glassblowing Workshops for their part in the fabrication of the major part of the apparatus used in the work.

The Science Research Council made a generous grant which enabled equipment and materials to be purchased.

The alumina catalyst carrier was supplied by Norton Industries, U.S.A.

Johnson Matthey Research Centre provided the palladium used in the catalyst and produced the catalyst itself.

During the period of this work I was supported by a Science Research Council Research Studentship.

CONTENTS

Page

LIST OF TABLES

LIST OF FIGURES

1. INTRODUCTION

1.1 Description of Reactor

A transport reactor consists of a vertical tube through which solid particles are conveyed upwards by a gas stream. At the reactor exit the solids are separated from the gases, usually by a cyclone either alone, or acting in conjunction with a disengaging chamber or filter. The particles may be fed to the gas stream by a variety of means; gravity feed through a valve, screw feeders, and pipes from fluidized beds have all been used. The particles may be a reacting solid, or a catalyst in which case they may be recycled to the process. The gases may be inert, their purpose being to transport the reacting solid (in a decomposition reaction for example), usually, however, they consist of or contain the reactants.

Several other terms have been used to describe the system referred to here as the Transport Reactor, for example: Riser Reactor, Transfer Line Reactor, Transported Bed Reactor and Dilute or Disperse Phase Transport Reactor.

Flowrates in a transport reactor may be such that the solids to gas mass flow ratio is in the range from just above zero to 250. The conveyed particles are usually in the size range of 30 μm to 300 μm diameter, but both smaller and larger particles have sometimes been employed. Conveying gas velocities of 2m/s to 30m/s giving residence times of up to 10s are possible in reactors of lengths rising to 20m. Tube diameters range from 0.01m in the laboratory to 2m in an industrial cracker.

The transport reactor has been said to have the following advantages:

(i) Plug flow of gas and particles leads to easy control of residence time and thus good selectivity.

(ii) The separation and subsequent recirculation of catalyst enables continuous catalyst regeneration to take place, which is of particular advantage for rapidly fouling catalyst. (Weekman, 1975).

(iii) The turbulent flow found in transport reactors may lead to uniform radial conditions, both of gas phase concentrations and of particle distribution.

(iv) Particle mass transfer is good and, unlike fluidized beds, there is no by-passing due to the presence of bubbles.

(v) Good particle heat transfer combined with the ability of the particles to act as a heat sink prevents formation of hot-spots.

(vi) Good heat transfer between the suspension and the reactor wall allows near isothermal operation. Alternatively it may be possible to impose an axial temperature gradient on the reactor in order to obtain the optimum yield of an intermediate product in a consecutive reaction system.

(vii) The reactor shows continuous operation.

(viii) Items (iii) to (vii) lead to stable operation and easy control.

(ix) The system is flexible, being able to cope with considerable variation in both gas and solid flowrates and in feedstock composition.

(x) Construction of the reactor should be cheap and relatively easy.

The transport reactor may suffer from the following disadvantages:

(i) The short residence times and high voidages inherent in transport reactors necessitate the use of high activity catalysts and/or high temperatures.

(ii) Efficient removal of small particles from the gas stream can be difficult and so loss of fines from a system employing a highly active, and thus probably expensive, catalyst may be a problem. This complexity of solids separation may result in the reactor being uneconomic.

(iii) Attrition of the solids may intensify the problem of item (ii).

(iv) Erosion of the system internals, particularly at pipe bends, may be severe when abrasive particles are being employed.

(v) Feeding of non free flowing particles to the gas stream may be difficult.

Industrial uses of the transport reactor have included catalytic cracking of oils, coal gasification and Fischer-Tropsch hydrocarbon synthesis. Other suitable reactions of both catalytic and non-catalytic types are oxidation, reduction and pyrolysis. The reactor has been successful industrially where processes depend, for their commercial viability, on obtaining very high conversions. The reactions involved had in common their need for high temperatures and short contact times.

1.2 Objectives of Work

Although the transport reactor has obvious advantages for certain types of reaction, little use has been made of it industrially. This

neglect appears to be the result of lack of experience, design data and design procedures. The aim of this work is to evaluate the possibility of wider use of the reactor and to assess suggestions for improving the performance of the reactor. One suggestion in particular is the imposition of an axial temperature gradient on the reactor to maximize the yield of a desired product.

To this end mathematical models have been developed to describe the behaviour of a catalytic transport reactor. By applying these models to known reaction systems the performance of the reactor has been evaluated.

An experimental investigation has been undertaken to test the validity of the models developed. It is hoped that this will add to the limited information currently available on the transport reactor, and will help to further the understanding and the wider use of the reactor.

2. LITERATURE SURVEY

2.1 Industrial Applications

The origin of the transport reactor may be traced back to fluidized bed cracking. Coke formation required that the catalyst was withdrawn from the reactor for regeneration. The regenerated catalyst was returned to the fluidized bed by a transfer line and it was found that a certain degree of cracking was obtained in this line. This led to a deliberate design for up to 90% of the cracking in the transfer line. The advantages of the use of a transport reactor followed by a secondary fluidized bed were recognised for feedstocks of varying composition and flowrate. The transport reactor minimized coke formation and unwanted cracking of the lighter gasoline fractions whilst the fluidized bed enabled cracking of the more difficult portions of the feedstock.

The industrial history and development of the transport reactor was discussed by Zenz and Othmer (1960). They also reported the use of the reactor for catalytic cracking and for hydrocarbon synthesis as well as for such non-catalytic applications as coal-gasification and retorting of oil shale. Several references to patents were made in the article.

More detailed discussion of the industrial use of the transport reactor for catalytic cracking of petroleum feedstocks has been made by Bryson, Huling and Glausser (1972); Strother, Vermillion and Conner (1972); Pierce, Souther and Kaufman (1972) and Saxton and Worley (1970).

Bryson et al reported the use of zeolite catalysts which were sufficiently active to produce high conversions of the feed for the short residence times employed. The short residence times meant that high reaction temperatures were possible; conditions which were best for the formation of the desired high octane components. Good selectivity was achieved by virtue of the short residence times which prevented further cracking of the gasoline products. Coke formation was reduced for the same reason, but that coke which was produced was burnt off at high pressure in the continuous process of catalyst regeneration. Particular design features, mentioned by the authors were the use of two or three stage cyclones for catalyst removal from the product gases and the careful consideration given to velocities and internal structure in order to minimize catalyst attrition. The reactor was said to have particularly good flexibility, stability and control.

Strother et al stressed the need for rapid separation of the catalyst from the product gases and for quenching the cracking reactions at optimum conversion times. Higher conversion to gasoline, for the same contact time (up to 3s), was obtained than in a fluidized bed as a result of the absence of backmixing and the resultant distribution of residence times.

Pierce et al considered that the excellent heat transfer and the disperse nature of the system were valuable in giving flexibility to the reactor. They also reported reductions in coke formation. Additional flexibility was provided by the ability of the cracker to deal with large variations in both composition and flowrate of feedstock. All of the system internals had erosion resistant linings and slide valves with hard surfaces were used.

2.2 Laboratory Studies

The use of the transport reactor as a laboratory reactor was discussed by Weekman (1974) who considered the straight through transport reactor and the recirculating type in a review article on laboratory reactors. Problems of construction and of sampling products were said to be major limitations of the reactor for catalytic studies.

Laboratory studies of the reactor may be classified into two categories: non-catalytic and catalytic reaction systems. The earlier studies were mainly concerned with non-catalytic reactions and catalytic reactions are the subject of many of the more recent papers.

2.2.1 Non-Catalytic Systems

The transport reactor has been used in the laboratory for the devolatilization of coal (Eddinger, Friedman and Rau, 1966; Friedman, Rau and Eddinger, 1968). For maximum devolatilization extremely rapid heating rates were needed together with very short residence times. The transport reactor provided these conditions and allowed the distribution of products to be altered by varying the residence times of the coal in the reactor. Heating rates of up to 2500°C/s with residence times of 8 to 40ms were reported.

Another non-catalytic study involved the reduction by hydrogen of powdered iron oxide (Lloyd and Amundson, 1961; Dalla Lana and Amundson, 1961). These papers were concerned with the determination

of the kinetics of the system used and found that the transport reactor eliminated sintering and particle surface mass transfer resistance. Short residence times of as low as one second were possible and small amounts of powder could be used to get sensitive and reproducible kinetic data.

Yannopoulos, Themelis and Gauvin (1966) presented a discussion of the transport reactor together with an experimental study, again of the reduction of iron oxide by hydrogen. Three different operating modes were discussed; co-gravity, counter gravity and counter gravity combined fluidized pneumatic transport and it was concluded that counter gravity flow requires the smallest height of reactor and that a combined system may be of advantage for a solids feed of wide particle size distribution. The authors assumed plug flow of solids, a flat gas velocity profile and a particle slip velocity (mean particle size, 45 μm) equal to the Stokes velocity. These assumptions, together with the rate equation for a single particle, allowed a good prediction of the performance of their experimental reactor.

Jepson, Poll and Smith (1965) also gave a short discussion of the transport reactor and reported on the thermal decomposition of sodium bicarbonate in a laboratory transport reactor. Some longitudinal mixing of solids was expected in the turbulent gas stream but the residence time distribution of the gas stream was examined using a benzene tracer in an air-sand system to check the common assumption of plug flow in the gas phase. It was found that for gas velocities of 20 ft/s (in a $1\frac{1}{2}$ in. diameter line) in the presence of up to 20:1 by weight of solids to air there was little deviation from plug flow.

At lower gas velocities, however, back mixing was more pronounced. The effects of particle size and of using a turbulence promoter on the heat transfer coefficients between the suspension and the reactor wall were also examined. The results showed that a turbulence promoter could greatly enhance the gas to wall heat transfer coefficient. Reaction rates measured in the transport reactor were found to agree with the theoretical predictions, and the heat and mass transfer rates from gas to solids and the heat transfer rate from gas to wall were said not to be limiting factors in the design of transport reactors.

2.2.2 Catalytic Systems

Echigoya, Yen and Morikawa (1969) used a bench-scale transport reactor for the catalytic cracking of cumene with a silica-alumina catalyst of 50 to 90 μm diameter particles. The reactor was 11 mm internal diameter by 1 m long and operated at 400 to 500°C. Particle slip velocities were found to be negligible under these conditions by use of a tracer technique employing inert gases and gases which adsorb on the solids. Conversions of the cracking reaction approached those achievable in conventional systems. Effects of axial diffusion of the gas were allowed for by determination of the residence-time distribution function of the reactor with tracers. An equation incorporating the residence-time distribution function was shown to be in good agreement with the experimental reaction data and the assumption of piston flow of the gas phase made little difference to these theoretical predictions of conversion.

Paraskos, Shah, McKinney and Carr (1976) also considered catalytic cracking in a transport reactor. Their study was of the cracking of gas oil by a zeolite catalyst of 60 μm mean diameter at 500 to 550°C using solid to gas mass flow ratios (W_s/W_g) of 3 to 8. Assumptions made by the authors in developing their model for the system were:

(i) No radial temperature or concentration gradients exist in the transfer line and plug flow may be assumed.

(ii) No slip velocity exists between particles and fluid.

(iii) No pressure drop occurs along the reactor.

(iv) The catalyst particles are of uniform size.

(v) The reactor is isothermal.

(vi) No film or intraparticle diffusion limitations exist.

The model, which allowed for catalyst activity decay, predicted that oil conversion and gasoline yield were, for a given catalyst, functions of temperature, pressure and flowing space time only. The model was shown to correlate the experimental data presented.

Wainwright and Hoffman (1974) used a transport reactor for the oxidation of o-xylene, on a vanadia on silica catalyst of 125 μm mean diameter, at 230 to 340°C. 1 to 3 mole percent o-xylene was oxidized by air using very high solids to gas mass flow ratios of up to 250:1. Stable operation of the reactor was obtained at these high loading ratios and reactor voidages of as low as 0.6 were found possible. The authors' analysis of the experimental results was based on a plug flow model with no slip velocity between particles and gas. Very high reaction rates were obtained using a freshly oxidized catalyst on a

once through basis whereas in a parallel fixed bed reactor study a rapid initial decay of the catalyst activity was found. It was suggested that the lower temperature needed, in the transport reactor, to achieve the required conversion of the feedstock would improve the selectivity relative to that obtained in a fixed bed; although the basis of this comparison is not made clear.

De Lasa and Gau (1973) investigated the effect of particle aggregation on the performance of a transport reactor operating at low gas velocity and high volumetric solids concentration. For gas velocities less than 6m/s, solids concentrations of 2 to 7 volume percent (solids to gas mass flow ratios of about 20 to 70), and particle diameters of 220 to 560 μm rapid formation and dispersion of agglomerates was observed. Two techniques were used for agglomeration detection; adsorption of ozone on a porous support and catalytic decomposition of ozone on a Fe_2O_3 catalyst on a porous silicagel support. The results for the transport reactor were compared with results obtained in a fixed bed reactor. The model used for the analysis of the transport reactor adsorption results allowed for the particle slip velocity, film mass transfer resistances and diffusion within the catalyst particles. For the analysis of the catalytic decomposition in the transport reactor, however, a model consisting of two sections was suggested. In the first section diffusion in the catalyst pores was said to be rate controlling since adsorption onto the porous solid was a rapid process. In the second section of the reaction the overall reaction rate was rate controlling since, in comparison, diffusion in the catalyst pores was a fast process. This second section only was considered in analyzing the results.

The comparison of the results for the effective intra-particle diffusivity obtained by adsorption in the fixed bed and in the transport reactor showed good agreement within experimental error and it was concluded that the agglomeration observed in the transport reactor had no effect on the particles external diffusional resistances. The mass transfer film resistance of the particles in the transport reactor was shown to be very small - neglecting it caused an error of less than 2%.

Comparison of the reaction rate constants obtained in the fixed and transported beds for the same catalyst particles was also made and again good agreement was found within the limits of experimental error. Thus aggregation had no measurable effect on the performance of the reactor and the authors concluded that the design of an industrial reactor should accordingly be relatively simple.

2.2.3 Similar Systems

Pruden and Weber (1970) discussed the three-phase transport reactor in which a liquid and catalyst slurry flowed co-currently with a gas, but this system has little in common with the gas phase systems under consideration here.

The falling cloud reactor has the same governing equations as the transport reactor and differs mathematically only with regard to boundary conditions. Gauvin and Gravel (1962) considered a falling cloud reactor in which atomized particles moved co-currently downward with a gas. The system was used for oxidation, reduction and pyrolysis.

Schiemann, Fetting, Prausner and Steinbach (1968) also studied a falling cloud reactor, but with a low upward gas velocity. They examined the catalytic oxidation of carbon monoxide and the hydrogenation of ethylene on palladium, supported on silica-alumina. The results were compared with those which would be expected for plug flow, and those expected for perfect mixing, and they were shown to lie between the two, indicating axial diffusion. A model incorporating the measured axial diffusion coefficients was shown to give good agreement with measured conversions for the carbon monoxide oxidation reaction. The particles were shown to increase the backmixing of gases compared with the same flow conditions for gases only.

2.2.4 Summary and Conclusions

Of the four laboratory catalytic transport reactor studies reviewed in section 2.2.2, three were mainly concerned with the investigation of a particular reaction system (i.e. catalytic cracking or o-xylene oxidation) and improving the yield of the desired products by the use of a transport reactor in place of a conventional reactor. Little attention was paid to axial temperature and concentration profiles; the exit concentrations being of prime concern. This lack of data combined with the problem of modelling the complex reactions occurring in the systems meant that the information obtained was of limited value in furthering the understanding of the transport reactor as such.

The study of De Lasa and Gau (1973) was concerned with the effect of agglomeration on the performance of the transport reactor at high solids to gas mass flow ratios. The use of a simple reaction system

with the absence of any side reactions and the measurement of axial concentration profiles enabled experimental results to be compared with those predicted by a model.

In order to gain a better understanding of the transport reactor it is necessary to obtain more detailed information regarding the conditions prevailing within the reactor. With this object in mind, the present work seeks to obtain axial temperature and concentration profiles, together with radial concentration profiles for a simple reaction system (carbon monoxide oxidation). The measurement of radial concentration profiles is of particular value in evaluating the efficiency of the reactant injector system and the importance of radial reactant dispersion in determining conversion. In contrast to previous catalytic studies, the present work is concerned with comparatively low solids to gas mass flow ratios ($W_s/W_g < 1$), and thus should be of value in extending the range of values of this parameter for which the system has been examined, whilst enabling the mathematical modelling of the system to be simplified.

2.3 Equipment and Measurement

2.3.1 Equipment

Reviews on laboratory equipment for use in circulating gas-solids suspensions were given by Boothroyd (1971) and Walton, Gammon and Boothroyd (1970/71). Other useful information regarding laboratory equipment may be found in the studies of Soo, Trezek, Dimick and Hohnstreiter (1964), Van Zoonen (1962), Doig and Roper (1967),

Richardson and McLeman (1960), Mehta, Smith and Comings (1957), Jepson, Poll and Smith (1963) and Depew and Farbar (1963).

The feeding of solids to the gas stream and their separation from it must be given careful consideration. A feeding device was discussed by Pratt and Byrne (1973), whilst Stairmand (1951b), Iinoya and Goto (1965) and Mori and Suganuma (1966b) considered design and performance of cyclone separators.

Abrasion can be a serious problem in suspension flow and it has been examined by Gluck (1971), Mason and Smith (1972) and Arundel, Taylor, Dean, Mason and Doran (1973). Boothroyd and Goldberg (1970a) discussed the protection of seals and bearings of shafts rotating in abrasive powders, which is of particular concern in screw feeders.

2.3.2 Measurement

The measurement of the most important parameters in gas-solids flow was reviewed by Beck and Wainwright (1968/69), Goldberg and Boothroyd (1969), Boothroyd and Goldberg (1970b) and Boothroyd (1971).

The majority of papers dealing with measurement have focussed on determination of solids flowrate as this is of prime concern in industrial pneumatic conveying (Arundel and Boothroyd, 1971; Beck, Plaskowski and Wainwright, 1968/69; Beck, Hobson and Mendies, 1971; Farbar, 1952 and 1953; Goto and Iinoya, 1963b and 1964b; McVeigh and Craig, 1971; Masuda, Ito and Iinoya, 1973 and King, 1973).

Solids velocity measurements have also attracted considerable interest (Reddy, Van Wijk and Pei, 1969; Reithmuller and Ginoux, 1973; Van Zuillichem, Bleumink and De Swart, 1973; Lovett and Musgrove, 1973 and Mendies, Wheeldon and Williams, 1973).

Correct sampling procedures must be used for suspensions to obtain an accurate picture of both phases and this isokinetic sampling has been examined by Boothroyd (1967a), Dennis, Samples, Anderson and Silverman (1957), Rao and Dukler (1971) and Stairmand (1951a).

Further measurement techniques may be found in the work of Soo and Regalbuto (1960), Soo, Trezek, Dimick and Hohnstreiter (1964), Van Zoonen (1962), Richardson and McLeman (1960), Mehta, Smith and Comings (1957) and Hellinckx (1962).

3. TRANSFER PROCESSES

3.1 Introduction

To enable realistic mathematical models of the transport reactor to be developed simplifying assumptions, preferably based on experimental evidence, must be made. The literature survey given in this chapter is an attempt to evaluate the experimental observations made on the major transfer processes of flowing gas-solids suspensions.

General works on gas-solids suspensions are those of Torobin and Gauvin (1959a,b,c; 1960a,b; 1961), Doig and Roper (1963a,b,c), Zenz and Othmer (1960), Owen (1969), Soo (1967), Boothroyd (1971), Clift and Gauvin (1971) and the B.H.R.A. bibliography (1972).

Attempts to model gas-solids suspensions theoretically have followed two approaches. The first, and least successful of these has been the extension of single particle dynamics to multi-particle suspensions made by Soo (1956, 1962a, 1967), Corrsin and Lumley (1967), Friedlander (1957), Soo and Tien (1960), Ranz, Talandis and Gutterman (1960), Davies (1966), Stannard (1967) and Chand (1971). The second approach was the application of the Navier-Stokes equation to the suspension which was assumed to behave as a continuum. This method was used by Van Deemter and Van der Laan (1961), Hinze (1962) and Soo (1962b, 1965a and b).

No theoretical work has yet modelled the real behaviour of suspension flow with any accuracy, thus emphasizing the need for experimental data. Dimensional analysis has often been used to correlate data. (Boothroyd, 1969c; Kovács, 1971b).

3.2 Momentum Transfer

3.2.1 Pressure Drop and Friction Factors

For the transport reactor a knowledge of pressure drop is necessary to calculate blower power requirements, but it is not expected to be a major factor in determining the reactor performance.

Much of the early work on suspension flow was concerned with the measurement of pressure drop, and the behaviour observed has been used to develop theories subsequently applied to other aspects of suspension flow, for example, heat transfer. This is the case as regards the dependence of the frictional pressure drop on the solids to gas mass flow ratio, where a distinction has been made between 'coarse' (~ > 100 μm diameter) and 'fine' particle behaviour. (Boothroyd, 1971; Mason and Boothroyd, 1971; Rossetti and Pfeffer, 1972; Kane, Weinbaum and Pfeffer, 1973). For coarse particles a relation of the form:

$$\frac{\Delta p_{fsg}}{\Delta p_o} = 1 + A_1 \frac{W_s}{W_g} \qquad 3.1$$

has been found, whereas a non-linear relationship exists for fine particles. The frictional pressure drop for fine particle systems, at mass flow ratios of about one, has been found to be less than that for air alone in some instances. (Boothroyd, 1966; Soo and Trezek, 1966; McCarthy and Olson, 1968; Rossetti and Pfeffer, 1972 and Kane, Weinbaum and Pfeffer, 1973). This has particular relevance where pressure drop is used to monitor the solids flowrate.

The dependence of pressure drop on particle to tube diameter ratio (d_p/d_t), density ratio of solids to gas (ρ_s/ρ_g), viscosity and density of gas (μ and ρ_g), electrostatic charging, Reynolds number (Re_t) and Froude number (Fr) has been investigated by Vogt and White (1948), Belden and Kassel (1949), Farbar (1949), Zenz (1949), Pinkus (1952), Mehta, Smith and Comings (1957), Rose and Barnacle (1957), Richardson and McLeman (1960), Stemerding (1962), Goto and Iinoya (1963a), Rose and Duckworth (1969), Duckworth and Kakka (1971) and Duckworth and Chan (1973). The results of these investigations are conflicting and inconclusive and it is suggested that, at present, pressure drop may be best estimated by use of correlations obtained in systems with the nearest geometry to that under consideration. Some of these correlations are to be found in the works of Razumov (1962), Julian and Dukler (1965), Jones, Braun, Daubert and Allendorf (1967), Konno and Saito (1969), Duckworth (1971), Leung, Wiles and Nicklin (1971a and b), Richards and Wiersma (1973), Yang (1974) and Khan and Pei (1973).

Haag (1967), Mori and Suganuma (1966c), Schuchart (1968), Kovács (1971a), Ikemori and Munakata (1973) and Mason and Smith (1973) give pressure drop data for suspension flow around bends.

3.2.2 Gas and Particle Velocities

3.2.2.1 Particle Slip Velocity and Drag Coefficient

A knowledge of the particle slip velocity, or the mean, absolute particle velocity, is essential to the development of a model of the transport reactor. For a given solids to gas mass flow ratio

(W_s/W_g), the solids slip velocity determines, and may be used to calculate, the reactor voidage (α). The reactor voidage (or the directly related catalyst holdup) is a major factor in determining the reactor performance.

For a single spherical particle moving at constant velocity in an unbounded, stationary fluid, the relationship of the drag coefficient (C_{Dp}) to the particle Reynolds number (Re_p) is well established. (Heywood, 1962). In pipe suspension flow, however, the presence of the pipe wall and of other particles will influence the particle drag coefficients, so it is necessary to determine their effects experimentally.

Hariu and Molstad (1949) and McCarthy and Olson (1968) found that the particle slip velocity was nearly equal to the particle terminal velocity. Jones, Braun, Daubert and Allendorf (1966) and Capes and Nakamura (1973) found that slip velocities were substantially less (up to 20% less) than the particle free-fall velocities at high solids loading ratios (W_s/W_g). In contradiction of this, at low solids loading ratios, Reddy and Pei (1969) and Chandok and Pei (1971) found that slip velocities were above the terminal velocities of the particles, and increased with solids loading.

Correlations for mean particle velocities have been given by Hellinckx (1962), Schuchart (1968), Rose and Duckworth (1969), Duckworth (1971) and Yanz (1973).

It appears, therefore, that particle slip velocity may be influenced by the solids loading ratio, but in view of the uncertainty

in the direction of this influence, it is considered that an assumption of a slip velocity equal to the particle terminal (i.e. free-fall) velocity is the most suitable.

3.2.2.2 Gas Velocity Profile

Gas velocity profiles have relevance to the modelling of a transport reactor in that they affect the residence time distribution of the system and transfer processes such as wall heat transfer, frictional losses, and diffusion.

In turbulent single phase pipe flow the mean (time-averaged) axial fluid velocity variation with radius is usually described either by the universal velocity profile or the 1/7th power law. In suspension flow, a power law relationship is often used owing to its simplicity and the ease with which the index (n_s) can be compared with that for air flowing alone (i.e. 7).

$$\frac{v_g}{v_{go}} = \left[1 - \frac{a}{a_o}\right]^{1/n_s} \qquad 3.2$$

Soo, Trezek, Dimick and Hohnstreiter (1964), Soo and Trezek (1966), Reddy and Pei (1969) and Kane, Weinbaum and Pfeffer found the index n_s to be the same as for air alone (7). Chandok and Pei (1971) found n_s to be in the range 9 to 32. McCarthy and Olson (1968) discovered less than 15% variation of air velocity with radius in the turbulent core ($a/a_o = 0 \rightarrow 0.8$). Kane, Weinbaum and Pfeffer (1973) found a thickening of the laminar sublayer.

Thus there appears to be considerable evidence to support the conclusion that addition of particles to an air stream does not affect the gas velocity profile in the turbulent region which covers the greater part of the pipe radius. For the purpose of developing a model, a 1/7th (or essentially flat) velocity profile may be used.

3.2.2.3 Solids Velocity Profile

Solids axial dispersion and residence time distribution are related to the solids velocity profile and may be of considerable interest in developing models for systems with rapid catalyst fouling.

By analogy with the power law relationship for the gas phase, Soo (1962a) has proposed the following equation, which allows for finite solids velocity at the pipe wall:

$$\frac{v_s - v_{sw}}{v_{so} - v_{sw}} = \left[1 - \frac{a}{a_o}\right]^{1/m} \qquad 3.3$$

Flat velocity profiles have been found by Kane, Weinbaum and Pfeffer (1973), Mori and Suganuma (1966a) and McCarthy and Olson (1968). Reddy and Pei (1969) and Chandok and Pei (1971) found slightly less flat profiles, determining m to be between 3 and 4. Van Zoonen (1962) found parabolic solids velocity profiles at high solids loadings, a result of general similarity to those of Soo, Trezek, Dimick and Hohnstreiter (1964) and Soo and Trezek (1966) who found m between 1 and 1.5.

The majority of the evidence seems to be in favour of solids velocity profiles similar in shape to those of the gas (i.e. following approximately a 1/7th power law). Even in those studies where a 1/7th power law was not obtained, the solids velocity profile has been found to be reasonably flat and so a flat solids velocity profile will be adopted here.

In summary it is thought that the conditions prevailing in a transport reactor can be best represented by using the particle free-fall velocity for the slip velocity, and by assuming a 1/7th power law for the gas velocity profile and a flat solids velocity profile. These conclusions are expected to apply only to cases of moderate solids loadings ($W_s/W_g < 50$), as it is for these cases that the majority of studies have been made.

3.2.3 Radial Solids Concentration and Mass Flow Distribution

Conversions obtained in transport reactors may be affected by a non-uniform radial distribution of particles, particularly if radial diffusion of the reactant is poor.

Soo (1962a) has proposed the following equation to describe the radial dispersed solids density profile:

$$\rho_p = \rho_{po} + (\rho_{pw} - \rho_{po}) \cdot \left(\frac{a}{a_o}\right)^{n_\rho} \qquad 3.4$$

Soo, Trezek, Dimick and Hohnstreiter (1964), Stemerding (1962), Arundel, Bibb and Boothroyd (1970/71), Saxton and Worley (1970) and,

at low solids loadings, Doig and Roper (1967 and 1968), found higher solids concentrations near the pipe walls, although generally this effect was slight. Van Zoonen (1962) found a parabolic concentration profile, with the minimum at the pipe centre, for high solids loadings. Kane, Weinbaum and Pfeffer, Reddy and Pei (1969), Chandok and Pei (1971), and, at moderate solids loadings, Doig and Roper (1967 and 1968), all obtained a uniform concentration distribution across the radius of the pipe.

The mass flow distribution was found to have a maximum at the pipe centre by Soo, Trezek, Dimick and Hohnstreiter (1964), Soo and Trezek (1966), Soo and Regalbuto (1960) and Goto and Iinoya (1964a), but here again this effect was not pronounced.

The increased particle density in the vicinity of the pipe walls has generally been attributed to electrostatic charging of the particles. If this effect is absent results indicate that at moderate solids loading ratio the particles are evenly distributed across the pipe diameter. The solids mass flow distribution may be calculated from the concentration distribution and the solids velocity profile; the evidence suggests that it is flat.

3.2.4 Turbulence Characteristics

Since the major means by which transfer processes occur in a turbulent suspension is eddy transfer (rather than molecular transfer), a study of the turbulence characteristics of both phases may enable an estimate of the importance of axial and radial diffusion to be made.

3.2.4.1 Particle Turbulence Intensity and Eddy Diffusivity

Turbulence intensities have received attention from Boothroyd (1967b), Chandok and Pei (1971), Reddy and Pei (1969), Mori and Suganuma (1966a) and Soo, Ihrig and El Kouh (1960).

Eddy diffusivities have been studied by Van Zoonen (1962), Soo and Trezek (1966) and Soo, Ihrig and El Kouh (1960).

The general conclusions reached are that both of the above quantities are smaller than for the gas phase but approach the gas phase values at high solids loadings.

3.2.4.2 Gas Phase Turbulence Intensity and Eddy Diffusivity

It has generally been found that fine particles are able to interact with the turbulence structure of the gas stream close to the pipe wall but that coarse particles have little effect on the gas turbulence intensity. Turbulence suppression by fine particles has been found by Boothroyd (1966), Mason and Boothroyd (1971), Kane, Weinbaum and Pfeffer (1973), Jotaki and Tomita (1971) and Boothroyd and Walton (1971 and 1973).

Work on coarse particle suspensions shown that radial eddy diffusivities are similar to those for gas alone (Van Zoonen, 1962) whereas gas eddy diffusivities are considerably reduced near the pipe wall for fine particle suspensions (Boothroyd, 1967b).

Thus for coarse particles at moderate loadings it seems reasonable to assume that the gas eddy diffusivity is about the same as for pure gas and that the particle eddy diffusivity is negligible in comparison. This is supported by the work of Jepson, Poll and Smith (1965) and Echigoya, Yen and Morikawa (1969) who found negligible axial diffusion of the reactant in studies on transport reactors.

3.3 Heat Transfer

The study of the heat transfer characteristics of a transport reactor may conveniently be divided into two sections: the gas to particle heat transfer and its relative importance in comparison to intra-particle heat transfer, and the wall to suspension heat transfer. Both of these aspects were the subject of review articles by Boothroyd (1969b and 1971).

3.3.1 Gas-Particle Heat Transfer

In addition to the above-mentioned reviews, Clamen and Gauvin (1968b), Pasternak and Gauvin (1960 and 1961) and Hughmark (1967) presented reviews on heat transfer from particles. All these papers give correlations, typically of the form:

$$Nu_p = 2 + a_1 Re_p^{b_1} Pr^{c_1} \qquad 3.5$$

The values of the constants a_1, b_1 and c_1 adopted for the present work are 0.6, 1/2 and 1/3 respectively (Hughmark, 1967).

The importance of intra-particle heat transfer may be evaluated using the following expression for the temperature rise in a spherical catalyst pellet (Petersen, 1965):

$$T - T_s = \frac{(-\Delta H)\, D_{eff}\, (c_s - C)}{\kappa_{eff}} \qquad 3.6$$

It is generally found that the temperature rise within a catalyst particle is small in comparison to the temperature difference existing across the gas film surrounding the particle. Satterfield (1970) states that, "Even for a particle of low thermal conductivity, essentially isothermal operation is likely at atmospheric pressure unless the heat of reaction is unusually high (> 40 kcal/mole) or the pores of the particle are so large that bulk diffusion occurs in them".

3.3.2 Suspension-Wall Heat Transfer

The wall to suspension heat transfer characteristics are of considerable interest in evaluating the suggestion that an optimum axial temperature profile may be imposed on a transport reactor.

Several theoretical models have been developed to represent wall heat transfer in suspension flow (Tien, 1961; Depew and Farbar, 1963; Boothroyd, 1969a) but they give poor predictions of real systems.

Various correlations for wall heat transfer are given by Boothroyd (1969b and 1971), Wen and Miller (1961) and Sadek (1972).

These give vastly differing results when applied to any one system and appear to be valid only for the system in which they were obtained.

The effects of the major system parameters on the ratio (Nu_s/Nu_o) or (h_s/h_o) are described below.

(i) Particle Size (d_p) and Mass Flow Ratio (W_s/W_g)

For fine particles (< 100 μm diameter) a minimum was often observed in the Nusselt number ratio at a mass flow ratio of about one. (Farbar and Morley, 1957; Jepson, Poll and Smith, 1963; Farbar and Depew, 1963; Depew and Farbar, 1963; Wilkinson and Norman, 1967; Boothroyd and Haque, 1970a). At higher values of (W_s/W_g) a large increase in the ratio (Nu_s/Nu_o) was observed.

For coarse particles only a very slight increase in heat transfer was found to result from increasing solids loading and no minimum was detected.

Briller and Peskin (1968) found that particle size had no effect on the heat transfer coefficient.

The evidence suggests the use of fine particles to obtain the maximum improvement in heat transfer at moderate solids loadings.

(ii) Tube Reynolds Number (Re_t)

Farbar and Morley (1957), Danziger (1963), Wilkinson and Norman (1967), Jepson, Poll and Smith (1963) and Yousfi, Gau and Le Goff (1973) concluded that the ratio (Nu_s/Nu_o) increased with decreasing Reynolds

number. Boothroyd and Haque (1970a) conclude that the Reynolds number is of minor and unclear significance and suggest the use of a dimensionless time scale ratio ($\rho_g \, d_t^2 \, / \, \rho_s \, d_p^2 \, Re_t$) for correlating data.

It appears that (Nu_s/Nu_o) increases with decreasing Re_t and that this may be due to greater backmixing of solids at the lower velocities. However, the relative heat transfer improvement (i.e. improvement in Nu_s/Nu_o) is of less importance than the absolute Nusselt number Nu_s and this generally increases with Re_t.

(iii) Pipe Diameter (d_t)

Boothroyd (1969b) concludes that increasing d_t increases (Nu_s/Nu_o).

(iv) Nature of Heat Transfer

Differing methods have been used to investigate wall heat transfer. Wilkinson and Norman (1967) and Depew and Farbar (1963) used a constant wall heat flux whereas Farbar and Morley (1957) used a constant wall temperature. The method used seems to make little difference to the results obtained.

Different values of the heat transfer coefficients have been obtained depending on whether the pipe has been heated or cooled (Boothroyd, 1969b) and the higher values of (Nu_s/Nu_o) obtained for heating may be due to thermophoresis.

Thermal Entry Region

Because of the time lag in establishing temperature profiles in a heat transfer process a thermal entry region exists where the flow may be said to be thermally undeveloped. If an axial temperature profile is to be imposed on the reactor, the length, and heat transfer characteristics of this region may be important. Depew and Farbar (1963), Boothroyd and Haque (1970b) and Wang and Heldman (1973) have studied the thermal entry region in suspension flow. The length of the entry region has been shown to increase with increasing mass flow ratio.

Radiation Heat Transfer

Boothroyd (1969b and 1971) suggested that the importance of radiation heat transfer to suspensions at high temperatures has been underestimated. The calculation of radiative heat transfer in a solids laden gas stream is complex involving the consideration of heat transfer between particle and gas, particle and reactor walls, particle and particle etc. Thus the simplification that radiative heat transfer can be neglected is necessary.

Temperature Profiles

Yousfi, Gau and Le Goff (1973) concluded that the presence of solids considerably flattens the parabolic radial gas temperature profile found for gas alone. It seems reasonable to suppose that the improved heat transfer found in suspension flow causes some flattening of the temperature profiles relative to gas alone.

Turbulence Promotion

The use of turbulence promoters to increase heat transfer has been investigated by Lodh, Murthy and Murti (1970), Boothroyd and Haque (1973) and Jepson, Poll and Smith (1965). The latter group of workers found greatly enhanced wall heat transfer coefficients whilst the former two groups obtained somewhat less improvement. This work may have particular significance for transport reactors where efficient removal of the heat of reaction is of utmost importance for many exothermic reactions.

Magnitude of Heat Transfer Improvement

The effect of particles in increasing heat transfer is much smaller than their effect in increasing the friction factors in suspension flow (Boothroyd and Haque, 1970a) and values of (Nu_s/Nu_o) of the order of 3 are often reported (Farbar and Morley, 1957; Jepson, Poll and Smith, 1963; Wilkinson and Norman, 1967). However, at low velocities and high loadings, where backmixing is prominent, values of (Nu_s/Nu_o) as high as 12 (Jepson, Poll and Smith, 1963) and 16 (Yousfi, Gau and Le Goff, 1973) have been reported.

To summarize: Wall heat transfer is best for small particles at high solids loading ratios, and although the best improvement in heat transfer coefficients relative to air is obtained at low Reynolds numbers, the best absolute heat transfer is found for high Re_t. Further improvement may be possible by the use of turbulence promoters.

It is suggested that a flat radial gas temperature profile may be adopted for moderate solids loadings.

3.4 Mass Transfer

Two types of mass transfer are important in transport reactors; film mass transfer and intra-particle mass transfer.

3.4.1 Intra-Particle Mass Transfer

Diffusion within the pores of the catalyst particle is described in detail in such works on catalysis as Satterfield (1970). Mass transfer rates within a particle depend on the particle pore structure and the nature of the reactant which together determine the effective diffusivity. The relative importance of diffusion and reaction in the particle depends on the effective diffusivity, the reaction rate law, and the particle size. These factors are incorporated in the dimensionless variable known as the Thiele Modulus which is of prime importance in any modelling of catalyst particles.

3.4.2 Film Mass Transfer

Reviews of mass transfer from single particles have been made by Zenz and Othmer (1960), Clamen and Gauvin (1968a and b), Pasternak and Gauvin (1960 and 1961) and Hughmark (1967). Correlations of data are usually of the form:

$$Sh = 2 + a_2 Re_p^{b_2} Sc^{c_2} \quad \text{or} \quad j_D = d_2 Re_p^{e_2} \qquad 3.7$$

where a_2, b_2, c_2, d_2 and e_2 are constants.

Nearly all these correlations have been arrived at in studies with single, fixed particles and have doubtful significance for the transport reactor. Jones and Smith (1962) allowed for multi-particle effects and for unsteady or spinning motion and found correlations of the type shown above to be inadequate. They presented the following correlations for use in dilute phase transport:

$$\left.\begin{aligned} Sh &= 2 + 0.25\ (Re_p.Sc.Re_t^{\frac{1}{2}})^{\frac{1}{3}} \text{ for } (Re_p.Sc.Re_t^{\frac{1}{2}}) < 10^4 \\ Sh &= 2 + 0.055\ (Re_p.Sc.Re_t^{\frac{1}{2}})^{\frac{1}{2}} \text{ for } (Re_p.Sc.Re_t^{\frac{1}{2}}) > 10^5 \end{aligned}\right) \qquad 3.8$$

The relative importance of intra-particle and film mass transfer resistance is of considerable interest. For moderately fast reactions in small particles where the effectiveness factor is about unity, film mass transfer is unlikely to be important. Where the effectiveness factor for a particle is well below unity, film mass transfer resistance may be an important consideration. In such a case, the above correlations (Equations 3.8) are recommended.

3.5 Summary

The available experimental evidence suggests that the transport reactor operating at moderate solids loadings may be modelled by making the following assumptions:

(i) Particle slip velocities are equal to the particle free-fall velocities.

(ii) Gas radial velocity profiles follow the 1/7th power law (or, less accurately, are flat).

(iii) Solids radial velocity profile is flat.

(iv) Solids radial concentration distribution is uniform.

(v) Solids eddy diffusivities may be neglected.

(vi) Gas axial and radial eddy diffusivities are equal to those for gas alone, allowing axial diffusion to be neglected in comparison to convective transport.

(vii) Catalyst particles are isothermal.

(viii) Particle film heat transfer should be allowed for.

(ix) intra-particle mass transfer may be dealt with by use of effectiveness factors based on the Thiele Modulus.

(x) Film mass transfer may be important for fast reactions and should be considered.

In cases where good wall to suspension heat transfer is desired to ensure efficient heat removal or to impose an axial temperature profile on the reactor, the system should be designed as far as possible to the following specifications:

(i) Fine catalyst particles.

(ii) High solids to gas mass flow ratios.

(iii) High tube Reynolds number.

(iv) Use turbulence promoters.

Fine particles also give the best film heat and mass transfer (per unit volume of catalyst) and the highest effectiveness factors, but they are most likely to agglomerate or deposit on the reactor wall since they are most affected by surface forces (for example

electrostatic forces). The major problem with small particles, however, is separation from the gas stream and this is likely to prevent the use of as fine a particle size as would otherwise be desirable.

4. MATHEMATICAL MODELLING

4.1 Introduction

4.1.1 Aims

The theoretical evaluation of the transport reactor involved the following aims:-

(i) To extend the existing analytic solution for first order kinetics in the transport reactor to the case of zero order kinetics.

(ii) To generalize the reactor equations to allow solution for any rate law.

(iii) To determine effectiveness factors for a first order reaction in the reactor and to compare them with the steady state effectiveness factor in order to evaluate the significance of the non steady state of the particles in the reactor.

(iv) To investigate the possibility of using the information obtained in (iii) to simplify the solution of the reactor equations and to determine under what circumstances this simplified solution is valid.

(v) To examine the importance of film heat and mass transfer resistance in the transport reactor.

(vi) To evaluate the possibility of maximizing the production of the intermediate B in a set of two consecutive first order reactions, $A \rightarrow B \rightarrow C$, by variation of the axial temperature profile and, by use of a particular example, to compare the results obtained by this approach with those obtained by use of an optimum isothermal temperature. Also, to determine

whether the wall heat flux required to impose an optimum temperature profile is a practical possibility.

4.1.2 Summary of Results

The results of the development detailed in the remainder of this chapter are outlined here to assist the reader in following the direction of the work:

(i) In addition to the existing analytic solution for first order kinetics an analytic solution has been obtained for the case of zero order kinetics, but it is cumbersome and alternative numerical solutions are preferable.

(ii) A computer program has been written to allow numerical solution of the reactor equations for a generalized rate law.

(iii) The first order effectiveness factors for the reactor may be closely approximated by their steady state values for the majority of the length of the reactor, excluding an entrance region of less than one tenth of the reactor length. Thus, kinetically, the catalyst particles are in a quasi-steady state.

(iv) Asymptotic solutions to the reactor equations for a first order rate law have been obtained. A solution valid at small distances along the reactor and a solution valid at large distances along the reactor (in practice corresponding to most of the reactor) have been combined to give a good approximation to the true solution.

(v) Film heat and mass transfer resistances have been shown to be important under certain conditions, particularly those

of high reaction rates. Expressions are presented which allow the magnitude of the film resistances to be estimated and an asymptotic solution has been obtained allowing for the effects of film mass transfer resistance for a first order reaction.

(vi) The optimization of the reactor by imposition of a wall heat flux has been shown to be theoretically feasible but limited in practice by the wall to suspension heat transfer rate. The operation of the reactor at the optimum isothermal temperature has been found to produce results comparable with those obtained using the optimum heat flux profile for the example considered.

4.2 Simple Analysis

An elementary analysis of the transport reactor may be made by making the following assumptions:

(i) Plug flow of both gas and solids.

(ii) Spherical catalyst particles of uniform size.

(iii) A single irreversible first order reaction is occurring under isothermal conditions with no volume change.

(iv) Axial diffusion of both phases is negligible.

(v) No film resistance to mass transfer exists at the catalyst surface.

(vi) The amount of reactant within the catalyst particles is negligible in comparison to the amount in the gas phase.

(vii) In kinetic terms the particles are in a quasi steady state, allowing particle reaction rates to be expressed using a steady state effectiveness factor.

A mass balance on an element of the reactor gives:

$$\alpha u_g \frac{dc}{dl} = -(1 - \alpha)\eta_{ss}\, kc \qquad 4.1$$

with the following boundary condition:

$$c = c_o \quad \text{at} \quad l = 0 \qquad 4.2$$

Integration gives:

$$c = c_o \exp\left[\frac{-\eta_{ss}(1 - \alpha)kl}{\alpha u_g}\right] \qquad 4.3$$

This may be put into dimensionless form for the purpose of comparison with later results:

$$\boxed{y = \exp(-PM\phi^2\eta_{ss}z)} \qquad 4.4$$

This dimensionless form, including the groups P and M, disguises the lack of dependence of the result on the particle voidage, ε, and the solids velocity, u_s, but demonstrates the dependence of y on the circulation ratio through the group P.

4.3 General Reactor Equations

The reactor model used in the previous section may be improved so that assumptions (vi) and (vii) are no longer necessary and assumption (iii) may be altered to allow for the possibility of any rate law.

A mass balance on an element of a spherical catalyst particle leads to the following equation:

$$\varepsilon \frac{\partial C}{\partial t} = D_{eff} \left[\frac{\partial^2 C}{\partial r^2} + \frac{2}{r} \frac{\partial C}{\partial r} \right] - S(C) \qquad 4.5$$

The surface boundary condition for the particle may be obtained by a mass balance on the gas phase of an element of the reactor:

$$u_g \alpha \frac{dc}{dl} = \frac{-3(1 - \alpha) D_{eff}}{R} \cdot \frac{\partial C}{\partial r} \Bigg|_{r = R} \qquad 4.6$$

The remaining boundary conditions are:

$$C(r,0) = 0 \qquad 0 \leq r < R \qquad 4.7$$

$$c(0) = c_o = C(R,0) \qquad 4.8$$

$$C(R,t) = c(1) \qquad 4.9$$

$$\frac{\partial C}{\partial r}(0,t) = 0 \qquad 4.10$$

Introducing the following dimensionless variables;

$$Y = \frac{C}{c_o} \; ; \quad y = \frac{c}{c_o} \; ; \quad x = \frac{r}{R} \; ; \quad z = \frac{l}{L} \; ; \quad \Psi = \frac{S(C)}{S(c_o)}$$

and the following dimensionless groups;

$$M = \frac{D_{eff} L}{\varepsilon R^2 u_s} \; ; \qquad P = \frac{\varepsilon u_s (1 - \alpha)}{u_g \alpha} \; ; \qquad \phi_g = R \sqrt{\frac{S(c_o)}{D_{eff} c_o}}$$

the above equation (4.5) and its boundary conditions may be made dimensionless:

$$\frac{1}{M}\frac{\partial Y}{\partial z} = \frac{\partial^2 Y}{\partial x^2} + \frac{2}{x}\frac{\partial Y}{\partial x} - \phi_g^2 \Psi \qquad 4.11$$

$$\frac{1}{M}\frac{dy}{dz} = -3P \left.\frac{\partial Y}{\partial x}\right|_{x=1} \qquad 4.12$$

$$Y(x,0) = 0 \qquad 0 \leq x < 1 \qquad 4.13$$

$$Y(1,0) = 1 = y(0) \qquad 4.14$$

$$Y(1,z) = y(z) \qquad 4.15$$

$$\frac{\partial Y}{\partial x}(0,z) = 0 \qquad 4.16$$

NB An alternative boundary condition to equation 4.16 is for the case of reactant exhaustion at $x = x_e(z)$. This is given by equations 4.17 and 4.18.

$$Y(x_e, z) = 0 \qquad 4.17$$

$$\frac{\partial Y}{\partial x}(x_e, z) = 0 \qquad 4.18$$

4.3.1 Analytic Solutions

For zero or first order rate laws equation 4.11 becomes linear and an analytic solution is possible. Appendices 1, 2 and 3 show the solution by Laplace Transformation for the cases of no reaction, zero order reaction and two consecutive first order reactions respectively. The zero order case is algebraically unwieldy and inconvenient to use so a numerical solution as described in the next section is preferable.

The first order case has been discussed by Pratt (1974) and the result is quoted below for comparison to the simplified forms derived later in this chapter.

Making assumptions (i) to (v) of section 4.2 leads to:

$$\frac{1}{M}\frac{\partial Y}{\partial z} = \frac{\partial^2 Y}{\partial x^2} + \frac{2}{x}\frac{\partial Y}{\partial x} - \phi^2 Y \qquad 4.19$$

This, together with equations 4.12 to 4.16, may be solved by Laplace Transformation to give:

$$\boxed{Y = \sum_{n=1}^{\infty} \frac{\sin(\sqrt{\beta_n} \cdot x)}{x \cdot \sin(\sqrt{\beta_n}) \cdot F_n} \cdot \exp(\gamma_n Mz)} \qquad 4.20$$

where $$F_n = 1 + \frac{3P}{2} - \frac{\gamma_n}{2\beta_n} + \frac{1}{6P} \cdot \frac{\gamma_n^2}{\beta_n} \qquad 4.21$$

and the β_n's and γ_n's are the roots of:

$$\beta_n = -\gamma_n - \phi^2 \qquad 4.22$$

and $$\frac{\gamma_n}{3P} = 1 - \sqrt{\beta_n} \cdot \cot\sqrt{\beta_n} \qquad 4.23$$

4.3.2 Numerical Solutions

For non-linear rate laws equation 4.11 must be solved numerically. The solution of equation 4.11 together with its associated boundary conditions (equations 4.12 to 4.16) has been accomplished by means of the Crank-Nicholson method.

The dimensionless rate law expressions, Ψ, were handled by linearization if necessary. The matrix equations resulting from the Crank-Nicholson treatment were solved by the Thomas algorithm (Bruce et al, 1953). The computer program used is given as programme 1 of appendix 9.

4.4 Effectiveness Factors

First order effectiveness factors for the transport reactor may be defined (Robertson and Pratt, 1975) in one of the following two ways:

$$\eta_f = \frac{4\pi R^2 D_{eff} \left.\frac{\partial C}{\partial r}\right|_{r = R}}{\frac{4\pi R^3}{3} k\, c_s} \qquad 4.24$$

or

$$\eta_i = \frac{\int_0^R 4\pi r^2 k\, C\, dr}{\frac{4\pi R^3}{3} k\, c_s} \qquad 4.25$$

These may be written in dimensionless form as:

$$\eta_f = \frac{3}{\phi^2 y} \cdot \left.\frac{\partial Y}{\partial x}\right|_{x = 1} \qquad 4.26$$

and $$\eta_i = \frac{3}{y} \int_0^1 x^2\, Y\, dx \qquad 4.27$$

Equation 4.24 defines the effectiveness factor in terms of the flux of reactant at the catalyst surface, whilst equation 4.25 defines an effectiveness factor in terms of the total rate of reaction integrated

throughout the catalyst particle. Thus η_i is the true effectiveness factor but η_f is of interest since it is easier to determine experimentally.

The above definitions mean that in general $\eta_i \neq \eta_f$; only in a steady state situation are the values of η_i and η_f always the same. Comparison of η_i and η_f with the first order steady state effectiveness factor will enable the effects of the non steady state nature of the system to be assessed and hence the validity of assumption (vii) of section 4.2 can be examined.

Using equations 4.26 and 4.27 with equation 4.20 the following expression for η_f and η_i are obtained:

$$\eta_f = \frac{-1}{\phi^2 P} \left[\frac{\sum_{n=1}^{\infty} \frac{\gamma_n . \exp(\gamma_n Mz)}{F_n}}{\sum_{n=1}^{\infty} \frac{\exp(\gamma_n Mz)}{F_n}} \right] \qquad 4.28$$

and

$$\eta_i = \frac{1}{P} \left[\frac{\sum_{n=1}^{\infty} \frac{\gamma_n . \exp(\gamma_n Mz)}{\beta_n . F_n}}{\sum_{n=1}^{\infty} \frac{\exp(\gamma_n Mz)}{F_n}} \right] \qquad 4.29$$

where β_n, γ_n and F_n are defined by equations 4.21 to 4.23.

Further mathematical development of these equations is given in Appendix 4.

Taking values of ϕ^2 from 10^{-2} to 10^5, of P from 0.005 to 0.1 and of Mz > 0.05 η_f and η_i were evaluated by computer using

equations 4.28 and 4.29. The results for η_i are shown in figures 4.1 and 4.2. The computational results for η_f are given in Robertson and Pratt (1975).

Figure 4.2 shows the approach of η_i to an asymptotic value as Mz increases, for various values of P and ϕ^2. It may be noted from figure 4.1 that, for values of Mz greater than 0.5, η_i becomes almost equal to the steady state effectiveness factor for all the values of ϕ^2 and P considered. Since, in practice, M will lie in the range 5 to 5000, η_i will be essentially equal (differing by a maximum of 2%) to the steady state effectiveness factor, η_{ss} after an entry region of less than one tenth of the reactor length.

Thus the results obtained reflect the model of the reactor used, where an entry region, characterized by the rapid diffusion of reactant into the catalyst particles, is followed by the major part of the reactor where concentration profiles within the catalyst pellets are established and a quasi steady state exists.

As a result of this examination of effectiveness factors it can be concluded that the steady state assumption (vii) of the elementary analysis (section 4.2) is a reasonable approximation outside the entrance region. The magnitude of the small errors incurred in making a steady state assumption are examined in Appendix 4 and an estimation of the entrance length as a function of the parameters M and ϕ^2 is made in Appendix 5.

FIGURE 4.1

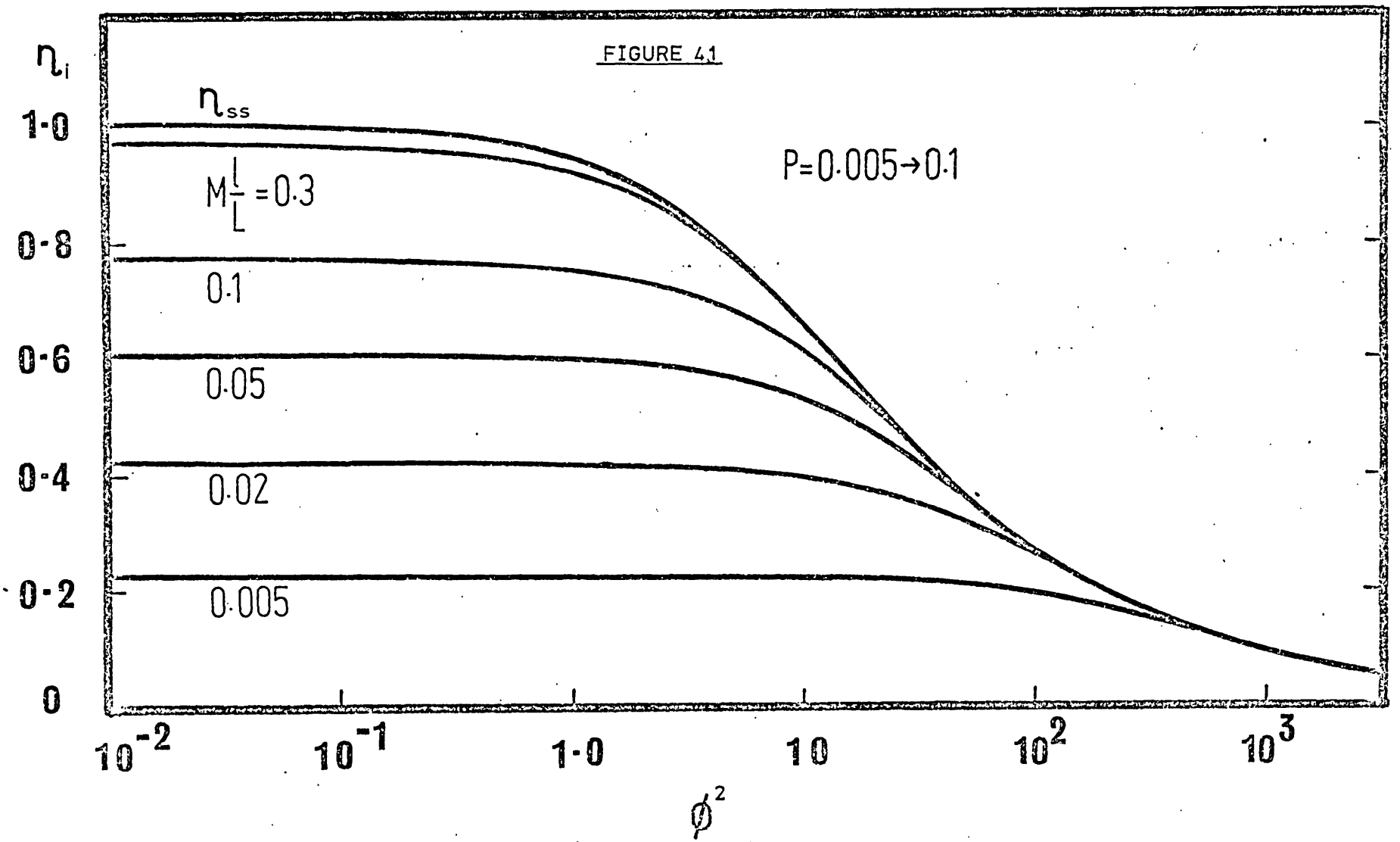
η_i
η_{ss}
1·0
0·8
0·6
0·4
0·2
0
$M\frac{l}{L} = 0.3$
0·1
0·05
0·02
0·005
P=0·005→0·1
10^{-2}
10^{-1}
1·0
10
10^2
10^3
ϕ^2

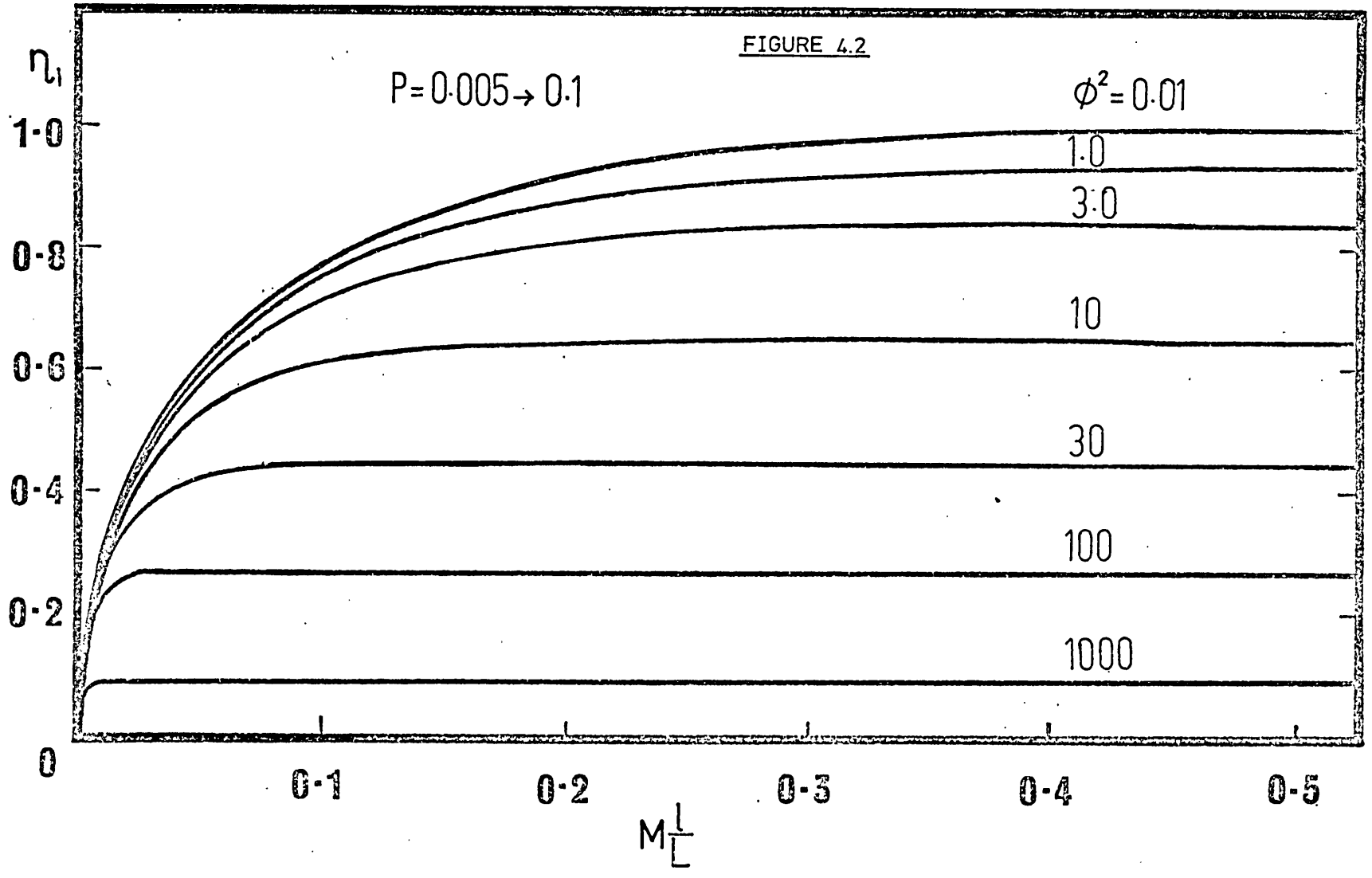
FIGURE 4.2
η_1
P = 0·005 → 0·1
ϕ^2 = 0·01
1·0
0·8
0·6
0·4
0·2
0
1·0
3·0
10
30
100
1000
0·1
0·2
0·3
0·4
0·5
$M\frac{l}{L}$

4.5 Asymptotic Solutions of the Reactor Equations

Using the results of section 4.4 the reactor equations may be simplified for the case of a first order reaction and a simpler and more convenient solution obtained. (See Appendix 5). Assumptions (i) to (v) of section 4.2 are made, together with assumptions (a) and (b) below:

(a) An entrance region exists where the major process is diffusion of reactant into the catalyst particles; the amount of reaction is negligible in comparison to this.

(b) Outside the entrance region the particles are in a quasi steady state and may be represented by a steady state effectiveness factor, i.e. concentration profiles within the catalyst particles are changing relatively slowly as the total reaction rate in the particle is slightly greater than the surface flux of reactant.

It is shown in Appendix 5 that assumption (a) is valid in the region $z < 1 / M\phi^2$ and assumption (b) is valid in the region $z \geq 1 / M\phi^2$. (The entrance length is defined as $z_a = 1 / M\phi^2$).

For a first order rate law an asymptotic solution, valid for $z > 0.1$ has been determined (Appendix 5):

$$y = \frac{1}{(1 + \eta_{ss} P)} \exp\left[\frac{-PM\phi^2 \eta_{ss} z}{(1 + \eta_{ss} P)}\right] \qquad 4.30$$

It can be seen that for small P this reduces to equation 4.4, the difference in the equations being due to the neglect of the reactant within the catalyst particle in the derivation of equation 4.4.

The greatest difference between the value of y calculated using equation 4.4 and the value calculated using equation 4.30 occurs for large η_{ss} and P (in practice the largest value of $\eta_{ss}P$ will be $\simeq 0.1$). Using this value the following differences between equations 4.4 and 4.30 may be calculated:

For $M\phi^2 > 100$ (i.e. entrance length $z_a < 0.01$); $y(4.30) - y(4.4) = 0.012$ 4.31

For $M\phi^2 < 10$ (i.e. entrance length $z_a > 0.1$); $y(4.4) - y(4.30) = 0.091$ 4.32

Thus for systems with a small entrance length differences of up to -1.2% of the entrance concentration are found between the value of y calculated from equation 4.4 and 4.30. These differences increase to up to +9.1% for systems with large entrance lengths (i.e. low reaction rates and residence times). These errors in equation 4.4 tend to zero as P tends to zero.

The derivations of both equation 4.4 and 4.30 involve the assumption that, in kinetic terms, the particles are in a steady state for at least the major part of the reactor. Equation 4.30 has been found to be valid to better than $\pm$ 1% of the entrance concentration for $z > 0.1$ even though the particles may not have reached a kinetic quasi-steady state. Presumably this is because the exponential decay due to reaction, described by equation 4.30, approximates for a first order reaction to the reduction in gas phase concentration of reactant as a result of diffusion into the particle.

An asymptotic solution for consecutive first order reactions is shown in Appendix 5.

Asymptotic solutions are not possible for any other rate law since for such laws the effectiveness factors do not reach a final steady value. The reason for this is that the effectiveness factor is a function of the Thiele Modulus which in turn is a function of the surface reactant concentration for non-first order kinetics. Appendix 5 gives further consideration to this point. A consequence of this point is that the elementary analysis of section 4.2, incorporating a constant, steady state effectiveness factor, cannot be used for reaction orders other than one.

4.6 Film Mass Transfer

By assuming that mass transfer across the film surrounding the catalyst particle may be represented by a steady state equation, the following expression has been obtained for the fractional drop in concentration across the film (Appendix 6):

$$\frac{y - y_s}{y} = \frac{2\eta_{gf}\,\phi_g^2\,\Psi_{x=1}}{3\,D_m\,Sh\,y} \qquad 4.33$$

By taking typical values of the parameters in this equation, the following regimes have been suggested; for reactions of order one and above (Appendix 6):

$\phi^2 \leq 1$ Film mass transfer resistance may be neglected, (a drop of concentration across the film of less than 2% will exist).

$1 < \phi^2 \leq 6.25 \times 10^6$ Film mass transfer resistance is important and may be estimated by use of equation 4.33.

$\phi^2 > 6.25 \times 10^6$ Film mass transfer is controlling and equation 4.34 applies, (a drop of concentration across the film of greater than 98% will exist).

$$y = \exp(-3PMD_m Shz/2) \qquad 4.34$$

For first order kinetics the following asymptotic solution has been derived for $z > 0.1$:

$$y = \frac{1}{\left[1 + \frac{\eta_{ss}P}{1 + 2\eta_{ss}\phi^2/3D_m Sh}\right]} \exp\left[\frac{-PM\phi^2\eta_{ss}z}{1 + \frac{2\eta_{ss}\phi^2}{3D_m Sh}}\right] \qquad 4.35$$

Values of ϕ^2 of over 10^6 are unlikely to be encountered in practice and so complete film mass transfer control will not be found in transport reactors for reactions of first and higher orders. Values of ϕ^2 greater than unity are commonly found and thus film mass transfer resistance must often be allowed for. It should be noted, however, that because of the much smaller particles used in transport reactors, film mass transfer resistance is generally not as serious as in fixed bed reactors even though much higher gas-particle slip velocities may be obtained for the latter.

As an example of the magnitude of film mass transfer resistance, values of parameters taken from the example used in section 4.8 (the oxidation of naphthalene) give values of ϕ^2 of up to 10. Thus using equation 4.33:

$\frac{y - y_s}{y} \simeq 0.06$ i.e. a 6% drop in concentration across the film.

For a reactor to operate successfully, $y(z = 1)$ must lie within the range 0.99 to 0 (or 1 to 100% conversion). These conversions are obtained for values of $MP\phi^2\eta_{ss}$ roughly in the range 0.01 to ∞. So it may be seen that a reasonable conversion may be achieved by several different policies of operation, the two extremes being:

(i) Short reactors with high gas flowrates and low loadings of either a highly active catalyst or a catalyst operating at high temperature, (low P, low M, high ϕ).

(ii) Long reactors with relatively low gas flowrates and high loadings of catalyst at moderate temperatures, (high M and P, low ϕ).

Policy (i) is most attractive from a practical aspect but the existence of the film mass transfer limitations described in this section mean that a shift towards policy (ii) is necessary since a low value of ϕ^2 is desired.

In an experimental system film mass transfer limitations may be detected by the same means as is often used in fixed bed reactors. Determination of rate constants over a wide temperature range enables activation energies to be determined. Changes in apparent activation energy with temperature can be used to detect both film and intra-particle mass transfer resistances. (Satterfield, 1970). This method may be of limited use in transport reactors, for the wide temperature range which must be examined necessitates measuring very large changes in reaction rates. The limited range of solids to gas loadings and solids residence times possible in the transport reactor may prevent this.

To gain information about film mass transfer in a transport reactor it is most convenient to compare rate constants and reaction orders measured in the reactor with those measured by a conventional method in a fixed bed reactor. Equation 4.34 shows that the existence of film mass transfer resistance will have the effect of shifting the apparent reaction order towards unity. For a first order reaction a comparison of reaction rate constants with fixed bed results should give some indication of film mass transfer as indicated by equation 4.35.

4.7 Film Heat Transfer

As a result of assuming that film heat transfer can be represented by a steady state equation the following regimes are suggested (Appendix 7) for reactions of first order and above:

$\phi^2 \leq 1000$ Film heat transfer may be neglected (a drop in absolute temperature of less than 1% across the film exists).

$\phi^2 > 1000$ Equation 4.36 may be used with caution to estimate the maximum film temperature drop.

$$[\tau_s - \tau_g]_{max} = - \frac{2\phi_g^2 \chi [\eta_g \Psi_x = 1]_{z_m}}{3(1 + P_T)\kappa_m Nu_p} \qquad 4.36$$

It is to be noted that the above equation was derived assuming the particles to have passed through the thermal entry region. No estimate of the length of this region has been developed but it is expected to be longer than the corresponding diffusional entry region on which it depends.

Again using the example of section 4.8 to show the magnitude of the film temperature drop it is found that less than 1°C drop in temperature occurs across the film. (Values of parameters used are given in section 4.8 and Appendix 7).

It is of interest to compare the behaviour of the transport reactor with a conventional reactor as regards film heat transfer. In a fixed bed reactor, for example, operating under steady state conditions, all heat produced by the reaction within the catalyst pellets must be transferred across the film to the surrounding gas. In the non-steady state conditions of a transport reactor, part of the heat of reaction is used in raising the temperature of the particles themselves. Since the thermal capacity of the solids is much higher than that of the gases, relatively little heat is transferred to the gas stream. This effect is described by the dimensionless group P_T which is the ratio of the thermal capacity of the solids to that of the gases. The low solids loadings used in transport reactors and the consequent need for a high catalyst activity (giving a high value of ϕ^2) offset this advantage of the transport reactor to some extent however.

Thus the ability of the catalyst particles to act as a heat sink reduces the importance of film heat transfer resistance. Generally the values of the Thiele Modulus found in transport reactors are not high enough to give rise to large film temperature gradients, but for reactions with large activation energies even a small change in temperature can mean an appreciable change in reaction rate. In such circumstances an estimate of film temperature drop should be made using equation 4.36. Conditions which minimize film mass transfer resistance will also minimize film heat transfer resistance.

4.8 Optimization

The possibility of maximizing the production of an intermediate in a set of consecutive reactions has been examined for a fixed bed reactor by Bilous and Amundson (1956) and Aris (1960). For such a plug flow reactor the optimum axial temperature profile was determined. However, for real systems, physical constraints (in particular heat transfer limitations) make realization of the optimum conditions impossible in practice.

The plug flow conditions of the transport reactor suggest that a similar attempt at optimization may be made for this reactor, and the lower thermal capacity and better wall heat transfer of the reactor relative to the fixed bed reactor, may mean that the optimum conditions can be achieved in a real system.

For the purpose of this study, a simple reaction scheme consisting of two, consecutive first order reactions has been taken:

$$A \rightarrow B \rightarrow C$$

where component B is the desired intermediate and C is the unwanted decomposition product.

The reaction chosen for the examination of the feasibility of optimizing the transport reactor was the oxidation of naphthalene by air using a silica supported V_2O_5 and $K_2S_2O_7$ catalyst.

Details of the kinetics of this reaction were given by De Maria, Longfield and Butler (1961). It has been suggested (Carberry, 1966)

that this reaction is particularly suited to the conditions of the transport reactor. The true kinetics of the reaction system are somewhat complex (De Maria, Longfield and Butler, 1961) but may be simplified to the scheme shown below (Westerterp, 1962):

$$\text{Naphthalene} \rightarrow \text{Phthalic Anhydride} \rightarrow CO_2 + H_2O$$

Two optimization procedures have been studied, the first being the calculation of the optimum isothermal temperature and the second being the determination of the optimum axial variation of the wall heat flux. Variation of the wall heat flux has been considered rather than variation of the reactor temperature as it was felt that the former is more related to the implementation of the optimum conditions in practice. The fixed bed reactor studies mentioned above showed that an infinite temperature was required at the reactor entrance and it should be noted that the choice of the wall heat flux as the variable to be studied precludes the possibility of obtaining this result. However, since an infinite temperature is meaningless in practice, this is of no consequence.

Optimization of the reactor wall heat flux has been called the 'full' optimization and the calculation of the optimum isothermal temperature was made for purposes of comparison only.

In addition to assumptions (i), (ii), (iv), (v) of section 4.2 the following assumptions have been made:

(i) No film heat transfer resistance exists at the catalyst particle surface.

(ii) The parameters M_A, M_B, M_T, P, P_T, G_A, G_B, $\phi_{\infty A}$, $\phi_{\infty B}$, $\sigma_{\infty A}$, $\sigma_{\infty B}$ are not temperature dependent.

4.8.1 Optimum Isothermal Temperature

For the reaction system $A \rightarrow B \rightarrow C$ consisting of two consecutive first order reactions where the objective is to maximize the production of component B, the optimum isothermal temperature may be found using the solutions of Appendix 3 (equations 3.13 to 3.21) or, less accurately, using the asymptotic solution of Appendix 5 (equation 5.30).

ϕ_A and ϕ_B are written in their Arrhenius forms:

$$\phi_A^2 = \phi_{\infty A}^2 \exp(-G_A/\tau) \qquad 4.37$$

and

$$\phi_B^2 = \phi_{\infty B}^2 \exp(-G_B/\tau) \qquad 4.38$$

Substitution of these equations into the appropriate equations listed above enabled y_B to be found as a function of dimensionless temperature τ. A computer search (Programme 2, Appendix 9) produced the optimum isothermal temperature and the maximum yield of component B.

The results of this section are discussed below together with the results of section 4.8.2.

4.8.2 Optimum Axial Variation of the Wall Heat Flux

The objective of this optimization was to maximize production of component B as above, but by imposing a wall heat flux on the reactor variation of temperature along the reactor was possible.

The analysis given in Appendix 8 determines the optimum axial variation of the radial, wall to suspension heat flux. The computer programme used for this determination is programme 3 of Appendix 9.

The method of optimization used was that of Denn, Gray and Ferron (1966). This consists of the solution of the linearized system variational equations by Green's functions combined with a steep ascent method for determination of the optimum heat flux. Firstly, the coupled partial differential system equations and their boundary conditions were integrated numerically along the reactor. The adjoint equations were then integrated numerically from exit to entrance of the reactor using the solution of the system equations previously obtained. The resulting values of the adjoint variables were used in a steep ascent method to choose a new heat flux profile to give improved conversion. This procedure was repeated until convergence was obtained. A Crank-Nicholson method was used for the numerical integration.

The values of the parameters used are given in Table 4.1.

TABLE 4.1

VALUES OF THE PARAMETERS USED IN THE OPTIMIZATION EXAMPLE

	Catalysts 1 and 2	Catalyst 1	Catalyst 2	Reference
ε	0.4			Satterfield (1970)
d_p	4.0×10^{-4} m			De Lasa and Gau (1973)
L/u_s	3.0s			Westerterp (1962)
ρ_s	1.2×10^3 kg/m^3			Satterfield (1970)
C_{ps}	10^3 J/kg			Al_2O_3, 500°C
T_{go}	600°K			Carberry (1966)
κ_{eff}	0.17 J/s m °K			Satterfield (1970)
ρ_g	0.6 kg/m^3			Air - 600°K, 1 atm
C_{pg}	1.04×10^3 J/kg			Air - 300°C
u_s/u_g	0.8 (u_s = 6.92 m/s)			Heywood (1962)
α	0.97			Zenz and Othmer (1960)
C_{AO}	2.04×10^{-1} moles/m^3 ($\simeq$ 1% by vol)			600°K 1 atm

TABLE 4.1 continued.....

	Catalysts 1 and 2	Catalyst 1	Catalyst 2	Reference
R	8.313 J/mole °K			-
D_{Aeff}	5.0×10^{-7} m^2/s)			Satterfield (1970)
D_{Beff}	5.0×10^{-7} m^2/s)			
ΔH_A	-1.881×10^6 J/mole)			Westerterp (1962)
ΔH_B	-3.282×10^6 J/mole)			
E_A		1.67×10^5 J/mole	8.49×10^4 J/mole)	Carberry (1966) De Maria, Longfield and Butler (1961)
$k_{\infty A}$		2.77×10^{14} s^{-1}	6.68×10^6 s^{-1})	
E_B		8.28×10^4 J/mole	1.86×10^5 J/mole)	
$k_{\infty B}$		1.88×10^5 s^{-1}	3.71×10^{13} s^{-1})	
M_A	93.8			
M_B	93.8			
M_T	17.7			
P	0.01 ($W_s/W_g \simeq 50$)			
P_T	28.9			

TABLE 4.1 continued.....

	Catalysts 1 and 2	Catalyst 1	Catalyst 2	Reference
G_A		33.6	17.0	
G_B		16.6	37.2	
$\phi^2_{\infty A}$		2.22×10^{13}	5.34×10^{5}	
$\phi^2_{\infty B}$		1.50×10^{4}	2.97×10^{12}	
$\sigma^2_{\infty A}$		-4.17×10^{10}	-1.00×10^{3}	
$\sigma^2_{\infty B}$		-4.94×10	-9.74×10^{9}	

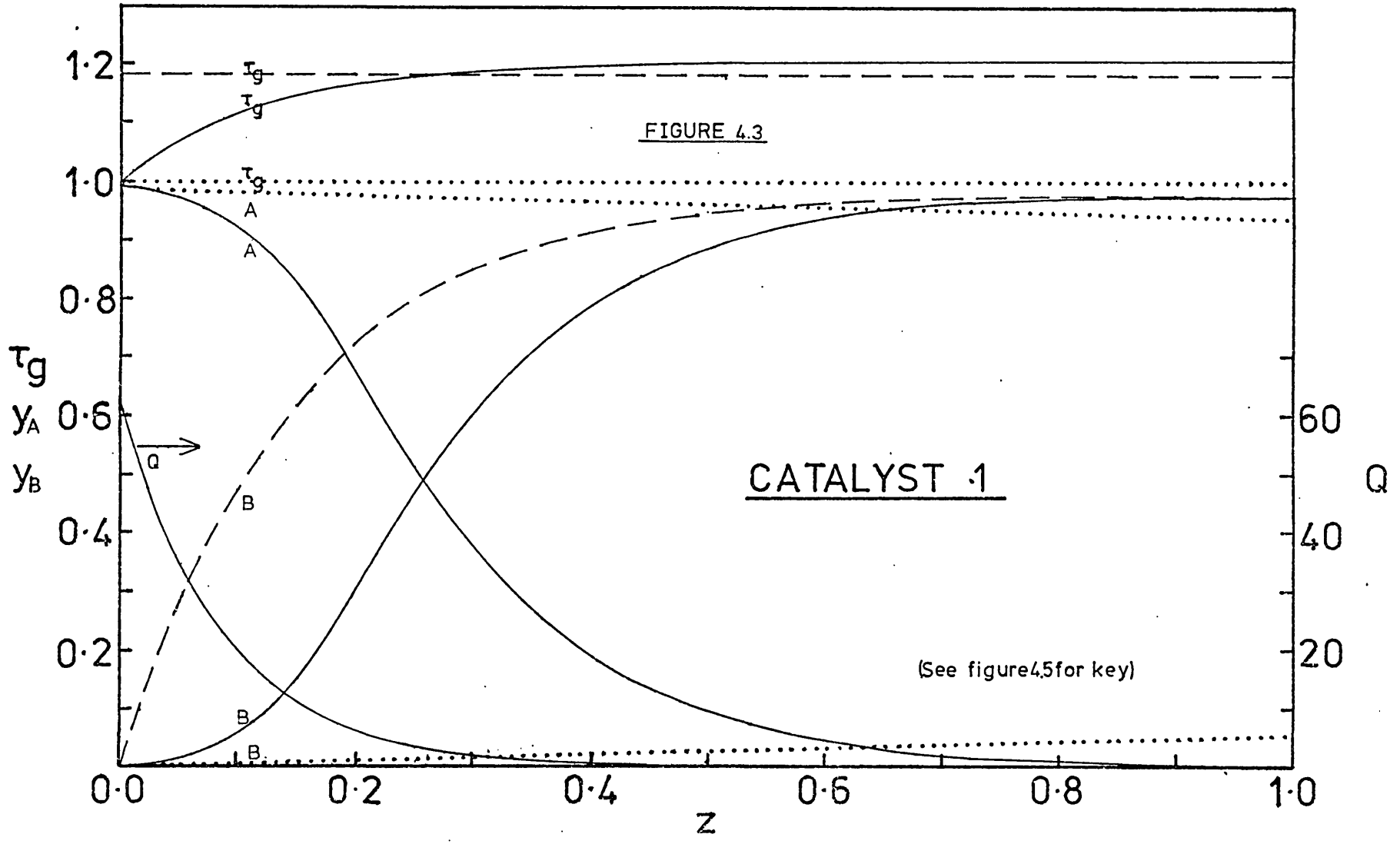
FIGURE 4.3
CATALYST 1
(See figure4.5for key)
τg
yA
yB
Q
z
1·2
1·0
0·8
0·6
0·4
0·2
0·0
0·2
0·4
0·6
0·8
1·0
60
40
20
A
B

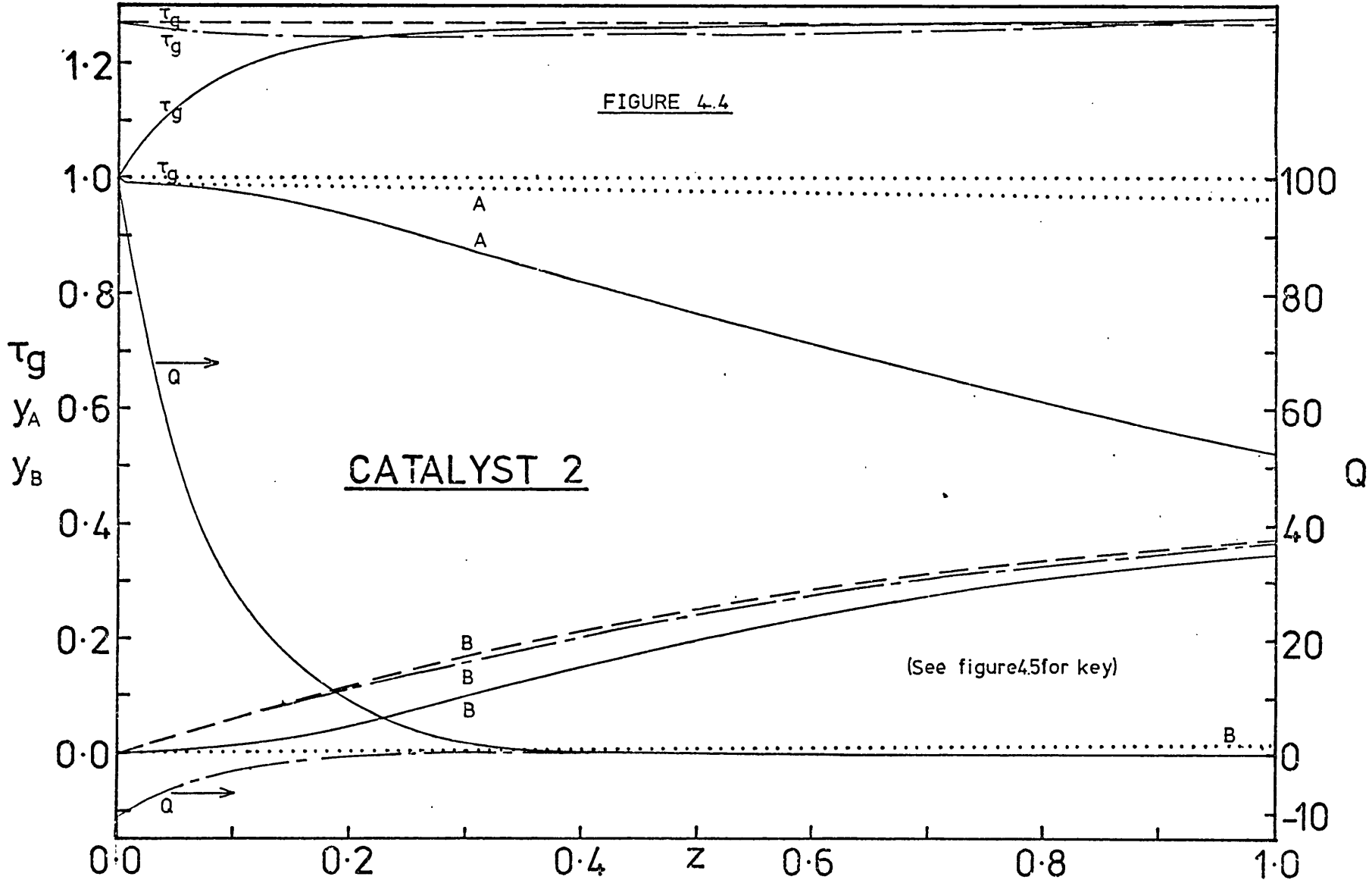
FIGURE 4.4
CATALYST 2
τ_g
y_A
y_B
Q
z
(See figure4.5for key)
1·2
1·0
0·8
0·6
0·4
0·2
0·0
100
80
60
40
20
0
-10
0·0
0·2
0·4
0·6
0·8
1·0
A
B

FIGURE 4.5

(Key to figures 4.3 & 4.4)

.....	Adiabatic conditions
————	Optimum heat flux conditions ($T_{go} = 600^{\circ}K$)
— — — —	Optimum isothermal temperature
———— – ————	Optimum heat flux conditions for entrance temperature approximately equal to the optimum isothermal temperature ($T_{go} = 762^{\circ}K$, for Catalyst 2)

Two catalysts have been considered. They have different characteristics and are catalysts A and B of Westerterp (1962) and Carberry (1966). The catalysts are referred to here as catalysts 1 and 2 respectively to avoid confusion with reactants A and B.

Figures 4.3 and 4.4 show the results obtained. Figure 4.5 is the key to these graphs.

Both figures 4.3 and 4.4 show that optimizing the wall heat flux increases the production of substance B (phthalic anhydride) greatly relative to the adiabatic conditions. The optimum isothermal temperature, whilst giving a different concentration profile to that obtained in the optimum heat flux case for B, produces an almost identical exit concentration of the intermediate B. From these results it is apparent that the main function of the large heat flux required at the reactor inlet is to raise the suspension temperature to the optimum isothermal temperature. This was investigated for catalyst 2 (figure 4.4) by optimizing the wall heat flux for an entrance temperature equal to the optimum isothermal temperature. The required wall heat flux was found to be small and negative, the amount of heat withdrawn from the system being sufficient to remove the heat of reaction along the reactor. The concentration profile of substance B was almost the same as that for the isothermal case.

It appears, therefore, that optimizing the wall heat flux offers no advantage over operating at the optimum isothermal temperature. This conclusion has been reached by the study of one particular system and to determine if it is of general validity the system parameters have been changed. For the non-reaction parameters, alteration of

their values had no effect on the conclusion reached, although this may have been a result of the initial assumption of the model that these parameters are independent of temperature.

In the naphthalene oxidation system studied, the intermediate (phthalic anhydride) is relatively stable, so to determine the effect of having a comparatively unstable intermediate, the rate constants k_A and k_B were interchanged in both catalysts 1 and 2. This had no effect on the conclusion that the optimum isothermal temperature conversion cannot be improved upon and thus it seems that this result is likely to be general.

An explanation of why the optimum temperature profile is isothermal may be suggested. Considering catalyst 2 (Figure 4.4) it may appear at first sight that an optimum temperature policy would involve the use of an infinitely high temperature at the reactor entrance (to maximize the rate of production of B relative to its decomposition to C) rapidly decreasing to zero as the concentration of B rises to unity. This type of policy has been suggested for a fixed bed reactor by Bilous and Amundson (1956) and Aris (1960). This picture, however, ignores the interior of the catalyst particles where the concentration of substance A decreases from the particle surface to its centre, the converse being true for substance B. So at the particle surface the ideal would be a high temperature, decreasing rapidly towards the particle centre. This situation cannot be achieved in practice as the thermal conductivity of the particles is such that they are almost isothermal (section 3.3.1). The best policy for the catalyst particles is therefore operation at the optimum isothermal temperature. Since this conclusion may be drawn for a particle at any point in the reactor,

the axial temperature profile of the reactor is itself isothermal for optimum performance.

As the optimum temperature profile is isothermal the results of section A 5.2 may be used to calculate the optimum temperature to a good approximation.

The heat sink role of the solids has been discussed in section 4.7 and it is of interest to compare the results of the fixed bed studies previously mentioned with the results for the transport reactor in this light. The solids in the transport reactor move along the reactor and, since they have a much larger heat capacity than the gas stream, they tend to make imposition of an axial temperature gradient on the reactor difficult. Thus the effect of the conveyed solids is to make imposed temperature gradients less steep. This effect does not explain why the optimum temperature of the transport reactor is isothermal but does show that a temperature profile similar to that suggested for a fixed bed reactor would be impossible to achieve in practice for a conveyed system.

The above analysis has assumed that, at the temperatures of operation, sintering of the catalyst is not important and, whilst this is probably true for the system considered, sintering may be a limiting factor in achieving optimum conditions for other reaction systems.

The conditions chosen (i.e. those of Table 4.1) are based on typical industrial systems and not on the conditions of the experimental reactor.

The wall heat flux which can be achieved in practice is clearly limited and its upper bound is considered below.

4.8.3 Maximum Wall Heat Flux

Heat transfer limitations between the reactor wall and the suspension result in a maximum value for the heat flux Q. This may be found from equation A 8.11.

The following values for the parameters are assumed:

$$L = 20.76m; \quad a_o = 0.04m; \quad Pr = 0.74; \quad Re_t = 1.384 \times 10^4$$

The wall to suspension Nusselt number is assumed to be about 16 times the value of that for air alone (section 3.3.2). This is the maximum enhancement of the heat transfer in suspension flow and is valid only at high loadings and very small particle sizes. For the loadings and particle size used in this example a much lower enhancement is to be expected (of the order of 2), but the figure 16 is used to obtain the limit of heat transfer under any conditions of operation.

$$\text{i.e.} \quad Nu_s = 16\, Nu_o$$

Nu_o is found from $Nu_o = 0.023\, Re_t^{0.8}\, Pr^{0.4}$ $(Re > 10^4)$ (Perry, 1973) giving $Nu_o = 41.9$ and $Nu_s = 671$,

$$\text{Hence} \quad Q = 68.0\, (\tau_w - \tau_{x=1}) \qquad 4.39$$

At the reactor entrance where Q is maximum $\tau_{x=1} = 1$ and $\tau_w = T_w/T_{go}$ with $T_{go} = 600°K$.

Assuming a temperature difference between the tube wall and the suspension of 300°K to be the maximum achievable, τ_w is calculated to be 1.5.

$$\text{Thus} \quad Q_{max} = 68.0\ (1.5\text{-}1) = 34.0 \qquad 4.40$$

It is concluded that physical constraints place an upper bound of 34 on the dimensionless heat flux Q. For the problem under consideration a value of Q of greater than 4 (i.e. $Nu_s/Nu_o \simeq 2$) cannot be obtained.

Removal of Heat of Reaction

In order to maintain the optimum isothermal temperature, the heat of reaction must be removed through the reactor walls and the heat flux required for this may be calculated.

Equation A 7.6 may be modified to include a wall heat flux:-

$$P_T\ (\eta_T \tau_s - 1) + (\tau_g - 1) = \frac{-P_T M_T \chi[(1-y) - \eta_* P y_s]}{PM} + Qz \qquad 4.41$$

where it is assumed that Q is constant along the reactor in order to simplify the estimation.

Assuming (i) $\eta_T \simeq 1$ (isothermal particles)

(ii) $\tau_g \simeq \tau_s$ (for isothermal system)

(iii) $\eta_* P y_s \ll (1-y)$ (since P small)

(iv) $y(1) = 0$ (complete conversion)

$\therefore$ at reactor exit:-

$$\left[\tau_s = \frac{-P_T M_T \chi}{(1 + P_T)\ PM} + \frac{Q}{(1 + P_T)} + 1\right]_{exit} \qquad 4.42$$

(cf equation A 7.22)

but for isothermal conditions $[\tau_s]_{exit} = 1$

$$\therefore\ Q = \frac{P_T M_T \chi}{PM} \qquad 4.43$$

$$Q = \frac{28.9 \times 17.7\ \chi}{0.01 \times 93.8} \qquad 4.44$$

(Using values from Table 4.1)

$$Q = 545.34\ \chi \qquad 4.45$$

From equation A 7.12 $\chi = -0.001481$

$$\therefore\ Q = -0.81$$

To remove all heat of reaction for complete conversion of component A, a mean value of Q of -0.81 is necessary. This value is well within the upper bound of 34 found above.

Maintaining isothermal conditions in a transport reactor by removal of the heat of reaction through the reactor wall should therefore be possible.

Thus the optimum heat flux for maximizing the production of an intermediate in a set of two consecutive first order reactions has been found. The optimum isothermal temperature has been shown to give the same conversions as the full optimization and isothermal conditions can be easily maintained by removal of the heat of reaction through

the reactor wall, whereas for the full optimization, heat fluxes in excess of the maximum limit of 34 were indicated.

The conditions used in making the evaluations of the maximum wall heat fluxes were, like all the parameters used in the optimization example, chosen to represent typical industrial conditions. It is thought that the conclusions reached in this section should thus be applicable to many industrial systems of the type examined here. The limiting factors involved in this study were the accuracy of the assumptions of the mathematical model used. (Section 4.3). In particular, the assumption of plug flow of the solid phase may break down at high solids loadings when backmixing may occur. Furthermore particle film heat and mass transfer resistances have been neglected for simplicity. Consideration of these factors seems likely to strengthen the conclusions reached, as the former brings the system closer to isothermality, whilst the latter add to the problems of heat transfer to the system when attempting to impose an axial temperature gradient on the reactor.

5. EQUIPMENT

5.1 Transport Reactor

A photograph of the experimental rig with the majority of the thermal insulation removed is given as Figure 5.1 and Figure 5.2 shows a line drawing of the rig. Appendix 10 gives details of the equipment used.

Air was drawn from outside of the laboratory, via a flexible rubber hose and a filter, by the blower. It then passed, via a short length of rubber hose (to damp vibrations), to a globe valve which controlled the air flowrate. After being metered by a rotameter the air entered the heater (Figure 5.3) where it was heated to about 600°C. 2 kW of the total 4 kW power of the heater were controlled by a temperature controller which had an input from a Chromel-Alumel thermocouple located at the pipe centre in a thermocouple well 4 in. before the reactor entrance.

The remaining section of the rig was fabricated throughout in stainless steel unless otherwise stated. The pipework was connected at the flanges to the supporting framework by sliding fixtures to allow for thermal expansion.

The hot air from the heater entered a horizontal section where the catalyst was added by means of a pipe inclined at 45° to impart a horizontal component of velocity to the particles. The catalyst was fed from a hopper via a modified gate valve (Figure 5.4) and fell under gravity into the airstream. Coarse control of particle feed rate was obtained by movement of the gate, whilst fine control

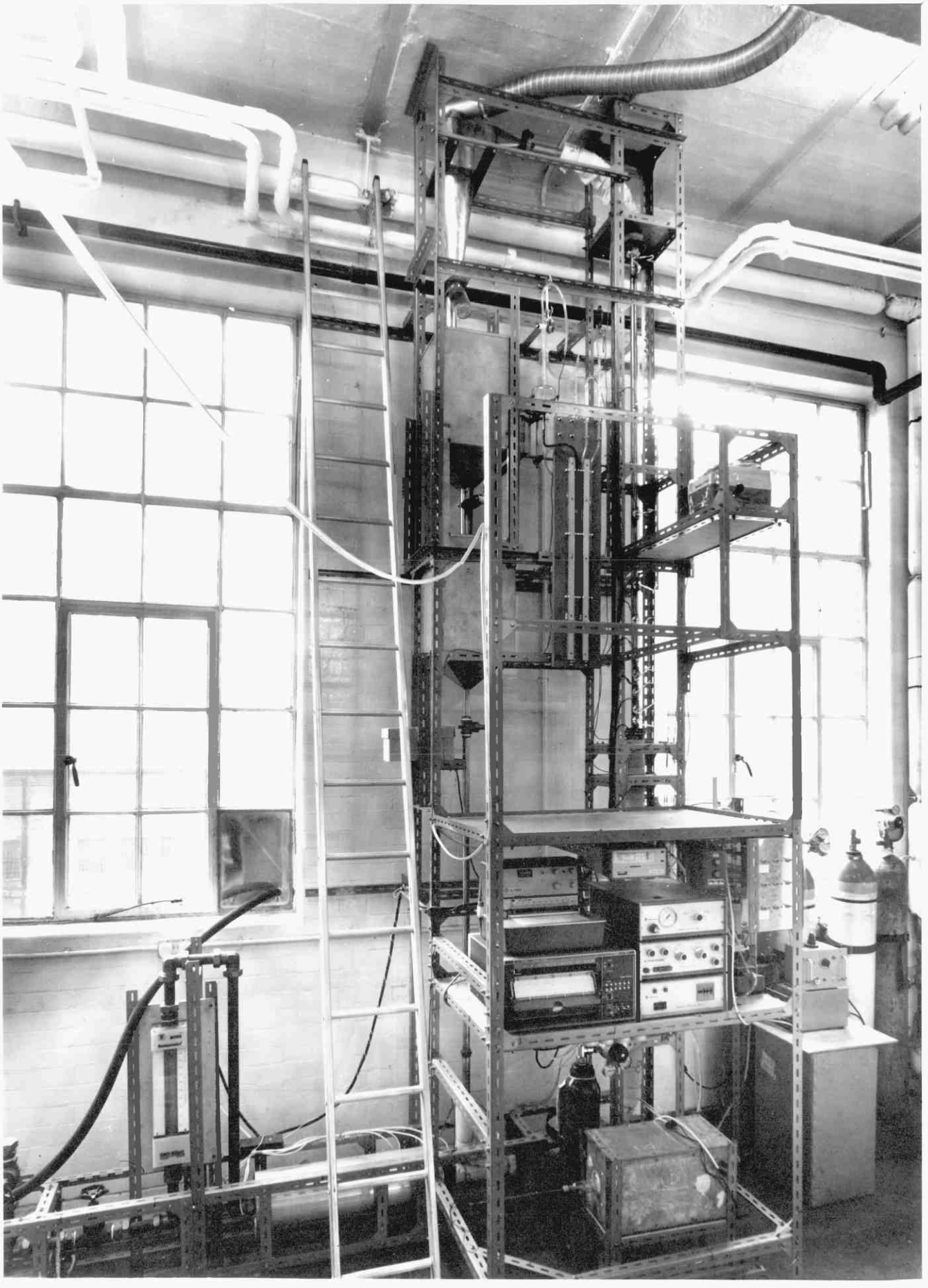

FIGURE 5.1

SCHEMATIC DIAGRAM OF EQUIPMENT

FIGURE 5.2

Scale 1:19·6

1 Blower
2 Globe Valve
3 Rotameter
4 Electric Heater
5 Solids Entry Pipe
6 Flow Straightener
7 CO Injector
8 Cock
9 Needle Valve
10 Reactor
11 Cyclone
12 Sampling Jar
13 Hopper
14 Slide Valve
15 Modified Gate Valve
16 Air Pump

P.T.- Pressure Tapping
T.C.- Thermocouple

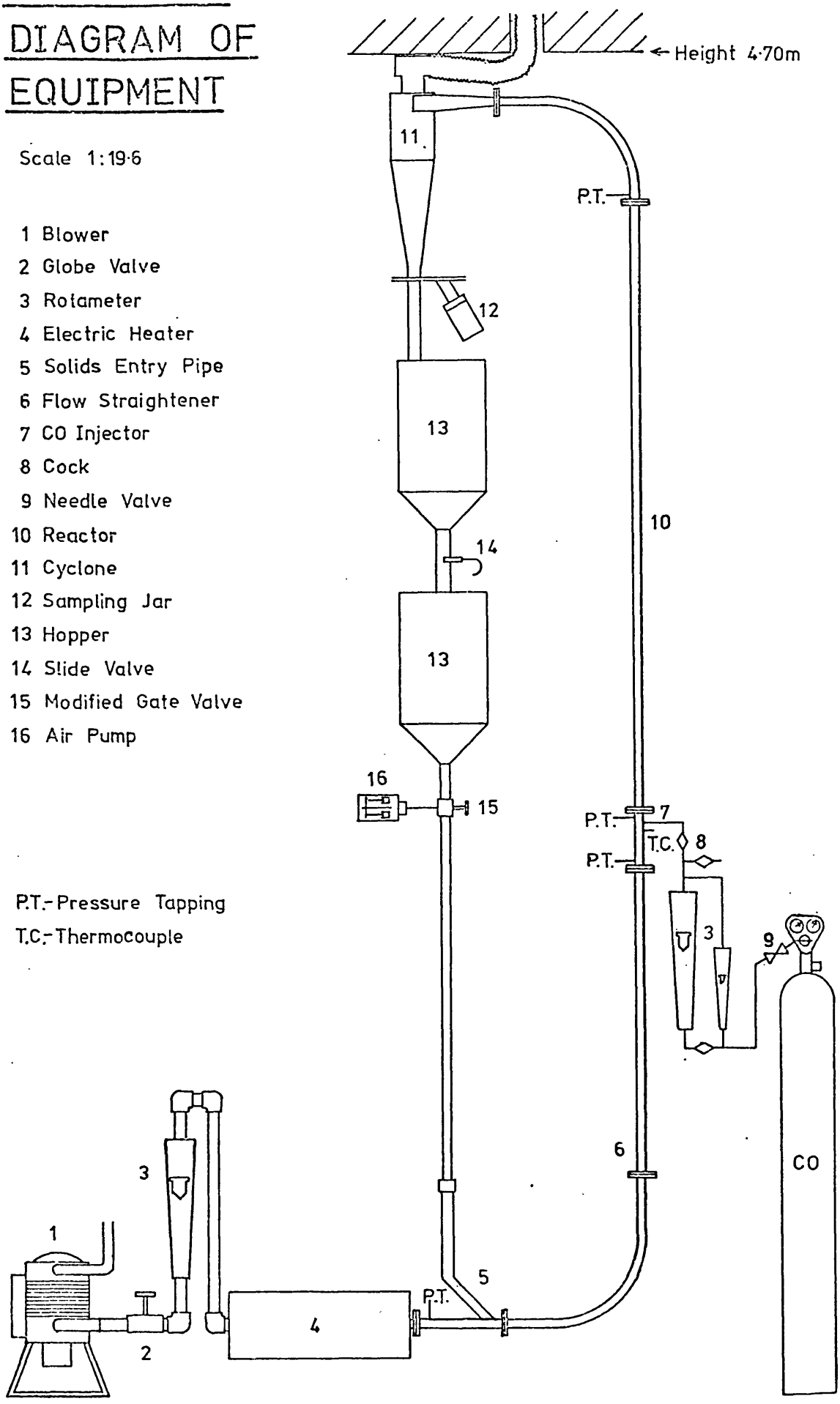

FIGURE 5.3

HEATER

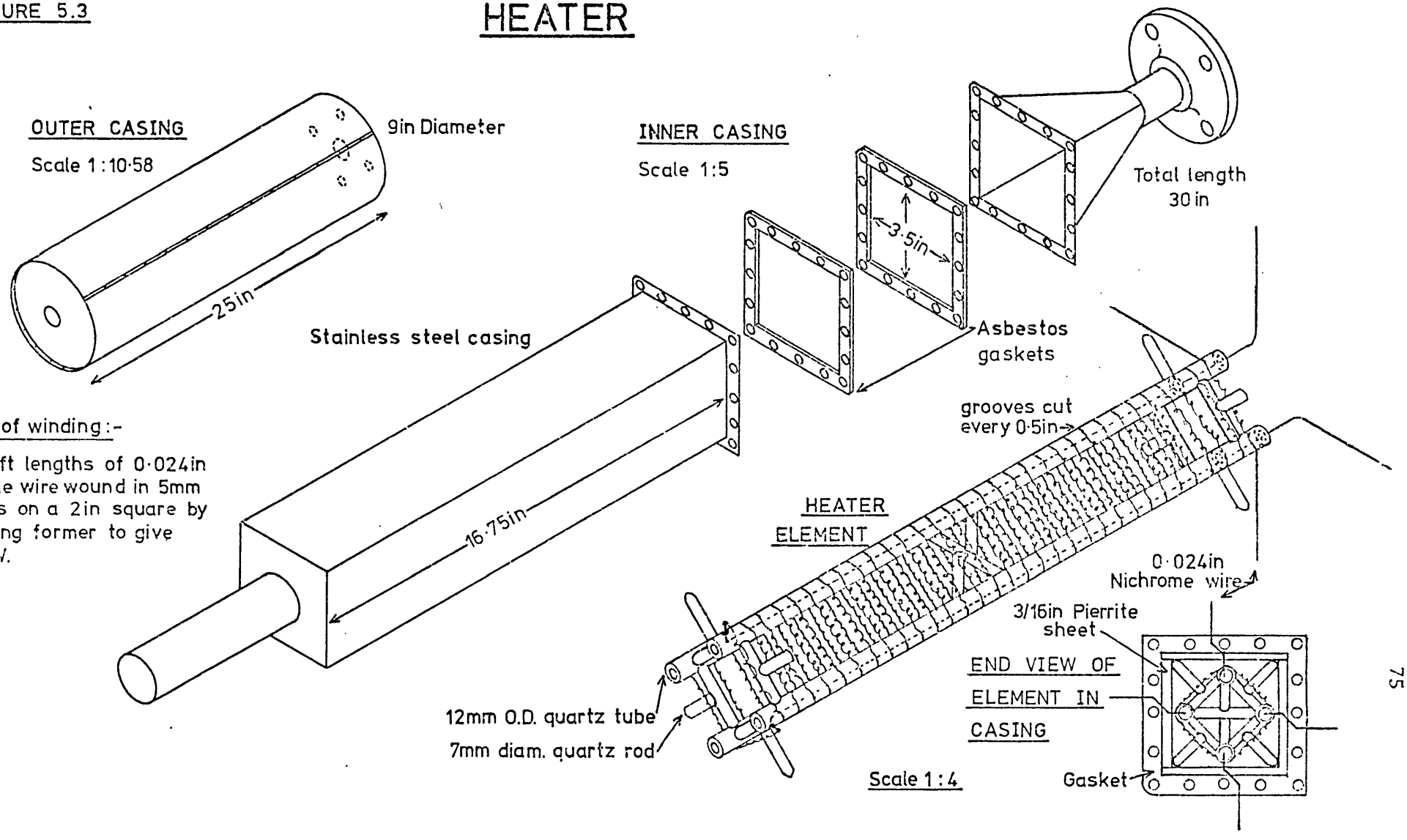

Details of winding:-

2 × 25·5ft lengths of 0·024in Nichrome wire wound in 5mm I.D. coils on a 2in square by 16·5in long former to give 2 × 2 kW.

SOLIDS FEED VALVE.

Scale 1:1

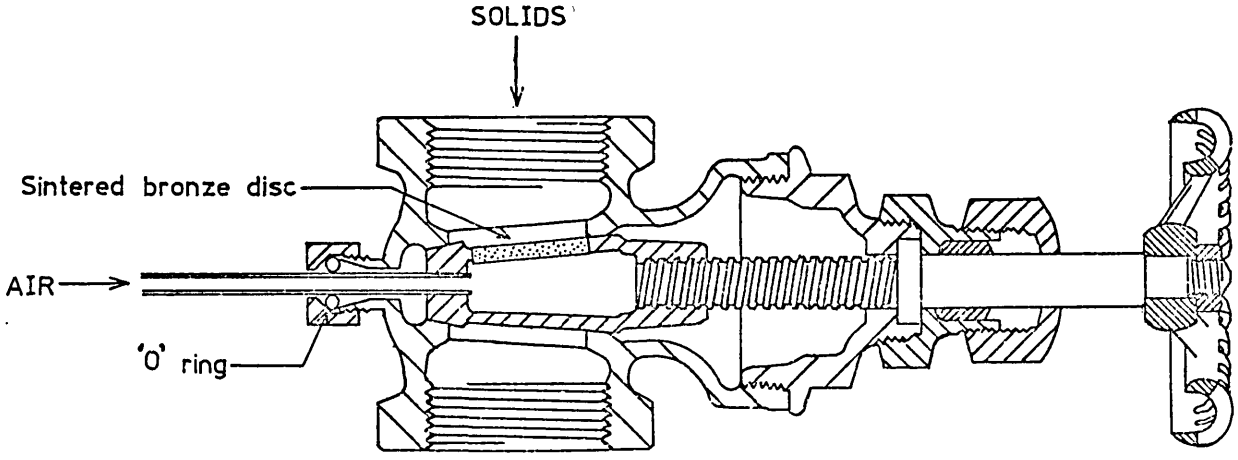

FIGURE 5.4

was achieved by varying the air flowrate through the sintered bronze disc in the upper surface of the gate.

The air and catalyst suspension passed round a 12 in. radius 90° bend, through a flow straightener followed by 44 in. of calming section and then entered the reactor.

Carbon monoxide of technical grade (99.5% CO) was fed from a cylinder through one of two rotameters (for different flowrate ranges) to an injector at the reactor entrance. The injector (Figure 5.5) consisted of a 1/8 in. O.D. tube which passed through the pipe wall and was bent through 90° to allign it co-axially with the reactor. From just below the sealed tube end, carbon monoxide was injected radially from 6 equally spaced holes located around the tube circumference. The end of the injector could be removed to allow replacement by alternative configurations if necessary.

The reactor (Figure 5.7) consisted of 7 ft. of 1 1/8 in. O.D. by 0.064 in. tubing.

Leaving the reactor, the suspension flowed round a second 12 in. radius 90° bend to a high efficiency cyclone which was mounted on flexible brackets to allow for thermal expansion of the pipework. Exhaust gases were vented to the atmosphere through a flexible metal duct.

Catalyst particles leaving the base of the cyclone passed through a 2 in. diameter tube to a second hopper. The two hoppers were connected by a 2 in. diameter tube containing a slide valve which enabled

CARBON MONOXIDE INJECTOR

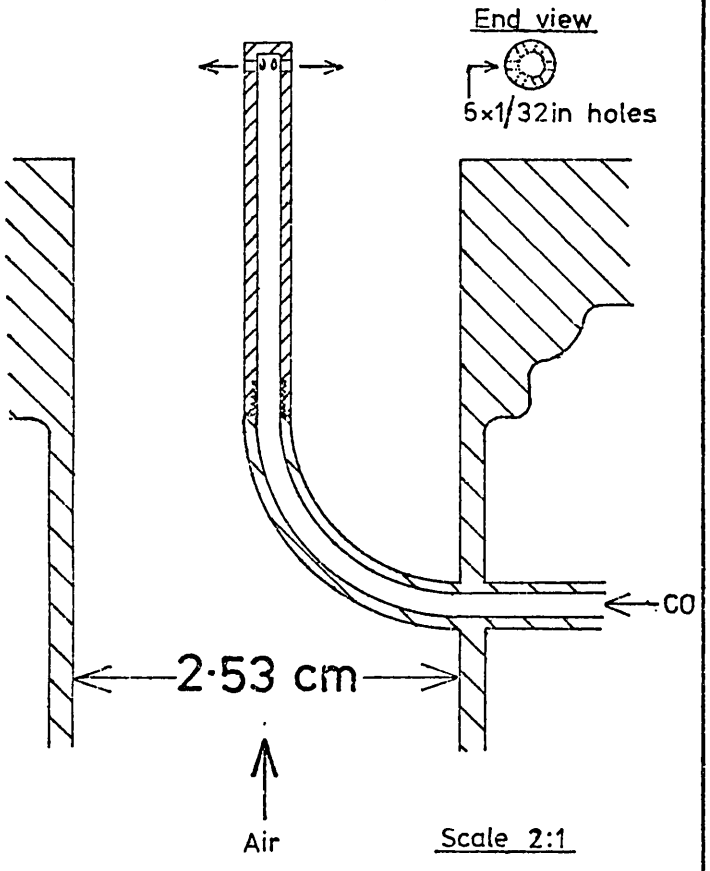

FIGURE 5.5

SAMPLING SYSTEM

FIGURE 5.6

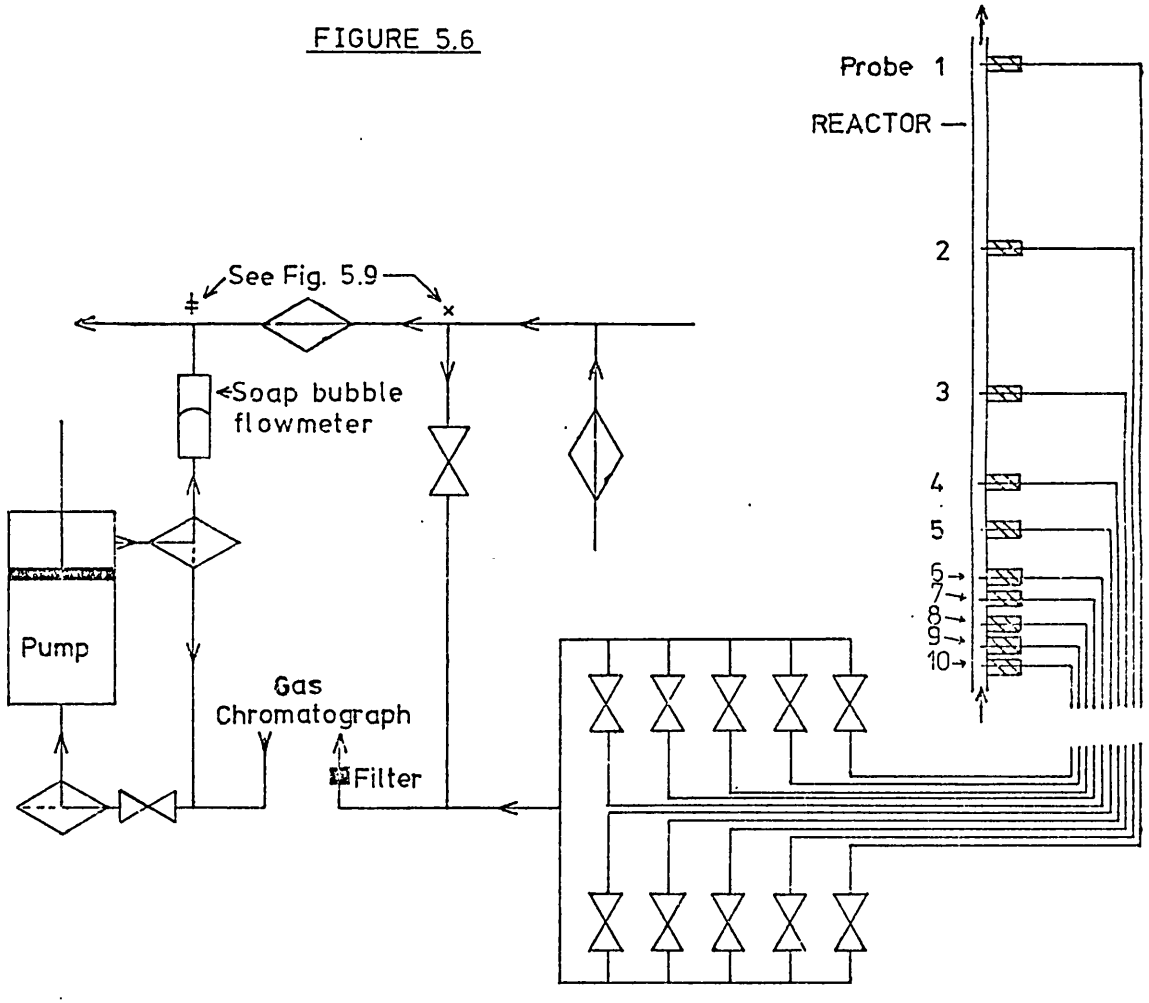

REACTOR

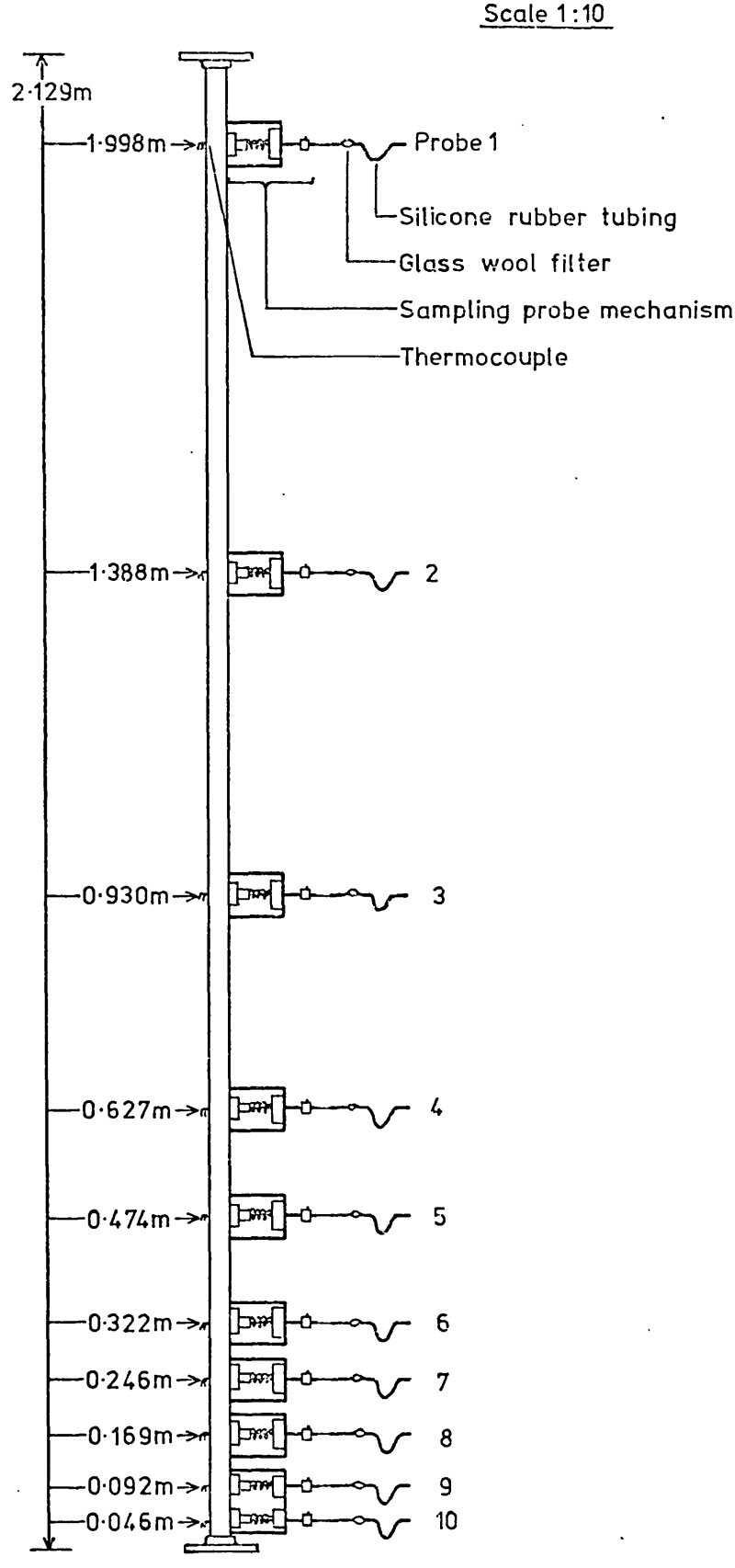

FIGURE 5.7

the system to be operated either batch-wise or, if left open, enabled recycling of the catalyst. Both hoppers had closely fitting lids to prevent escape of fines or gases to the atmosphere. At the base of the cyclone a sampling tube could be moved manually into position to collect samples of catalyst for mass flowrate determination. A collecting jar could be screwed on to the end of the sampling tube giving a gas tight seal. The sliding surfaces of the sampling mechanism were machined flat to prevent gas leakage.

All of the stainless steel pipework following the heater was insulated with preformed glass fibre insulation to prevent heat loss. The cyclone and hoppers were insulated with woven ceramic fibre matting and asbestos yarn was used to insulate the remaining exposed metal surfaces. The heater (Figure 5.3) was enclosed in a 9 in. diameter aluminium cylinder packed with ceramic wool insulation.

The total system was supported by a "Handy-angle" framework which was anchored securely to the wall and earthed to prevent electrostatic charging. Instruments and control panels were positioned in front of the rig at chest height. A platform above the instruments allowed easy access to the upper half of the equipment. A further small platform below the level of the cyclone base held a balance for weighing samples from the cyclone.

Pressure tappings at the reactor entrance and exit were used to measure the pressure drop across the reactor and to monitor the solids flowrate. A two fluid manometer was used for this purpose. A further pressure tapping at the heater exit was connected to a single fluid manometer and provided an alternative means of measuring solids flowrate.

Ten hypodermic sampling tubes, with their ends facing downstream to prevent blockage with particles, were positioned in an approximately exponential fashion along the reactor (Figure 5.7). Radial movement of these tubes was controlled by a mechanism attached to the reactor wall (Figure 5.8). A threaded rod, fitted with a spring to ensure correct positioning, allowed movement of the hypodermic tube by the turning of an engraved metal disc. The rod was fitted with a stop to prevent damage to the hypodermic tube by collision with the far wall of the reactor and the position of the end of the tube was accurately determined by measuring rotation of the engraved metal disc. A gland containing graphitised asbestos prevented gas leakage around the hypodermic tube.

Sample gases were withdrawn from the reactor by a diaphragm pump via a glass wool filter, to trap any particles present, and a selector panel (Figure 5.6). The gas flow direction could be reversed, by means of two 3-way cocks, to clear particles from blocked sample tubes. A particular sample line could be selected by opening the appropriate valve on the selection panel. Gases passed through a removable micron filter to the sampling chamber of a gas chromatograph. The chromatograph output was recorded by an integrater recorder. Waste gases were passed to a fume cupboard via a soap bubble flowmeter for measurement of sampling rate.

Opposite all ten sampling points iron-constantan thermocouples were attached to the external wall of the reactor by ceramic cement. All of these temperature measurement points were monitored continuously by a twelve channel chart recorder. The eleventh channel of the recorder was used for measuring the external wall temperature opposite the

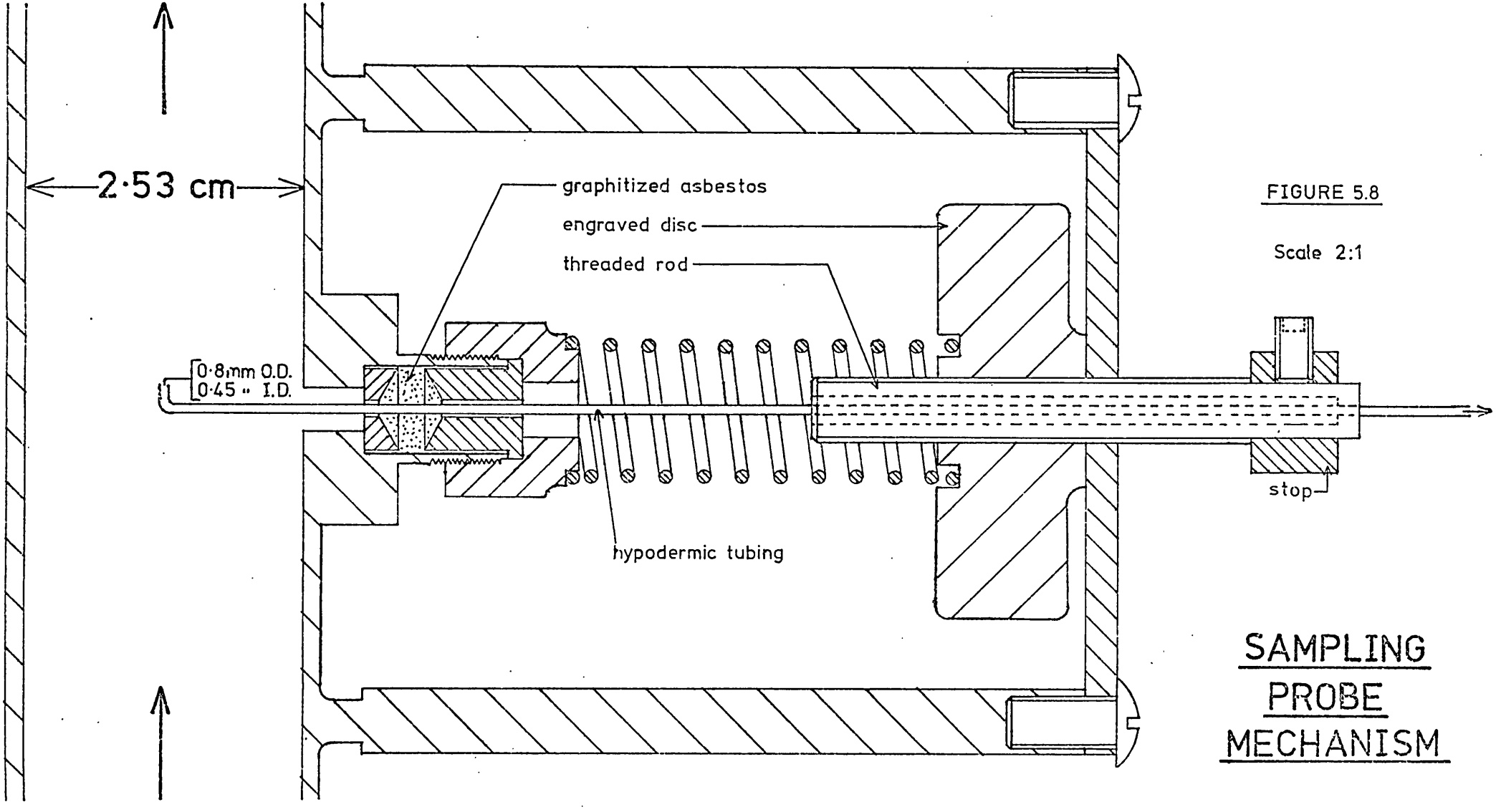

FIGURE 5.8

Scale 2:1

SAMPLING PROBE MECHANISM

thermocouple well used for temperature control. This enabled measurement of the temperature difference between the external tube wall and the gas at the tube centre (where the control thermocouple was positioned) so that a correction factor could be used to estimate the mainstream gas temperature from the measured wall temperature at the sampling points.

5.2 Catalyst Test Rig

A line drawing of the catalyst test apparatus is given in (Figure 5.9). Catalyst activity was measured in a fixed bed reactor consisting of a pyrex glass tube of either 9 mm or 25 mm internal diameter. The catalyst bed was held in position in the tube by glass wool plugs at both ends. The bed temperature was measured by an iron-constantin thermocouple located axially at the bed entrance and connected to the twelth channel of the recorder mentioned in section 5.1. The reactor was heated externally by a 1.2 kW tube furnace.

Carbon monoxide, either as a 1% or as a 5% mixture with nitrogen, was passed from a cylinder through a rotameter at up to 500 cc/min. Air from a cylinder was passed through a rotameter at up to 500 cc/min. and mixed with the carbon monoxide / nitrogen stream. Having passed through the reactor, the gases were released into a fume cupboard. Samples of the exit gases were analysed by the gas chromatograph mentioned in section 5.1. The pressure drop across the bed and the pressure at the reactor exit were measured with a mercury manometer.

CATALYST TEST APPARATUS

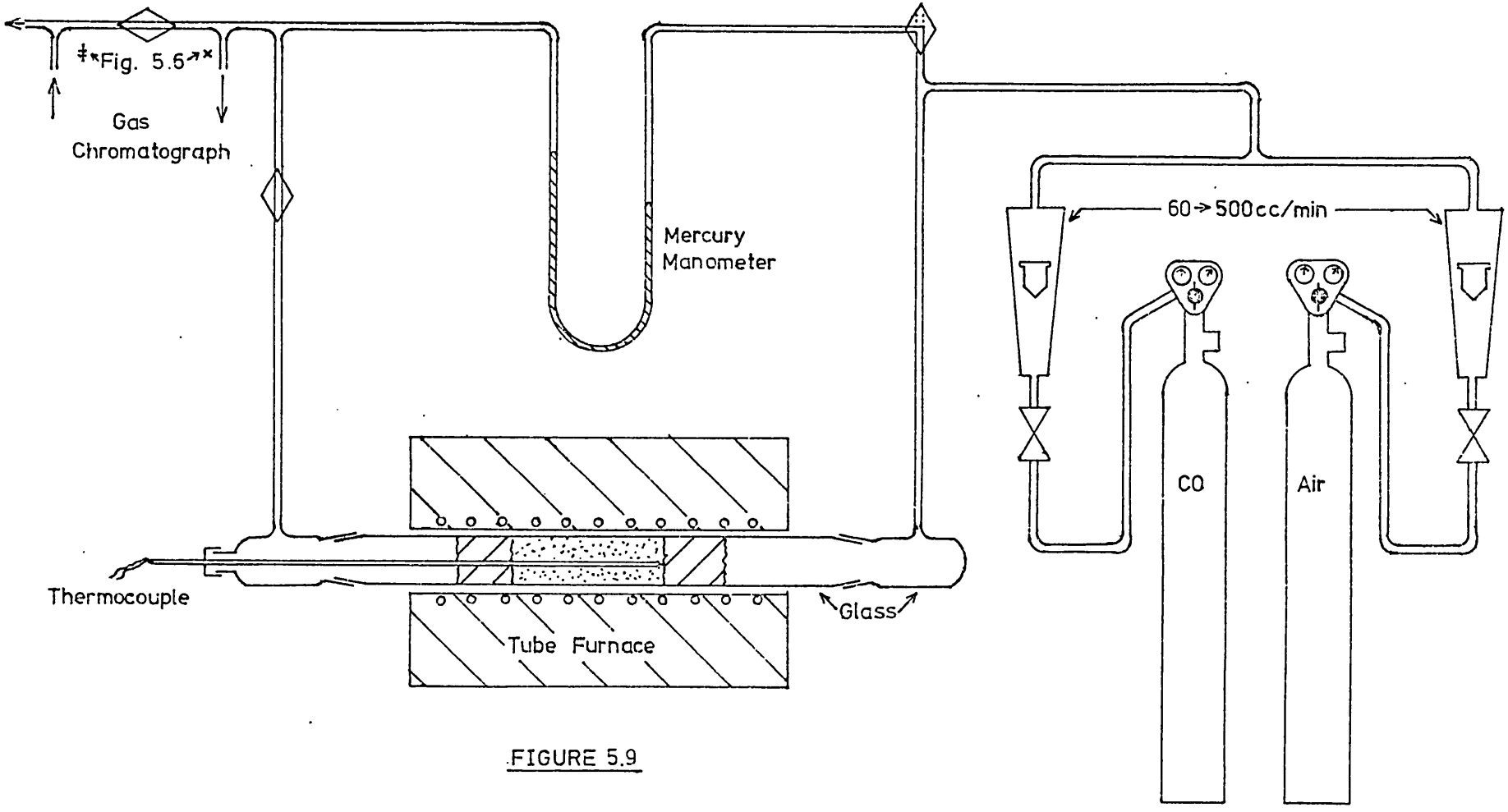

FIGURE 5.9

6. CATALYST CHARACTERISATION

6.1 Reaction and Catalyst

The test reaction used to study the behaviour of the transport reactor was the oxidation of carbon monoxide on a palladium catalyst, supported on γ-alumina.

The choice of an oxidation reaction enabled air to be used as the conveying gas and carbon monoxide oxidation is one of the simplest and most convenient reactions of this type. The palladium catalyzed oxidation of carbon monoxide has received a considerable amount of attention: Dixon and Longfield (1960); Dwyer (1972); Katz (1953); Thomas and Thomas (1967); Baddour, Modell and Heuser (1968); Close and White (1975); Matsushima and White (1975); Matsushima, Almy, Foyt, Close and White (1975); Wei (1975a and b). Generally the following kinetic expression has been found to apply:

$$S = k_{CO} \frac{[O_2]}{[CO]} \qquad 6.1$$

with an activation energy in the range 22 to 30 kcal/mole. In contrast to many of the above-mentioned studies in which the palladium was in wire or foil form, Tajbl, Simons and Carberry (1966) studied a 0.5 wt % Pd on α-alumina catalyst. The form of the catalyst does not appear to affect the activation energy greatly.

6.2 Catalyst Physical Data

The palladium metal loading on the γ-alumina support was 0.17 wt % palladium. The surface area of the support (determined by B.E.T.) was 185.5 m^2/g.

6.2.1 Particle Size (d_p)

A sieve analysis conforming to British Standard 1796 was conducted to determine the particle size distribution of the catalyst support, as supplied, and the result is shown in Figure 6.1. The mean (on a weight basis) particle size was found to be 180 μm diameter. (See section 7.3.3).

Three kilograms of catalyst were continuously circulated in the transport reactor for 42 hours. The sieve analysis was repeated on this sample and no significant change in particle size distribution was detected. No measurable loss of particles from the system occurred over this period. Thus it was concluded that particle attrition in the system was negligible.

6.2.2 Particle Density (ρ_s) and Particle Voidage (ε)

The density and voidage of the catalyst particles was determined by the method given in Satterfield (1970):

(i) Add a known weight of carrier to a known weight (and volume) of water in a measuring cylinder. (Sufficient water to cover carrier).

PARTICLE SIZE DISTRIBUTION

FIGURE 6.1

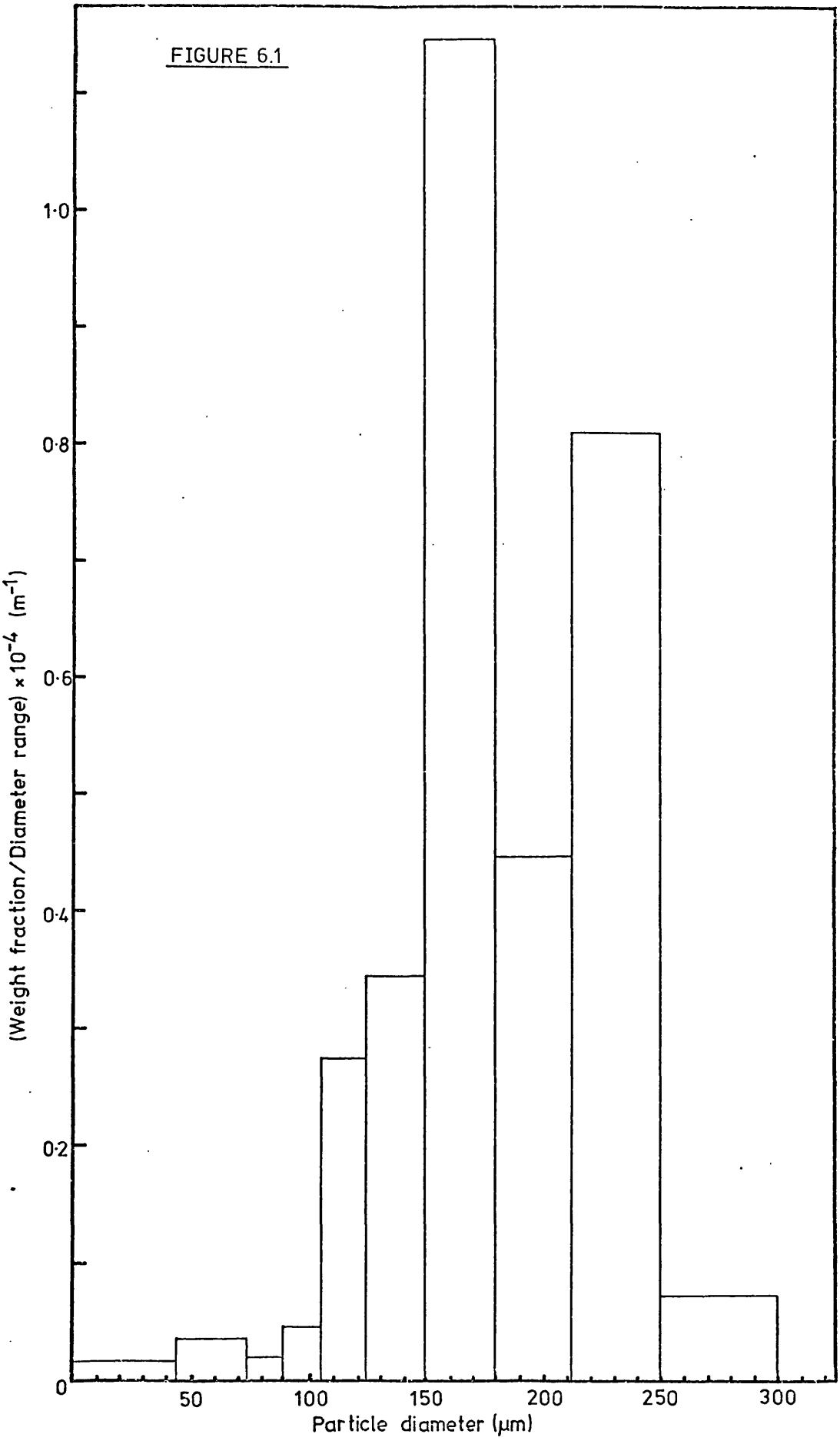

(ii) Note initial and final volumes of water - hence the volume of the particle material (excluding pores) may be calculated.

(iii) Filter the catalyst and dry the outside surfaces of the particles carefully with filter paper.

(iv) Weigh the dried particles - hence the weight of water in the pores and so the pore volume may be found.

(v) The volume of water outside the pores may be found by subtraction of the weight of absorbed water from the total weight of water. Thus the volume of the particles may be found by subtraction of volume of water outside the pores from the total volume of particles plus water.

(vi) Division of the pore volume by the particle volume gives the particle voidage.

(vii) Division of the weight of the carrier by the particle volume gives the particle density.

(viii) Division of the weight of the carrier by the material volume gives the density of the particle material.

The following results have been obtained:

Particle Voidage (ε)	=	0.46	) pore volume = 0.28 cc/g
Particle Density (ρ_s)	=	1.66×10^3 kg/m^3	) cf B.E.T. result → 0.31 cc/g
Material Density	=	3.08×10^3 kg/m^3	

6.2.3 Effective Diffusivity and Effective Thermal Conductivity

These were estimated to be 10^{-6} m^2/s and 0.22 W/m°K respectively by comparison with values for similar supports and reaction systems given by Satterfield (1970).

6.3 Kinetic Data

6.3.1 Experimental

The equipment used for the kinetic data determinations has been described in section 5.2.

Samples of pure catalyst and of catalyst diluted with carrier by ten and one hundred times (to allow measurement of activity over a wide temperature range) were dried in an oven at 120°C to remove adsorbed water. A weighed sample was placed in the reactor and the bed length was measured. By varying the flowrates of the carbon monoxide mixture and the air, the composition of the gases entering the reactor was varied between 0.3 and 0.9% by volume of carbon monoxide. Oxygen to carbon monoxide concentration ratios of 5 to 60 were obtained by the same means. The total gas flowrate entering the reactor was varied between 400 and 600 cc/min. (R.T.P.) and the reactor temperature was in the range 172 to 207°C.

The system was allowed to reach steady state by allowing one hour before measurements were made, after any change in furnace temperature. The gas chromatograph was calibrated using standard 1% and 5% mixtures of carbon monoxide in nitrogen and the sample size was checked by measurement of the nitrogen peak area.

A blank run using pure carrier showed that the carrier itself had no catalytic activity.

6.3.2 Analysis of Results

A mass balance on carbon monoxide for an element of the reactor gives:

$$\frac{d\{[CO]q\}}{dV} = -(1-\alpha_f)\, k_{CO}\frac{[O_2]}{[CO]} \qquad 6.2$$

Or, rearranging:

$$\int_{IN}^{OUT} \{[CO]q\}d\{[CO]q\} = -\int_{0}^{V_B} (1-\alpha_f)\, k_{CO}[O_2]q\, dV \qquad 6.3$$

This expression may be integrated analytically if the following assumptions are made:

(i) The reactor is isothermal, i.e. k_{CO} is constant.

(ii) Either the conversion of carbon monoxide is small or a large excess of oxygen is present, i.e. the molar flowrate of oxygen, $[O_2]q$ may be considered constant.

Making these assumptions and integrating:

$$1 - (1-y_{ex})^2 = \frac{2(1-\alpha_f)\, k_{CO}[O_2]_{in}\, V_B}{q_{in}\, [CO]_{in}^2} \qquad 6.4$$

where y_{ex} is the fractional conversion of carbon monoxide:

$$y_{ex} = 1 - \frac{[CO]_{ex}\, q_{ex}}{[CO]_{in}\, q_{in}} \qquad 6.5$$

Thus a plot of $(1-y_{ex})^2$ vs $\frac{2(1-\alpha_f)\ [O_2]_{in}\ V_B}{q_{in}\ [CO]_{in}^2}$ should give a straight line of slope - k_{CO}.

Figure 6.2 shows this plot of the data obtained. Figure 6.3 is a graph of $\ln(k_{CO})$ vs 1/T used to determine the activation energy of the reaction.

Straight lines have been fitted to the data by the method of least squares. It may be seen that the catalyst therefore obeys the following rate law:-

$$S = k_{CO} \frac{[O_2]}{[CO]} \qquad 6.6$$

where k_{CO} is given by:-

$$k = 6.03 \times 10^8 \exp\left[\frac{-31,439}{\mathcal{R}T}\right] \text{ moles/s. (cc catalyst)} \qquad 6.7$$

$\mathcal{R}$ is the gas constant; $\mathcal{R}$ = 1.98 cals/mole°K.

6.3.3 Discussion

In the preceding analysis several factors have been ignored or neglected; the most important of these are considered here.

CATALYST KINETIC DATA

FIGURE 6.2

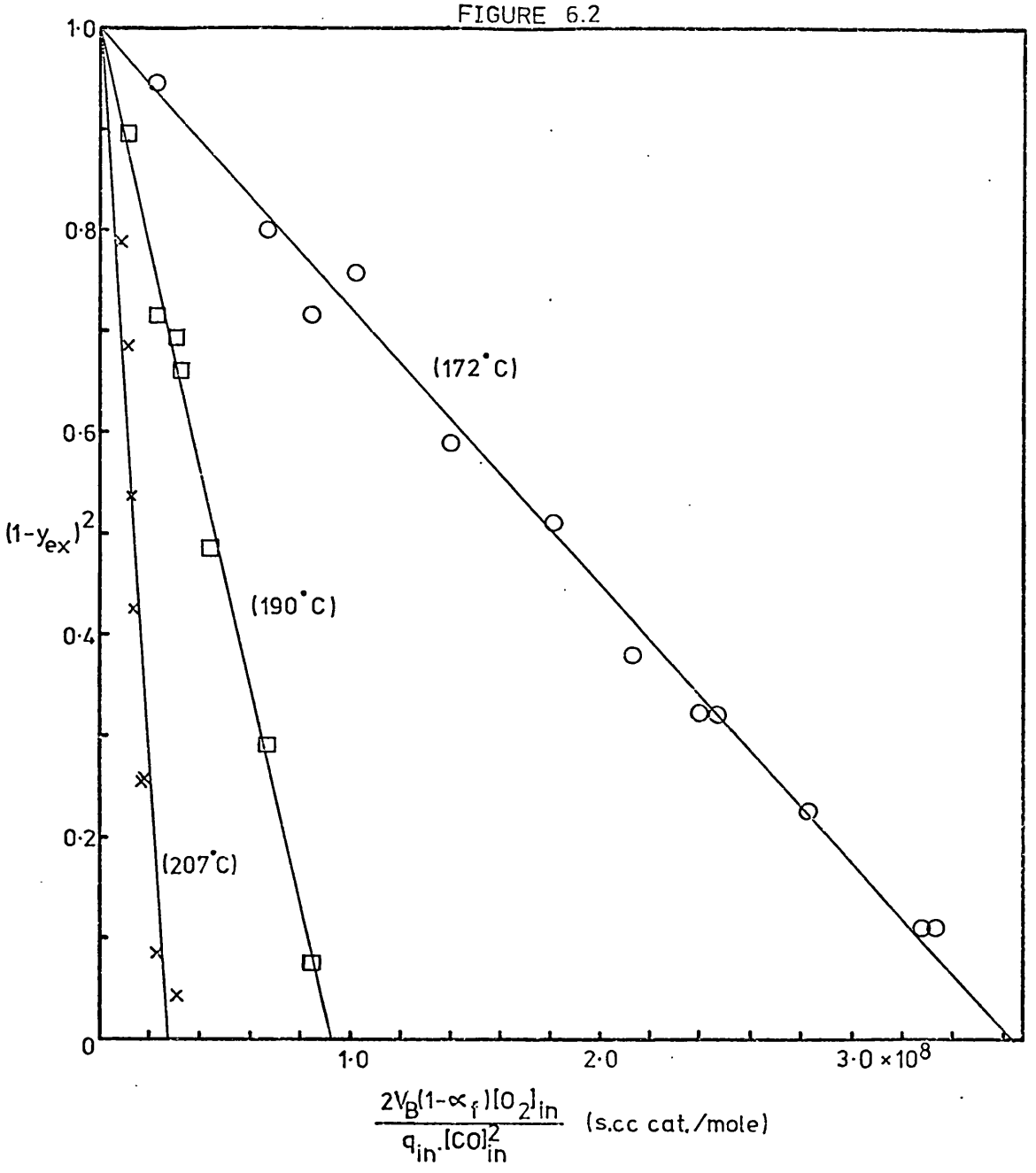

FIGURE 6.3

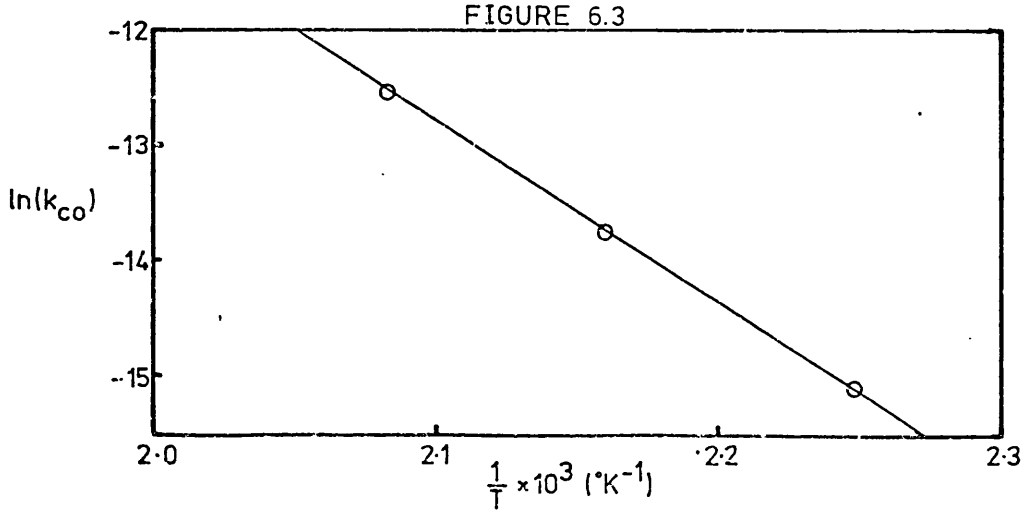

6.3.3.1 Validity of Assumptions

(i) Isothermality of Reactor

The maximum adiabatic temperature rise along the catalyst bed for 100% conversion of 1% by volume of carbon monoxide may be calculated using:

$$C_{pg}.m_f.\Delta T_B = 0.01\ m_f\ (-\Delta H_{CO}) \qquad 6.8$$

$$\therefore \quad \Delta T_B = \frac{0.01 \times 67 \times 10^3 \times 4.19}{1.01 \times 29} = 96°K$$

Generally, a smaller temperature rise is to be expected than the 96°K predicted above since the highest conversions of carbon monoxide which were obtained (about 80%) were for smaller concentrations of carbon monoxide (0.7%). Higher concentrations of carbon monoxide gave smaller conversions due to the form of the rate law and thus under the conditions of the investigation a maximum adiabatic temperature rise of 54°K may be calculated.

The real temperature rise will be less than the adiabatic value as heat losses occur through the reactor walls, however, poor radial transfer of heat will reduce these losses to some extent. (See section 6.3.3.3).

Nevertheless a substantial rise in temperature can occur across the catalyst bed and will lead to over-estimation of the rate constant and activation energy for the reaction.

(ii) Excess Oxygen or Small Carbon Monoxide Conversion

These assumptions were generally good due to the form of the rate law. Thus for high reaction rates and high conversions high oxygen to carbon monoxide ratios (giving an excess of oxygen) were required. When an excess of oxygen was not present only a small amount of carbon monoxide was oxidized. For the range of variables used a maximum error of about 2% was to be expected in making the above assumption.

(iii) Range of Validity

Strictly, the range of validity of equations 6.6 and 6.7 is 172°C to 207°C, the range of temperatures over which measurements were made, and the equations may not necessarily apply at the much higher temperatures (about 350°C) used in the transport reactor (chapter 7).

Determination of kinetic data at temperatures higher than 207°C proved impossible using the equipment described. Further elevation of the reaction temperature led to reaction rates so high that complete conversion was obtained in the reactor. For the measurements at 207°C the catalyst was diluted by one hundred times with pure carrier, but further dilution to a 0.1% mixture proved unsatisfactory for giving accurate and reproducible results. Decreasing the catalyst bed length was unsatisfactory for the same reason and increase of the gas flowrate through the reactor was prevented by excessive pressure drop.

6.3.3.2 Particle Effectiveness Factors

An estimate of the catalyst utilization may be obtained from an examination of the value of ϕ_{CO}, the Thiele Modulus for the carbon monoxide oxidation reaction.

$$\phi_{CO} = R \sqrt{\frac{k_{CO}\,[O_2]}{D_{eff}\,[CO]^2}} \qquad 6.9$$

At the reactor entrance a maximum value of ϕ_{CO}^2 (for 207°C) may be calculated:

$$\phi_{CO}^2 = \frac{(1.8 \times 10^{-4})^2 \times 3.6 \times 13}{4 \times 10^{-6} \times 0.2} = 1.9$$

It should be noted that ϕ_{CO} is a function of the length of the reactor and so a value of ϕ_{CO}^2 of 2 at the reactor entrance may become as large as 50 (for 80% conversion of CO) at the reactor exit.

For the rate law found in this system, the effect of a high value of the Thiele Modulus is to make the particle effectiveness factor very much larger than one, rather than to diminish it as for positive order rate laws. For the rate law of equation 6.6 no mathematical solution for the effectiveness factor is possible for values of ϕ_{CO} greater than about 0.8 (Aris, 1975). This point is discussed further below (section 6.3.3.5).

Another check on effectiveness factors is an examination of the apparent activation energy of the catalyst. For positive order reactions intra particle diffusional limitations cause reduction of

the apparent activation energy to half its true value (i.e. for complete diffusional control).

The calculated value of the activation energy of 31.4 kcal/mole is somewhat higher than typical values of 22-30 kcal/mole reported in the literature, but not excessively so.

Thus for high reaction rates and/or high conversions, the calculated reaction rates, and thus the rate constant and activation energy, may be somewhat high.

6.3.3.3 Axial and Radial Dispersion

These effects are described by axial and radial Peclét numbers, Pe_{ax} and Pe_{rad}.

For the conditions used in the kinetic measurements, the Reynolds number was of the order 2 to 3. Thus the values of Pe_{ax} and Pe_{rad} could be estimated to be 2 and 8 respectively by means of the charts given by Petersen (1965).

(i) Axial Dispersion

Axial dispersion may be estimated by use of a dispersion number N_{dis} which may be written as:

$$N_{dis} = \frac{u\, L_B}{2\, E_{ax}} = \frac{Pe_{ax}\, L_B}{2\, d_p} \qquad 6.10$$

but $Pe_{ax} \simeq 2$, so $N_{dis} \simeq L_B/d_p$ 6.11

Now N_{dis} is the ratio of convective transport to diffussive transport and dispersion can be considered to arise from N_{dis} mixing voids in series. For $N_{dis} > 8$ the system approximates to plug flow.

$$d_p = 180\ \mu m\ ; \quad L_B > 0.01\ m$$

$$\therefore\ N_{dis} > 55$$

Thus axial diffusion may safely be neglected.

(ii) Radial Dispersion

In the same way that the small size of the particles relative to the bed length reduced axial dispersion, radial dispersion will also be reduced. The small radial diffusivity of both reactant and heat can lead to non-uniformity of radial concentration and temperature profiles. This is a possible source of error in the kinetic determinations but will only be important if non-isothermal conditions occur in the catalyst bed (section 6.3.3.1 (i)).

The effects of axial and radial dispersion have been examined experimentally by variation of the ratio of the catalyst bed length to its diameter using two reactors of different diameters (9 mm and 25 mm I.D.). No effects of dispersion could be detected for bed length to diameter ratios of 0.5 to 8.

6.3.3.4 Film Mass Transfer and Film Heat Transfer

For Reynolds numbers of less than 3 as were used in the kinetic determinations the particle Sherwood and Nusselt numbers are

close to the limiting value for an isolated particle of 2. (Satterfield, 1970).

$$\text{i.e.} \qquad Sh = 2 \; ; \qquad Nu_p = 2$$

(i) Mass Transfer

Assuming an effectiveness factor of one, a mass balance at the particle surface leads to the following expression for the fractional drop in reactant concentration across the particle film at the reactor entrance:

$$\frac{(c - c_s)}{c} = \frac{k_{CO}}{c} \frac{[O_2]_{in}}{[CO]_{in}} \frac{d_p^2}{6 \; Sh \; D_{12}} \qquad 6.12$$

Thus for the maximum reaction rate (at 207°C):

$$\frac{(c - c_s)}{c} = \frac{3.6 \times 13 \times (1.8 \times 10^{-4})^2}{0.2 \times 6 \times 2 \times 4.7 \times 10^{-5}} = 0.013 \text{ or } \underline{1.3\%}$$

(ii) Heat Transfer

By a heat balance at the particle surface the following expression relating film temperature drop to film concentration drop may be obtained:

$$k_f (c - c_s) (-\Delta H_{CO}) = h_p (T_g - T_s) \qquad 6.13$$

Thus

$$T_g - T_s = \frac{Sh \; D_{12} \; (-\Delta H_{CO})}{Nu_p \; \kappa_g} \left[\frac{(c - c_s)}{c}\right] c \qquad 6.14$$

$$T_g - T_s = \frac{2 \times 4.7 \times 10^{-5} \times 67 \times 10^3 \times 4.19 \times 0.013 \times 0.2}{2 \times 3.5 \times 10^{-2}} = \underline{0.98°K}$$

A maximum film concentration drop of about 1.3% and a maximum film temperature rise of about 1°K will occur at the reactor entrance. As discussed in section 6.3.3.2 the reaction rate towards the reactor exit increases as the carbon monoxide concentration decreases so the above figures may be up to 25 times larger for the film concentration drop and 5 times larger for the temperature drop (calculated for an 80% conversion). For the majority of the results obtained, however, film heat and mass transfer resistance can be neglected.

Variation of the total gas flowrate through the reactor can enable film heat and mass transfer resistance to be detected since the transfer coefficients are functions of the Reynolds number. For the range of flowrates considered, however, giving Reynolds numbers of up to 3 the particle Sherwood and Nusselt numbers do not differ substantially from their limiting value of 2.

Thus as expected no film resistance effects were detected in the experimental work. Higher values of the Reynolds number could not be attained without incurring excessive pressure drop.

6.3.3.5 Rate Law

(i) Reaction Order with respect to Oxygen Concentration

The use of excess oxygen in the kinetic determinations allowed the order of the reaction with respect to carbon monoxide concentration to be determined. In order to determine the dependence of reaction rate on oxygen concentration, an excess of carbon monoxide was required. This investigation was not performed since the conditions used in the

transport reactor involved excess oxygen (i.e. about 1% CO in air). By using either a 1% or a 5% CO/N_2 mixture though, the same carbon monoxide concentration could be achieved for two different oxygen concentrations. For this limited variation the rate law equation 6.6 appeared to hold within the limits of experimental error. Numerical integration of equation 6.2 was necessary here since the oxygen was no longer in large excess.

(ii) Langmuir-Hinshelwood Rate Equation

The rate law equation 6.6, although easy to fit experimental data to, is inaccurate. This must be so, for it predicts infinite reaction rate at zero carbon monoxide concentration. This causes considerable difficulty mathematically as a singularity occurs at zero concentration. Aris (1975) shows that, for values of the Thiele Modulus greater than 0.765 for a slab, no solution for the effectiveness factor exists.

A more accurate rate law and one which avoids the mathematical difficulties is one of the Langmuir-Hinshelwood forms obtained by Baddour, Modell and Heuser (1968) and may be written:

$$S = \frac{k^1 [CO][O_2]}{(1 + K[CO])^2} \qquad 6.15$$

(The other Langmuir-Hinshelwood form quoted in the above reference does not overcome the problem of the singularity).

Whilst equation 6.15 is convenient to use mathematically, it involves the experimental determination of two independent constants.

(Nb $k^1/K^2 = k_{CO}$ of equation 6.6). The determination of K independent of k^1 could not be achieved with the apparatus used. Equation 6.15 reduces to equation 6.6 at high carbon monoxide concentration, i.e. $K[CO] >> 1$. In fact a concentration of carbon monoxide low enough to make $K[CO] < 1$, and thus to allow independent determination of the two constants, could not be measured with the equipment used.

The only solution to this problem appears to be an assumption of a value for K equal to the minimum value consistent with the experimental results (in order to simplify any numerical analysis) and calculation of k^1 from:

$$k^1 = k_{CO} \times K^2 \qquad 6.16$$

$K = 500\ m^3/mole$ gives $K[CO] \simeq 1$ for [CO] = 0.01% by volume; the smallest measurable concentration.

6.3.3.6 Conclusions

(i) Non-isothermal conditions in the reactor and high effectiveness factors may have caused over-estimation of the rate constant and activation energy especially at high conversions of reactant.

(ii) The rate law and rate constant defined by equations 6.6 and 6.7 may not be valid at 350°C.

(iii) For mathematical evaluations a Langmuir-Hinshelwood form of the rate law is necessary (equation 6.15).

7. EXPERIMENTAL EVALUATION OF THE TRANSPORT REACTOR

7.1 Introduction

The aims of the experimental investigation were:

(i) To construct and commission an experimental system which could be used for evaluating the dependence of the performance of the transport reactor on the operating variables.

(ii) To find a reaction system and catalyst, suitable for use in the laboratory reactor, which provided reliable and easily measured results.

(iii) To design and produce a sampling system which could be used for the measurement of axial and radial concentration profiles within the reactor.

(iv) To use the sampling system to determine the efficiency of the reactant injector and the consequences of an inefficient injector.

(v) To test the validity of the theoretical models of the reactor performance developed in Chapter 4.

(vi) To use the experimental results obtained to simplify (or to elaborate) the theoretical models.

7.2 Preliminary Investigations

7.2.1 Catalytic Activity of the Reactor Walls

After calibration of the Gas Chromatograph with standard carbon monoxide and nitrogen mixtures as described in Chapter 6, the stainless steel tubing used for the transport reactor was tested for any catalytic

action by two methods. Firstly, tests were performed in the transport reactor under similar conditions to those used in later studies with catalyst, but with carrier rather than catalyst flowing. No reaction was detected, (see Figures 7.2, 7.3 and 7.10). Secondly, pieces of 1/8 in. tubing made of the same steel as the reactor were placed in the tubular reactor used in Chapter 6. No reaction was detected for temperatures in excess of the 350°C used in the transport reactor and for residence times over 100 times greater than those found in the transport reactor. Thus it was concluded that no catalytic action was produced by the stainless steel reactor walls or sampling lines.

7.2.2 Sampling System

7.2.2.1 Volume of Sample Lines

To ensure correct sampling it was necessary to determine the residence time of the sampled gases in the sample lines between the reactor and the gas chromatograph. Under the conditions used for later reaction studies but with carrier instead of catalyst flowing, carbon monoxide was injected into the reactor by opening a cock and a stopwatch started. Gases were withdrawn continually through the sample probe most distant from the gas chromatograph (Probe 1) and the sampling rate was measured with a soap bubble flowmeter. After a measured time the sample valve on the gas chromatograph was turned and the carbon monoxide concentration measured. By repeating this procedure, at different times, the time of appearance of the carbon monoxide at the chromatograph was found. After making an allowance for the residence time of the carbon monoxide in the transport reactor, the volume of the sample line was calculated.

The volume of sample line 1 was 19.6 ccs giving a residence time of 3.9 seconds at a sampling rate of 5 cc/sec.

Thus the maximum delay required between selecting a probe by opening the appropriate valve, and operating the chromatograph sample valve was 4 seconds.

7.2.2.2 Effect of Sampling Rate

The effect of the rate of sampling on the measured CO concentration was investigated before catalyst was added to the system and it was found to have no influence on the accuracy of the concentration measurement. However, when the system was tested under reaction conditions with flowing catalyst, anomalous results were noted at low sampling rates and so the investigation was repeated. Figure 7.1 shows the effect on measured concentration for sampling rates up to 5 cc/s. These results were obtained with Probe 6, its end being positioned against the most distant reactor wall. Clearly a reaction was occurring in the probe or sample line. Since the stainless steel tubing of which the probe and sample line was constructed has been shown to be catalytically inactive, the conclusion was drawn that a layer of fine catalytic particles had become deposited on the walls of the sampling probe (a filter prevented particles from entering the sample lines). This conclusion was confirmed by making measurements with the probe end at the far reactor wall so that about 1 in. of the probe length was at reaction temperature, and with the probe end at the near reactor wall so that only the tip of the probe was at reaction temperature. The results (Table 7.1) show that at the highest sampling

FIGURE 7.1 Effect of Sampling Rate on Measured Concentration

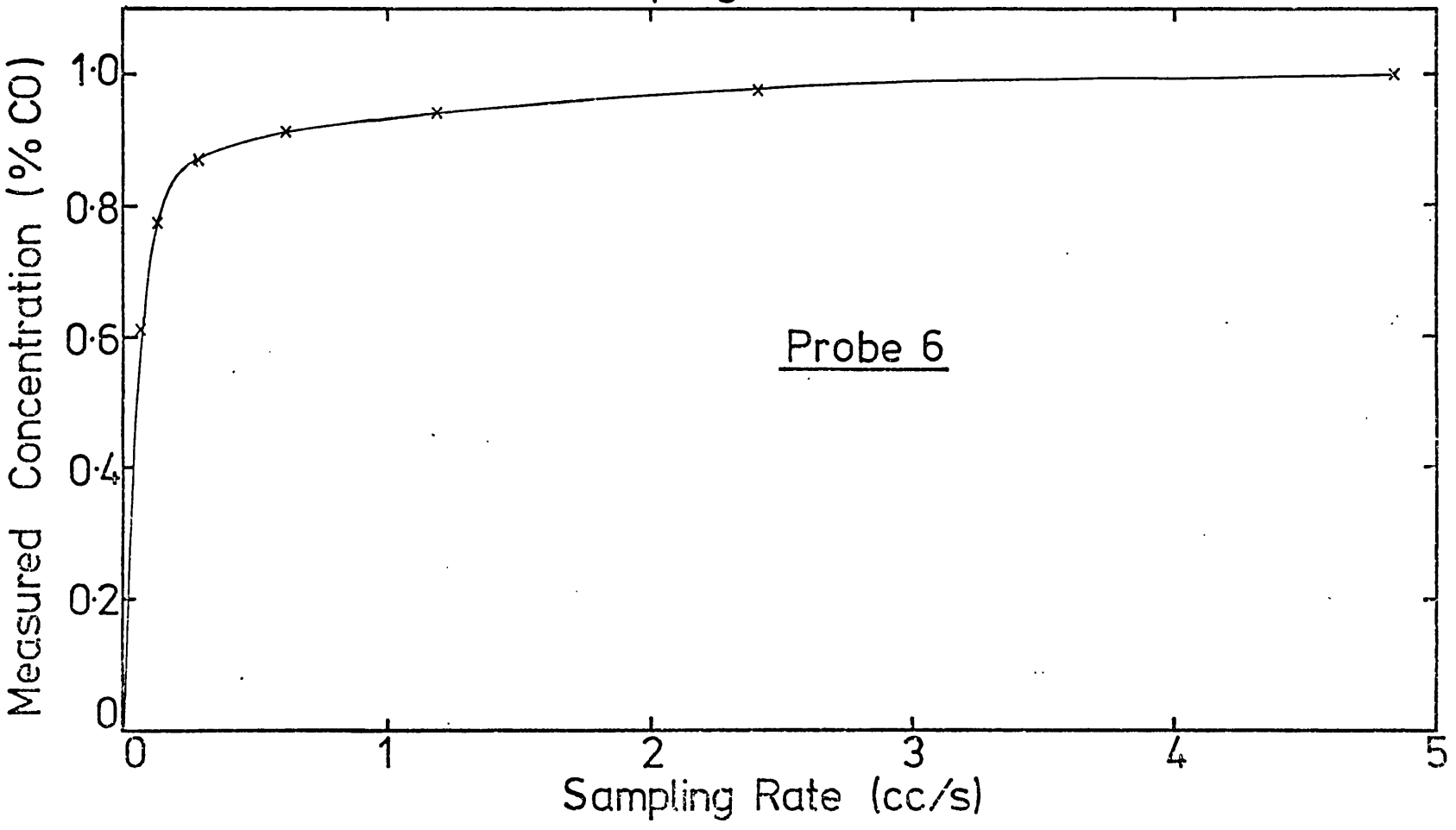

rate, the measured concentration for the two probe positions was identical, whilst for the lowest sampling rate the measured concentration with the probe at the near wall was much higher than that for the probe at the far wall. Thus a fluid mechanical effect (i.e. non-isokinetic sampling conditions) was ruled out.

TABLE 7.1

MEASURED CARBON MONOXIDE CONCENTRATION VS. SAMPLING RATE

Sampling Rate (cc/s)	Measured CO concentration (vol %)	
	Probe at far wall	Probe at near wall
5.17	0.85	0.85
0.076	0.66	0.83

Various means were tried to prevent catalyst adhering to the inner walls of the probes. After thoroughly washing the probes to remove the catalyst fines, (a visible quantity of fines were removed by washing), sampling was attempted at the lowest rate possible without unduly lengthening the residence times of reactant in the lines. After each sample, the direction of flow was reversed and the maximum possible flowrate of air was blown through the probe to remove any particles which might have entered. This process proved ineffective, so the solution adopted was always to sample at the maximum possible rate (in order to minimize reaction in the probe) and to reverse the flow direction after each sample to prevent build-up of fines in the probes.

7.2.3 Reactant Injector

The efficiency of the reactant injector was tested under similar conditions to those later to be used for reaction studies but with carrier flowing instead of catalyst. Figures 7.2 and 7.3 show the radial concentration profiles obtained, whilst Figures 7.4 and 7.5 show the same data plotted to show axial concentration profiles. The profiles have been integrated assuming a 1/7 th power law velocity profile and the resulting mean concentration is shown as a function of the reactor length coordinate in Figure 7.10. For an efficient injector a flat radial concentration profile should be obtained in as short a distance as possible since homogeneous conditions are important in ensuring optimum performance of a reactor. Figure 7.2 shows that an essentially flat profile is obtained after less than 50 cm of reactor length. Although this corresponds to about one quarter of the reactor length, the experimental reactor has a much smaller length to diameter ratio than would be used in practice so the injector used performs reasonably well.

7.2.4 Flow of Solids

Although a fluidizing valve was used for feeding solids to the system, considerable difficulty was experienced in maintaining solids flow at certain times. This problem was identified as being almost entirely due to the effects of static electricity. Although all parts of the system were earthed, charging of the particles occurred and could be detected visually at times, by observing the solids in the hoppers or in the glass sampling jar used to collect the particles at the cyclone base. The particles had the appearance of

FIGURE 7.2 Radial Concentration Profiles - Carrier

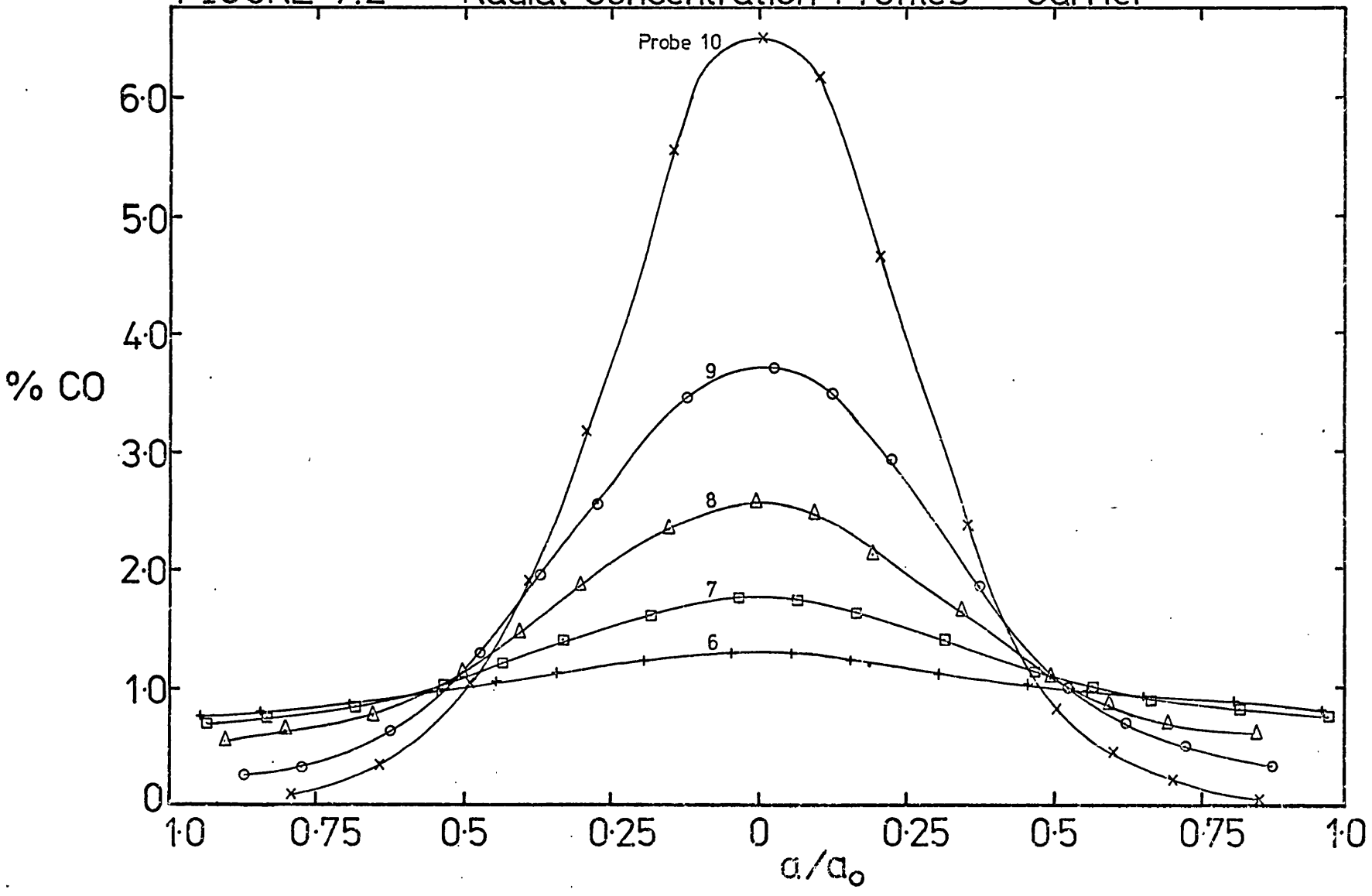

FIGURE 7.3 Radial Concentration Profiles - Carrier

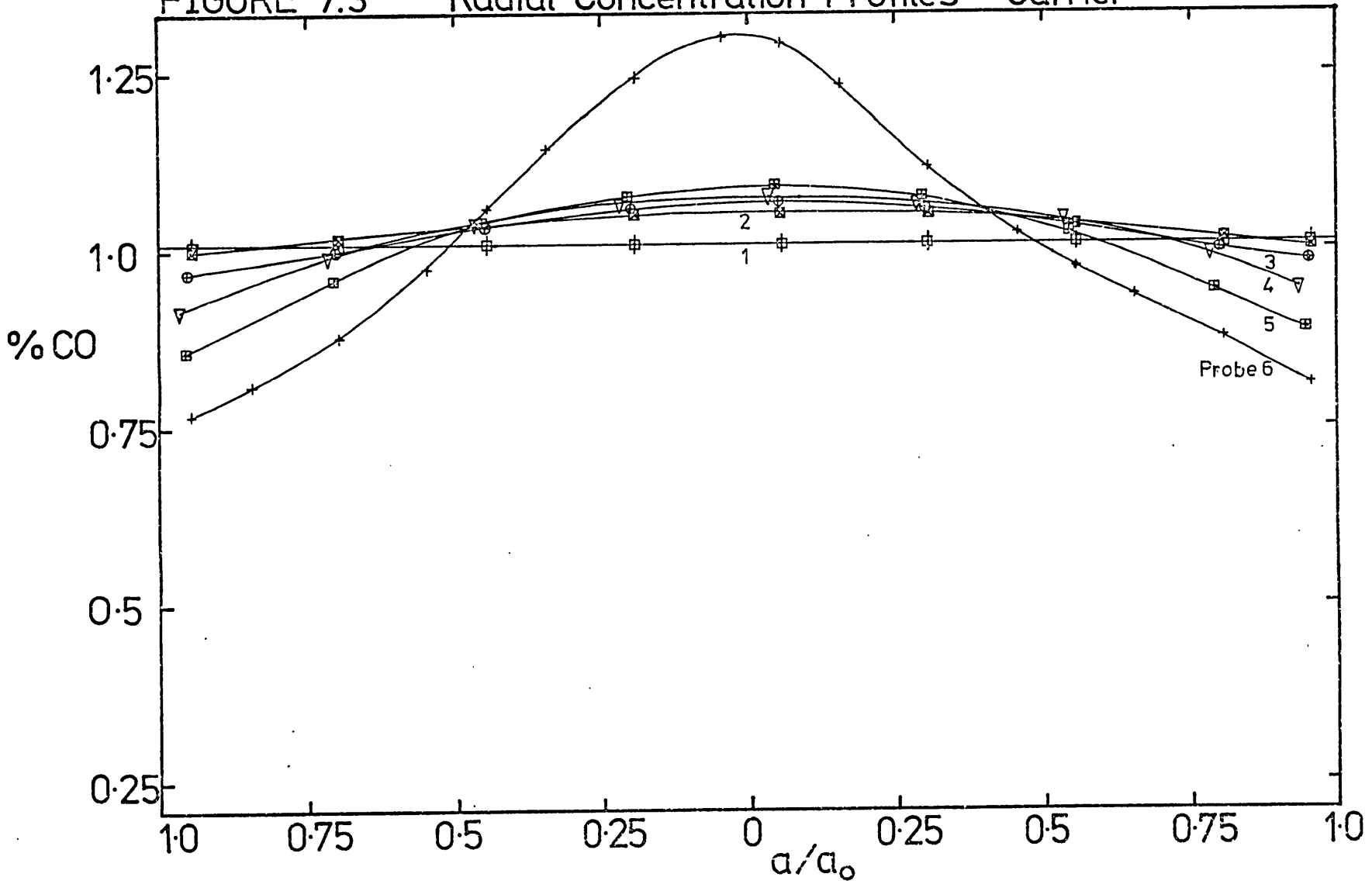

FIGURE 7.4 Axial Concentration Profiles - Carrier

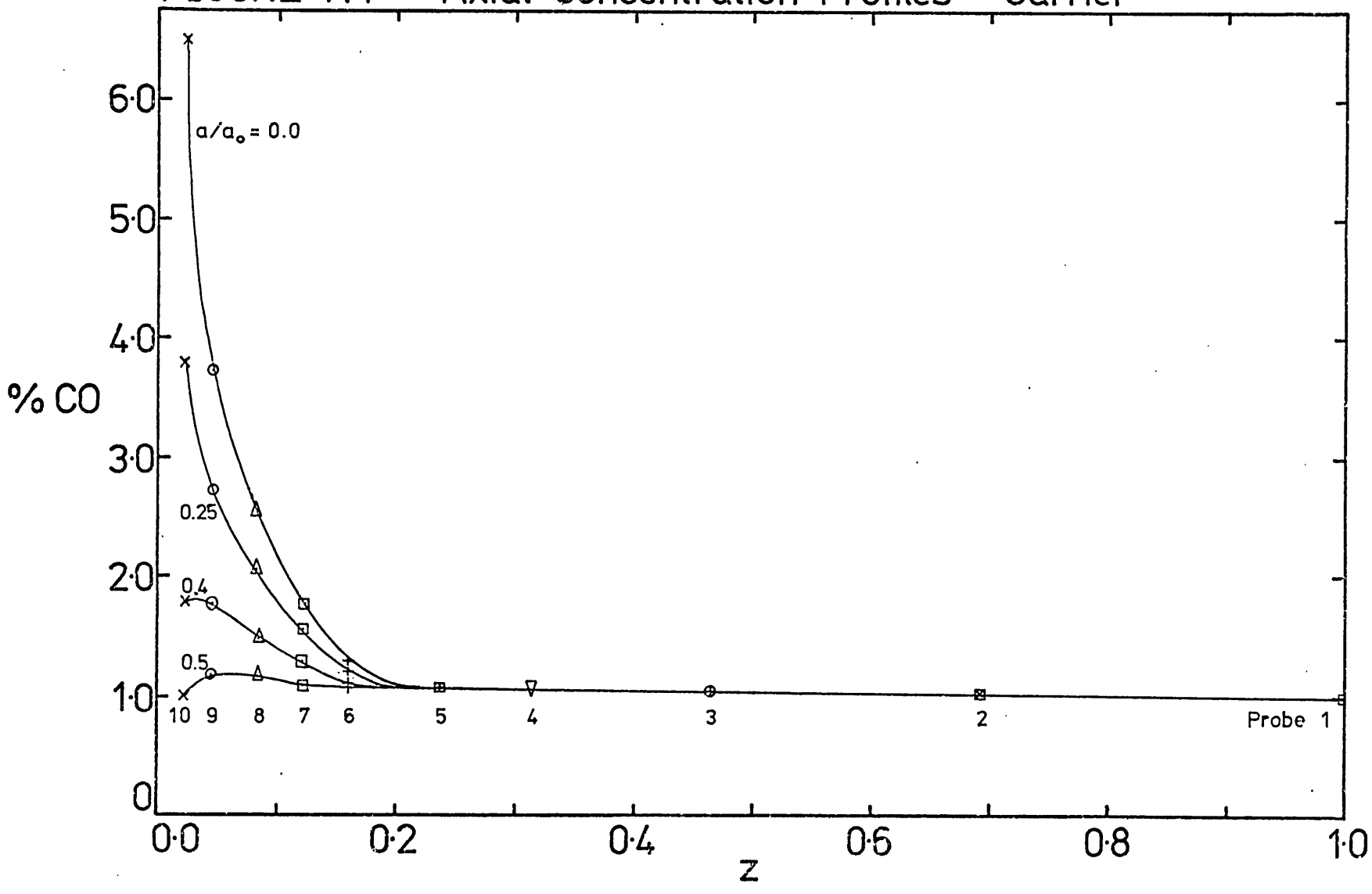

FIGURE 7.5 Axial Concentration Profiles - Carrier

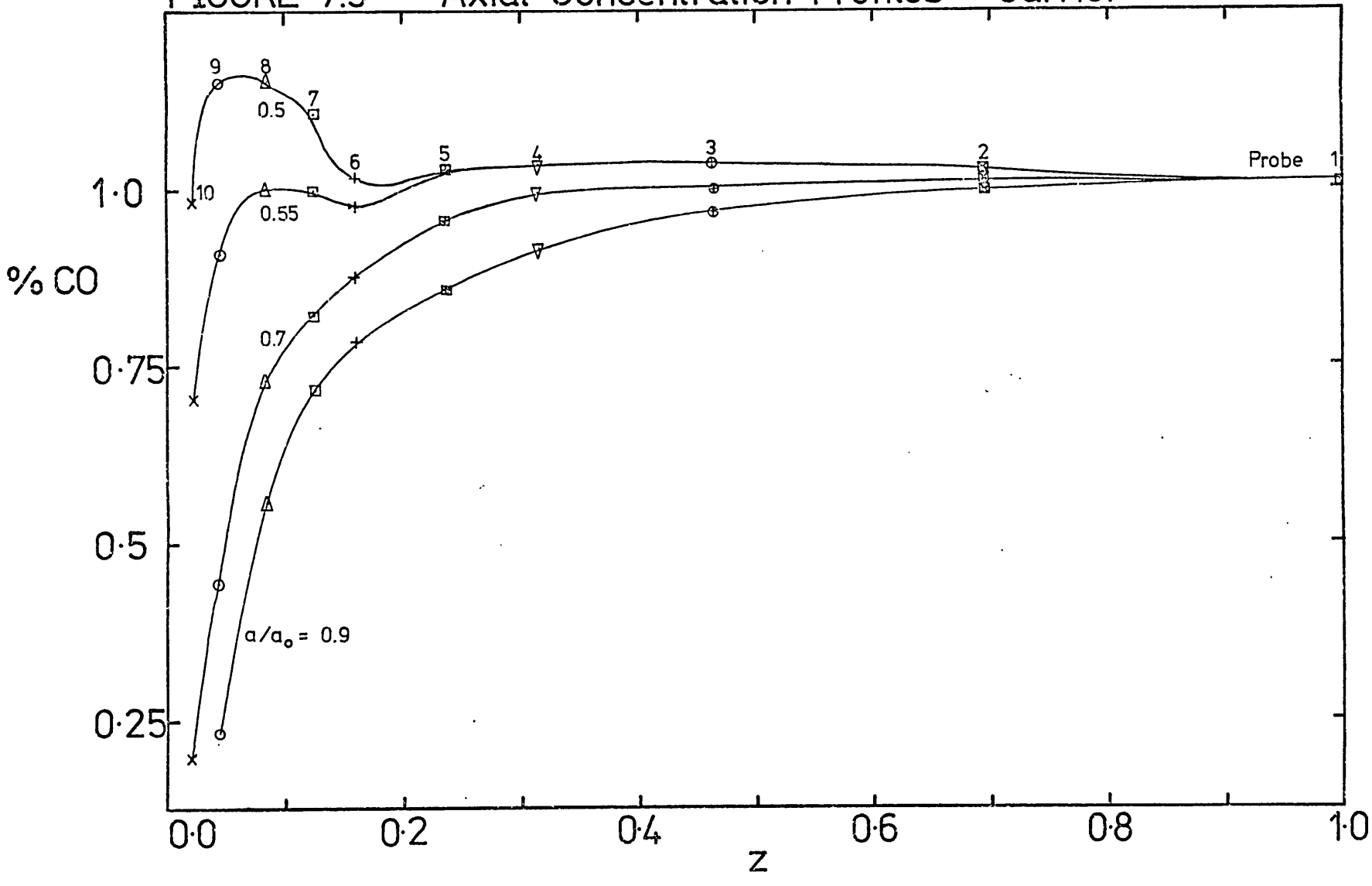

iron filings under the influence of a magnetic field, hanging down in groups for as much as 4 in. below the end of the sampling tube held together by their own electric charges.

These electrostatic effects occurred sporadically and appear to show no simple relationship to the humidity of the air, earthing of the system or the temperature of the system. Attempts to humidify the air stream failed to prevent electrostatic effects. These observations of electrostatic effects may explain the adhesion of catalyst fines to the inside walls of the sampling probes mentioned in section 7.2.2.2.

Difficulties in maintaining solids flow from the lower hopper could be seen to be a result of 'bridging' of particles across the exit from the hopper due to electrostatic charging. This problem was alleviated to some extent by the following actions:-

(i) The solids charge was continuously recirculated and kept at a minimum level, sufficient only to provide enough head of solids for smooth flow.

(ii) The solids returning to the hopper were diverted by a chute to the side of the hopper rather than falling directly above the hopper exit.

(iii) A metal rod about 2 ft. in length was placed in the pipe loading from the hopper and was rested on the upper surface of the solids-feed gate valve. This proved particularly effective and it could be seen that charged particles were attracted towards the rod leaving an apparently uncharged annular region around the rod through which particles could pass unhindered.

Calibrations of pressure drop versus solids flowrate allowed a required solids to gas mass flow ratio to be readily obtained, but because of the problems involved with the flow of solids, measurement of solids flowrate was made periodically during the experimental runs by collecting solids over a known period of time. Monitoring of the pressure drop through the system enabled any change in solids flowrate to be detected immediately.

TABLE 7.2

VALUES OF VARIABLES USED IN THE TRANSPORT REACTOR UNDER REACTION CONDITIONS

(i) Dimensional

(a) Gas Phase

T_{go} = 350°C (= 623°K)

ρ_g = 0.5720 kg/m^3

C_{pg} = 1016 J/kg°K

D_{12} = 7.542 x 10^{-5} m^2/s (CO/Air)

u_g = 18.00 m/s

p = 767.3 mm Hg (= 1.0196 x 10^5 Pa)

μ = 3.116 x 10^{-5} Ns/m^2

κ_g = 4.274 x 10^{-2} W/m°K

C_o = 0.189 moles/m^3

W_g = 5.236 x 10^{-3} kg/s

(b) Solids Phase

ρ_s = 1.66 x 10^3 kg/m^3

C_{ps} = 910 J/kg°K

D_{eff} = 10^{-6} m^2/s (CO/Air)

u_s = 17.42 m/s

d_p = 155 μm (see section 7.3.3)

κ_{eff} = 0.22 W/m°K

W_s = 0.877 x 10^{-3} kg/s

u_{sl} = 0.5783 m/s

(c) Reactor

L = 1.9976 m

d_t = 2.53 x 10^{-2} m

(d) Kinetic Parameters

$k_{\infty CO}$ = 6.03×10^{14} moles/s.(m^3 cat) E = 131.6 kJ/mole

K = 500 m^3/mole ΔH = 280.5 kJ/mole

b = 94.5 = ($K \times C_o$)

(ii) Dimensionless

%(vol) CO = 0.958 %(vol) O_2 = 20.75) All at entrance of reactor

$\frac{[O_2]}{[CO]} = \frac{1}{X} = 21.66$)

ε = 0.46 $(1 - \alpha) = 5.964 \times 10^{-5}$

W_s/W_g = 0.1675

Pr	= 0.7407	Sc	= 0.7223
Re_p	= 1.645	Re_t	= 8360
P_T	= 0.08101	P	= 2.655×10^{-5}
M_T	= 5.149	M	= 41.50
Nu_o	= 28.01(1)	Nu_p	= 2.696(2)
κ_m	= 0.1943	D_m	= 75.42
ϕ_g^2	= 3836	Sh	= 3.193(3)
χ	= -3.868×10^{-4}	G	= 25.41

(1) $Nu_o = 0.023\ Re_t^{0.8}\ Pr^{0.4}$ (Perry, 1973)

(2) $Nu_p = 2.0 + 0.6\ Re_p^{1/2}\ Pr^{1/3}$ (Equation 3.5)

(3) $Sh = 2.0 + 0.25\ (Re_p\ Re_t^{1/2}\ Sc)^{1/3}$ (Equation 3.8)

7.2.5 Ranges of System Variables

(i) Air Velocity

The air flowrate was chosen to be as low as possible in order to achieve the maximum residence time in the reactor and hence maximum conversion, whilst being sufficiently high to provide good heat transfer in the air heater. Operating experience showed that a minimum flowrate of 250 l/min. (R.T.P.) of air was required to prevent melting of the heater elements when the full 4 kW of power was being applied.

(ii) Reaction Temperature

This was chosen to be as high as the system would permit (350°C) in order to achieve sufficient reaction to be measured satisfactorily.

(iii) Solids Flowrate

For maximum reaction the solids flowrate was required to be as high as possible. However, to achieve a high enough temperature for reaction an upper bound of about 0.2 for the solids to gas mass flowrate ratio was found for 250 l/min. of air. The problem in achieving the reaction temperature at higher solids flowrates may be appreciated by considering that only the air stream is heated. Since the specific heat of air and catalyst, per unit mass is about the same, an air temperature of at least 700°C would be required to bring a suspension, with a solids to gas mass flowrate ratio of one, to 350°C.

A listing of the values of the system variables used is given in Table 7.2.

7.3 Theoretical Predictions

7.3.1 Entrance Length and Steady State Type Assumptions

Although equation A 5.24 of Appendix 5 giving the entrance length is valid only for a first order case with a step input of reactant, it may be used to give an order of magnitude estimate for the dimensionless entrance length for other rate expressions. Hence:

$$z_a \simeq \frac{1}{M\phi_g^2} = \frac{1}{41.5 \times 3836} = 6.3 \times 10^{-6} \qquad 7.1$$

Thus it may safely be assumed that even with a reactant injector which does not give a step input of reactant the entrance length in the experimental reactor is very small. Physically, this corresponds to the rapid establishment of a concentration profile in the catalyst particles. For a first order reaction, this means that although the concentrations are changing outside the entrance region, the change is slow enough relative to the rate of diffusion of reactant within the particles, to allow representation by the steady state effectiveness factor. It seems reasonable to assume that for other rate laws the same situation exists, allowing a representation by steady state effectiveness factors, but with one major difference: for non-first order rate laws the steady state effectiveness factor is dependent on the concentration of the reactant at the particle surface. Thus a solution to the reactor equations may be found by making the assumption that, at any point outside the very short entrance region, the reaction rate may be calculated by use of the steady state effectiveness factor calculated using the gas phase concentration of reactant at that point.

Equation A 6.4:

$$\frac{dy}{dz} = -\frac{3PMD_m}{2} Sh(y-y_s) \qquad 7.2$$

may be used to calculate the conversion of reactant if y_s is known. This is considered below in section 7.3.6.

7.3.2 Rate Law, Effectiveness Factors and Film Mass Transfer Resistance

(i) Rate Law

As discussed in section 6.3.3.5(ii), a Langmuir-Hinshelwood form for the rate law is most convenient for analysing experimental results. The rate law 6.15 may be written in a dimensionless form:-

$$\Psi = \frac{Y(1+b)^2}{(1+bY)^2}\left[1 - \frac{X}{2}(1-Y)\right] \qquad 7.3$$

where $b = K[CO]_I = Kc_o$ 7.4

and $X = [CO]_I/[O_2]_I$ 7.5

(ii) Effectiveness Factors and Film Mass Transfer Resistance

The value of the steady-state effectiveness factor in a spherical particle may be calculated numerically for a rate law of the form of equation 7.3. For high values of the Thiele Modulus (ϕ_g) however, an asymptotic solution may be found, (Petersen, 1965).

Petersen shows that for large ϕ_g the asymptotic value of the steady state effectiveness factor becomes:

$$\eta_{gf} = \frac{3}{\Psi_{x=1}\,\phi_g} \left[2\int_0^{y_s} \Psi\,(Y)\,dY \right]^{1/2} \qquad 7.6$$

Substituting equation 7.3 into equation 7.6:

$$\frac{\eta_{gf}\,\Psi_{x=1}\,\phi_g}{3} = \sqrt{2}\,\frac{(1+b)}{b} \left[\frac{-y_s\{1 - \frac{X}{2}(1 - y_s)\}b}{(1 + b\,y_s)} + 2Xy_s + \left(1 - \frac{X}{2} - \frac{2X}{b}\right) \ln\,(1 + by_s) \right]^{1/2} \qquad 7.7$$

Thus the effectiveness factor may be found from equation 7.7 if the value of y_s at that point is known.

Equation A 6.9 may be written:

$$\frac{\eta_{gf}\,\Psi_{x=1}\,\phi_g}{3} = \frac{D_m\,Sh\,(y - y_s)}{2\,\phi_g} \qquad 7.8$$

Thus y_s may be found by iteration from equations 7.7 and 7.8 and hence η_{gf} found from equation 7.7 or 7.8.

Using the values in Table 7.2 for the variables in the above equations, the following are obtained for particles of mean diameter 155 μm at the reactor entrance (y = 1).

$$y_s = 0.1073$$
$$\eta_{gf} = 1.3 \times 10^{-3}$$

More than 99.5 wt % of the particles used in the reactor lie in the diameter range 20 to 300 μm (see Figure 6.1) so the smallest

value of ϕ_g (and hence the largest value of η_{gf}) which will be of practical importance is for the 20 μm particles evaluated at the reactor entrance. Particles much smaller than 20 μm would not be removed from the air stream by the cyclone and so would be lost from the system.

For the 20 μm particles ϕ_g may be calculated to be 7.99 at the reactor entrance under the conditions existing in the reactor. From equations 7.7 and 7.8 (at y = 1):

$$\left.\begin{aligned} y_s &= 0.8263 \\ \eta_{gf} &= 0.56 \end{aligned}\right\} \quad d_p = 20\ \mu m$$

Thus the effectiveness factors in the reactor will always be less than 0.56 since the effectiveness factors decrease along the reactor as the surface concentration of reactant decreases. The film concentration drop will always be significant and is more important as the reaction rate increases (as a result of reactant concentration decrease) along the reactor.

The assumption of an asymptotic value for η_{gf} is valid only at large ϕ_g and the lower limit of validity is usually taken to be that value of ϕ_g which gives $\eta_{gf} = 1$ (Petersen, 1965b). This value is taken here, although an even lower limit of ϕ_g is probably acceptable in this case since values of η_{gf} greater than one are possible for the rate law used here.

(iii) Conclusions

(a) All sizes of particles present in the reactor are in the intra-particle diffusion controlled regime and may be represented by asymptotic values of η_{gf} found from equations 7.7 and 7.8.

(b) Film resistance to mass transfer is important for all particle diameters used and must be allowed for.

7.3.3 Mean Particle Diameter

It has been determined (section 6.2.1) that the mean particle diameter on a weight basis is 180 μm, however, use of this value in calculating the mean value of the Thiele Modulus will lead to errors. A mean effectiveness factor, based on a reaction equivalent Thiele Modulus, has been discussed by Pratt and Wakeham (1975) but that was for a log normal particle size distribution and so is not applicable here.

(i) Intra-Particle Diffusion Control

The total reaction rate in a particle is proportional to R^2 (since the reaction is confined to a narrow surface region).

Dividing the particles into n_t groups of diameter ranges: Total reaction rate is proportional to:-

$$\sum_{n=1}^{n_t} N_n R_n^2 = N_t R_{AV}^2 \qquad 7.9$$

where $$N_t = \sum_{n=1}^{n_t} \frac{N_n R_n^3}{R_{AV}^3} \qquad 7.10$$

but $$W_n \alpha N_n R_n^3 \qquad 7.11$$

$$\therefore \quad R_{AV} = \frac{\sum_{n=1}^{n_t} W_n}{\sum_{n=1}^{n_t} (W_n/R_n)} \qquad 7.12$$

but $$\sum_{n=1}^{n_t} W_n = 1 \qquad 7.13$$

Thus $$R_{AV} = 1/\sum_{n=1}^{n_t} (W_n/R_n) \qquad 7.14$$

Using equation 7.14 on the data of figure 6.1 the reaction mean diameter is calculated to be 166.36 μm.

The above analysis has ignored the effects of film mass transfer resistance and this will now be considered.

(ii) Total Film Mass Transfer Control

This is not encountered in the system under consideration but this, and the case considered above (i.e. no diffusional film resistance) will enable upper and lower bounds to be put on the effective mean particle diameter.

The transfer of reactant to any particle is proportional to $R^2 \times k_f$. Now k_f is approximately proportional to 1/R since $k_f = D_{12}\ Sh/2R$ and the Sherwood number is a very weak function of particle Reynolds number (and hence particle diameter) for the range of particle diameters

present in this system. (Equation 3.8). The rate of disappearance of reactant in a particle is therefore proportional to its radius (R). By similar reasoning to (i) above, the film diffusion mean diameter is given by:-

$$R_{AVfilm} = \sqrt{\frac{n_t}{\sum_{n=1} \frac{1}{(W_n/R_n^2)}}} \qquad 7.15$$

which gives a value of 139.86 μm for the film diffusion mean particle diameter.

In the reactor, the degree of film mass transfer resistance varies both with particle diameter and with the axial position of the particle so that in practice, the effective mean diameter will vary between 139 and 167 μm. Because of the difficulty in allowing for this variation, an intermediate value of 155 μm was taken for the effective mean particle diameter.

7.3.4 Film and Intra-Particle Temperature

The maximum temperature rise within the particles may be calculated using equation A 7.11:

$$\tau_{max} - \tau_s = -\chi y_s \qquad 7.16$$

So for $y_s = 1$

$$T_{max} - T_s = 3.868 \times 10^{-4} \times 623 = \underline{0.24°C}$$

which is negligible.

The film temperature rise may be related to the film concentration drop by combining equations A 6.9 and A 7.18:

$$\text{Since } P \ll 1,\ \eta_{gf} \simeq \eta_g \quad \therefore \quad \frac{[\tau_s-\tau_g]_{max}}{[y-y_s]_{z_m}} = \frac{-\chi\, D_m\, Sh}{(1+P_T)\kappa_m\, Nu_p} \qquad 7.17$$

So using values from Table 7.2:

$$\frac{[\tau_s-\tau_g]_{max}}{[y-y_s]_{z_m}} = \frac{3.868 \times 10^{-4} \times 75.42 \times 3.193}{(1 + 0.081) \times 0.1943 \times 2.696} = 0.1645$$

The value of $[y-y_s]_{z_m}$ is not easily obtained, so the maximum value of $[y-y_s]$ is used, i.e. at the reactor entrance ($y = 1$, $y_s = 0.1073$),

$$\therefore \quad [T_s-T_g]_{max} = (1 - 0.1073) \times 623 \times 0.1645 = \underline{91.48°C}$$

Therefore film temperature rises of up to 92°C may occur in the reactor and this fact must be allowed for in calculations of conversion in the reactor.

7.3.5 Adiabatic Temperature Rise Along Reactor

This may be found by using equation A 7.6, putting $\eta_T = 1$ (since particles are essentially isothermal):

$$P_T\,(\tau_s - 1) + (\tau_g - 1) = \frac{-P_T M_T \chi[(1-y) - \eta_* Py_s]}{PM} \qquad 7.18$$

but P is small so that $\eta_*\, Py_s \ll (1-y)$ and thus

$$P_T\,(\tau_s - 1) + (\tau_g - 1) = \frac{-P_T M_T \chi(1-y)}{PM} \qquad 7.19$$

This equation, together with equation A 7.3 and boundary conditions for τ_s and τ_g, can be solved numerically for τ_s at any point in the reactor if y is known as a function of z. From this, it is apparent that solution of the reactor equations for both temperature and concentration must proceed simultaneously since the equations are coupled. This is considered below.

7.3.6 Solution of Reactor Equation

Sections 7.3.1 to 7.3.5 have resulted in the following assumptions for solution of the reactor equation:

(i) The reactor entrance length is short and the steady-state effectiveness factor may be used.

(ii) The particles are all internally diffusion limited and an asymptotic value of the effectiveness factor may be used.

(iii) Film mass transfer resistances are important and must be considered.

(iv) A mean particle diameter based on reaction rate considerations may be used in calculating conversions.

(v) Particles are isothermal.

(vi) Film heat transfer resistance is important and must be considered.

(vii) The reactor is adiabatic

A version of equation 7.3, modified to allow for the temperature rise along the reactor may be written:

$$\Psi = \frac{Y(1 + b)^2}{(1 + bY)^2} \left[1 - \frac{X}{2}(1-Y)\right] \exp[-G(1 - 1/\bar{\tau})] \qquad 7.20$$

If the above equation is used in equation 7.6 in place of equation 7.3 the result is (cf. equation 7.7):

$$\eta_{gf}\,\Psi_{x=1}\,\phi_g / 3 = \frac{\sqrt{2}(1+b)}{b}\left[\frac{-y_s.\{1-\frac{X}{2}(1-y_s)\}b}{(1+by_s)} + 2Xy_s + \left(1-\frac{X}{2}-\frac{2X}{b}\right)\ln(1+by_s)\right]^{1/2}.\exp[-G(1-1/\bar{\tau})] \qquad 7.21$$

Combining equations 7.8 and 7.21 (with $\bar{\tau} = \tau_s$ since $\eta_T \simeq 1$):

$$D_m\,Sh\,(y-y_s)/2\phi_g = \frac{\sqrt{2}(1+b)}{b}\left[\frac{-y_s.\{1-\frac{X}{2}(1-y_s)\}b}{(1+by_s)} + 2Xy_s\left(1-\frac{X}{2}-\frac{2X}{b}\right)\ln(1+by_s)\right]^{1/2}.\exp[-G(1-1/\tau_s)] \qquad 7.22$$

Writing equations 7.2, 7.19 and A 7.3 respectively:-

$$\frac{dy}{dz} = -\frac{3PMD_m}{2}\,Sh\,(y-y_s) \qquad 7.23$$

$$P_T\,(\tau_s - 1) + (\tau_g - 1) = \frac{-P_T M_T \chi(1-y)}{PM} \qquad 7.24$$

$$\frac{d\tau_g}{dz} = -\frac{3P_T M_T \kappa_m}{2}\,Nu_p\,(\tau_g - \tau_s) \qquad 7.25$$

Assuming that the variation of P, M, D_m, Sh, P_T, M_T, κ_m, Nu_p, χ and G with temperature may be neglected in comparison to the effect of temperature on the reaction rate, equations 7.22 to 7.25 may be integrated numerically using the boundary conditions $y = 1$; $\tau_g = \tau_s = 1$ at $z = 0$.

The calculated axial concentration profiles and gas temperature profiles are shown on Figure 7.10.

7.4 Results and Discussion

The system was allowed one hour to reach a steady state after switching on the heater. During this time the temperature controller was set at the reaction temperature and the solids and gas flowrates were set at the required values. The reactant was only injected when a steady state had been reached and the system was then allowed a further period of 20 minutes to regain equilibrium. Measurement of the solids flowrate was made, under reaction conditions, by collecting samples of about 250 g of catalyst over a measured period of time whilst ensuring that the manometer readings remained steady. Any adjustment of the solids flowrate required that the air flowrate was brought back to its original value. Measurements of concentration were made all at 10 axial positions and at 16 radial positions across the whole diameter of the reactor. Measurements under reaction conditions were made for the same values of variables as were used for the dispersion study.

Figures 7.6 and 7.7 show the radial reactant concentration profiles for probes 1 to 10 for flowing catalyst under the conditions given by Table 7.2. Figures 7.8 and 7.9 show the radial concentration of reactant for probes 1 to 10 when no solids were flowing under conditions otherwise identical to those in Table 7.2. These figures may be compared with those for the case of no reaction, i.e. with carrier flowing, again under the conditions given by Table 7.2 (Figures 7.2 to 7.5). Figure 7.10 shows the axial variation of the reactor wall temperature for the three cases detailed above.

In obtaining the radial mean concentration, a 1/7th power velocity profile (section 3.2.2.2) has been assumed in order to

FIGURE 7.6 Radial Concentration Profiles - Catalyst

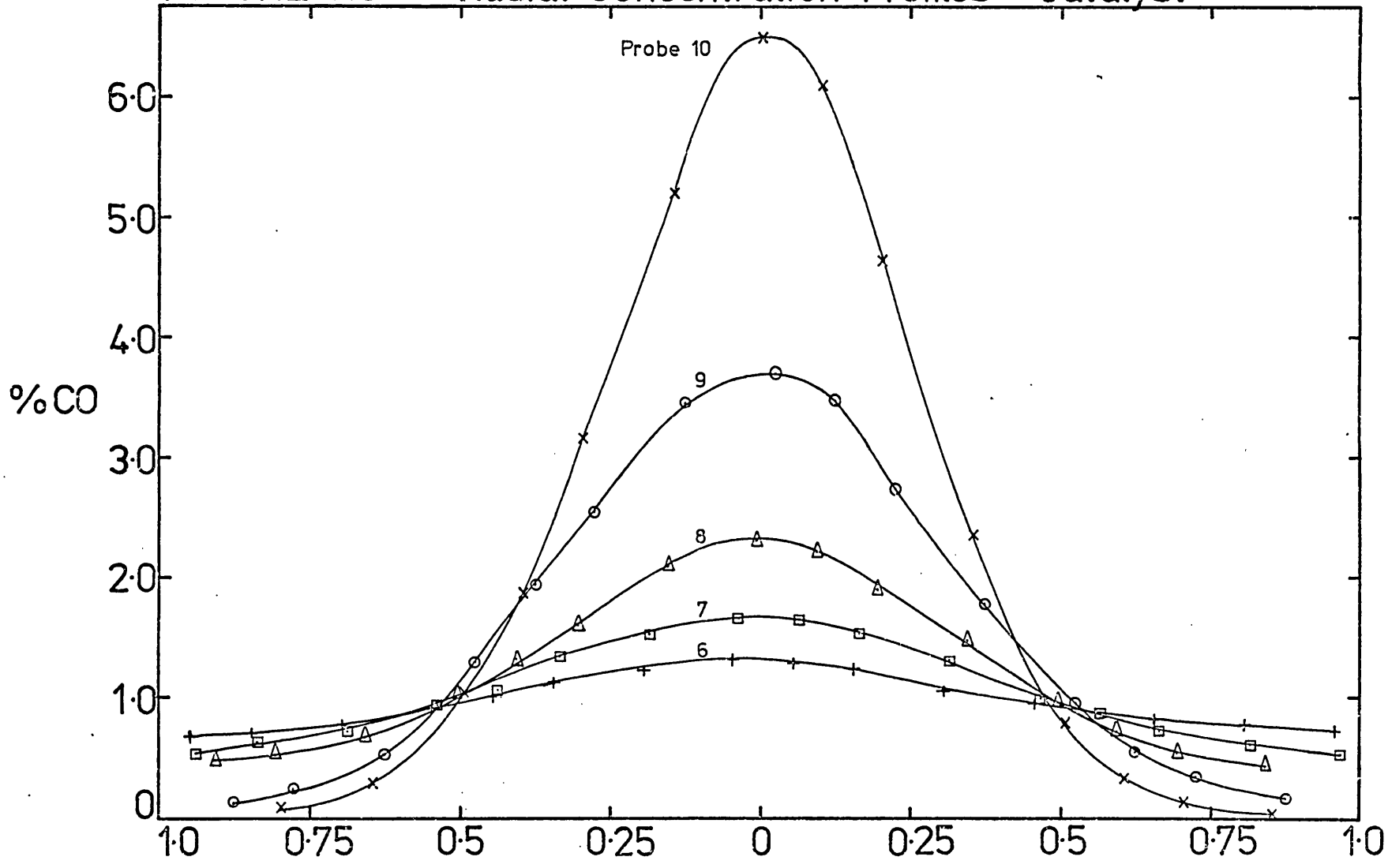

FIGURE 7.7 Radial Concentration Profiles - Catalyst

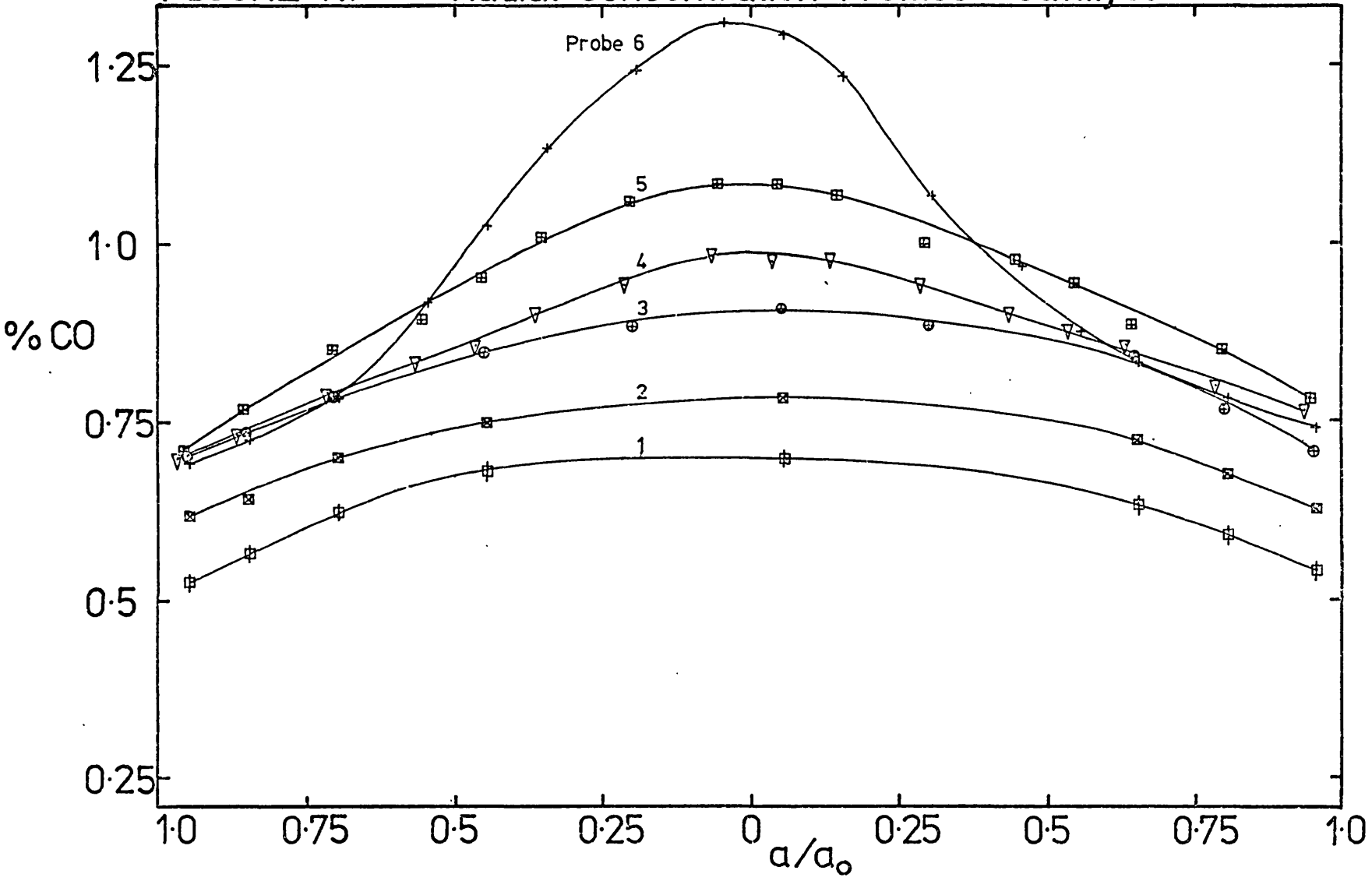

FIGURE 7.8 Radial Concentration Profiles - No Solids

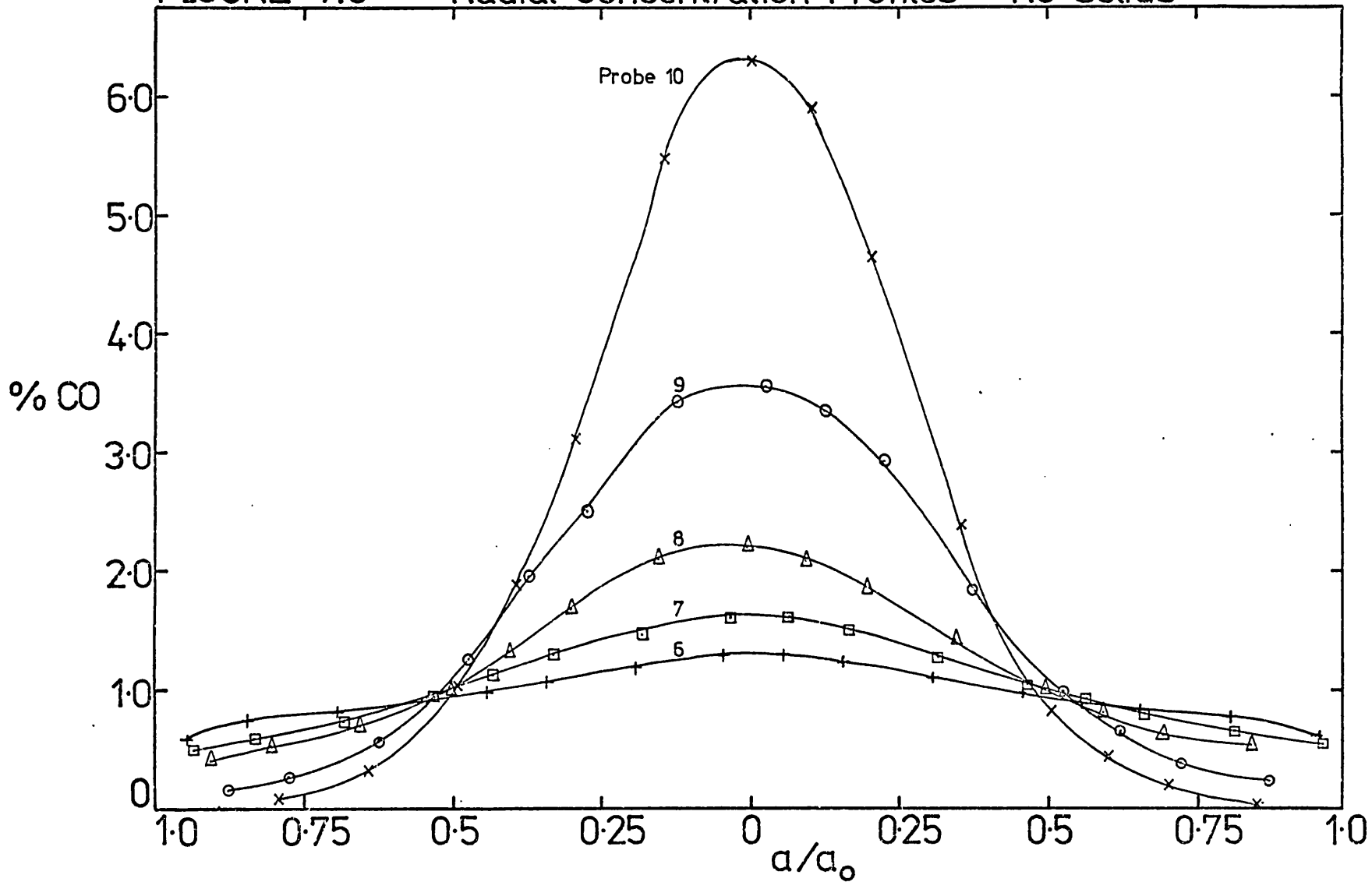

FIGURE 7.9 Radial Concentration Profiles - No Solids

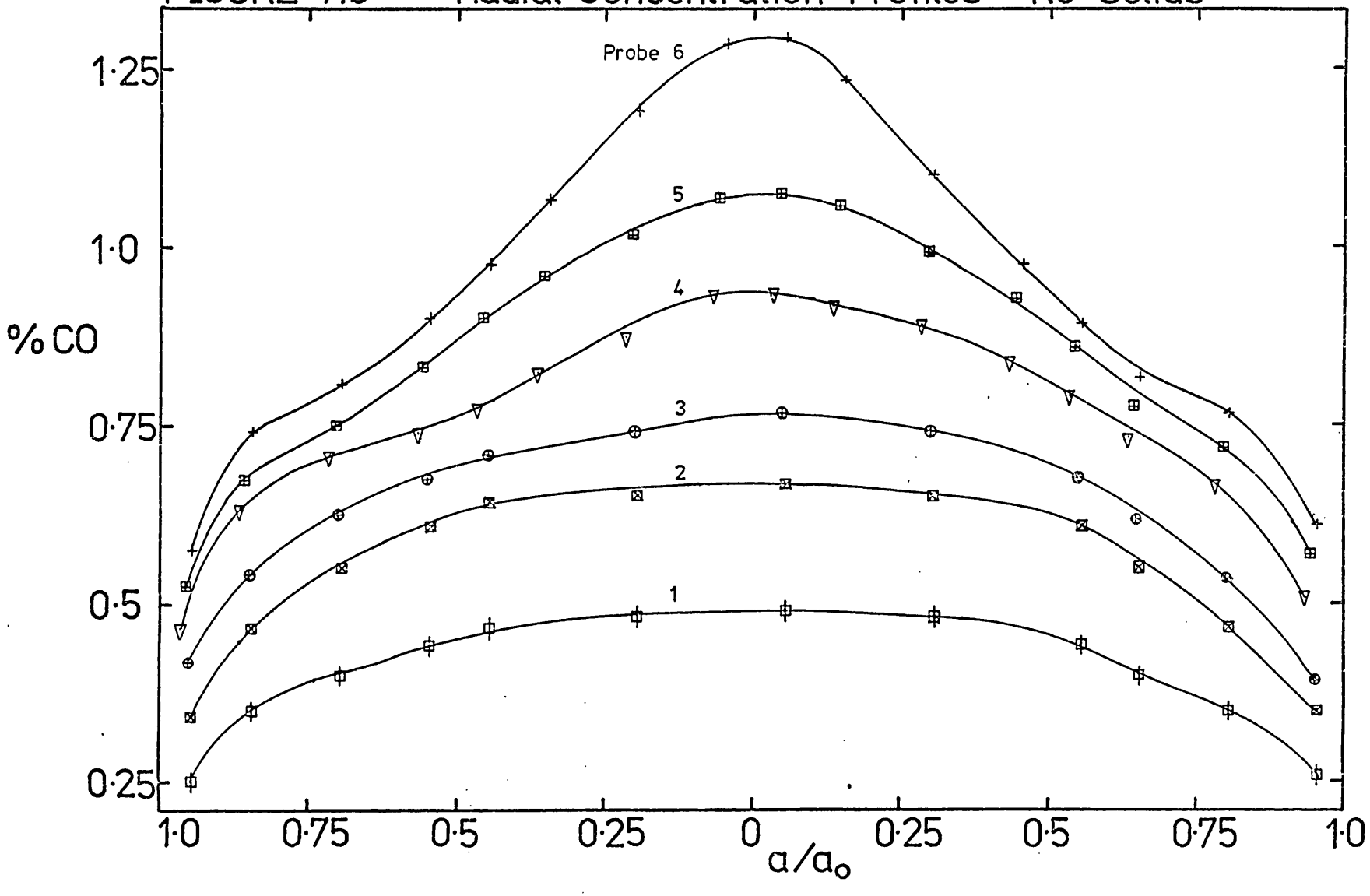

FIGURE 7.10 Axial Concentration & Temperature Profiles

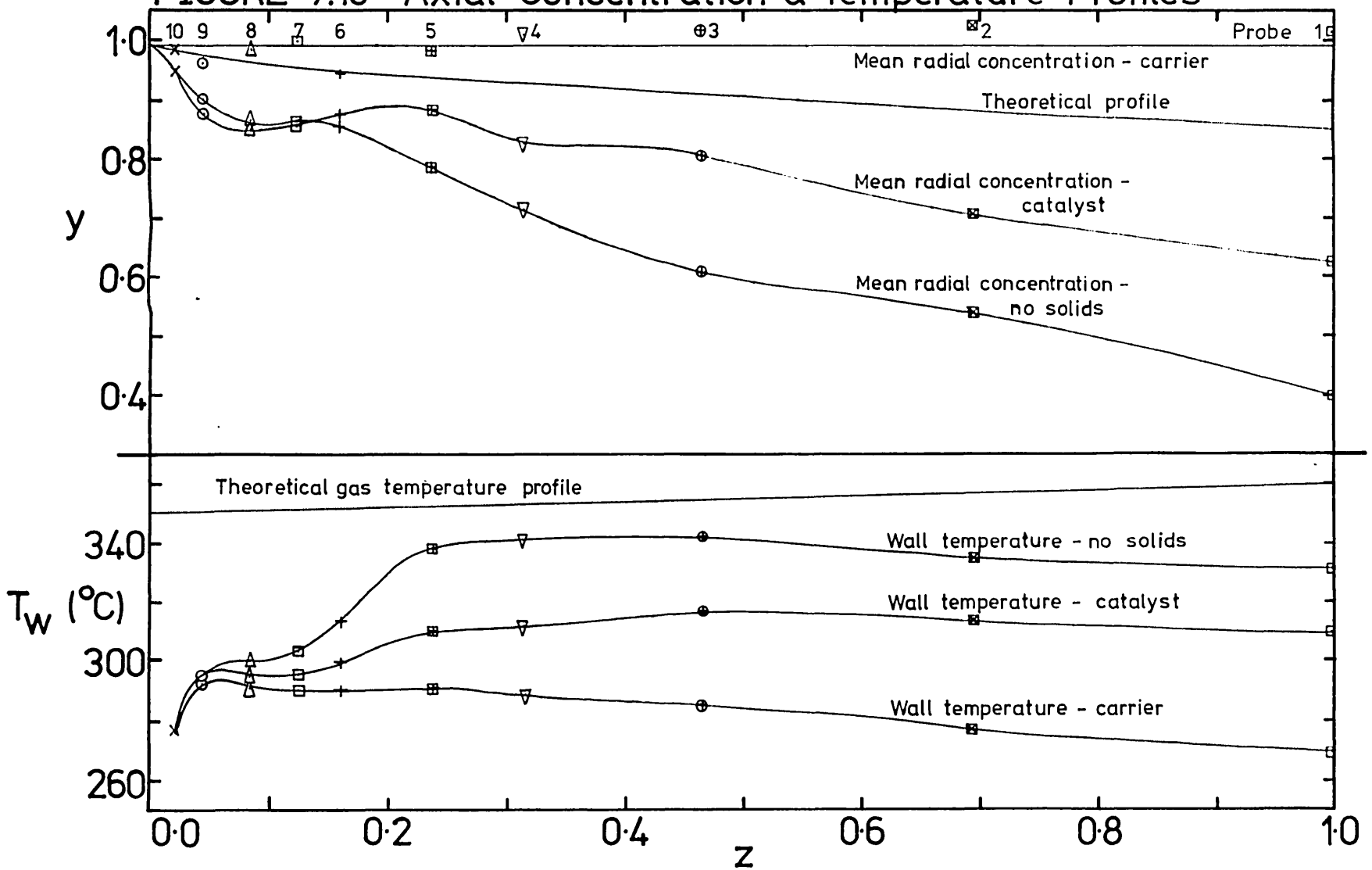

integrate the radial profiles. That this assumption is reasonable can be seen by consideration of the no reaction case. Since the shape of the radial concentration profile varies from a sharp peak to being flat as it moves down the reactor, any error in the velocity profile will have the effect of either gradually increasing or decreasing the apparent mean concentration of reactant along the length of the reactor. Figure 7.10 shows that this is not the case for the no reaction situation so that any errors in assuming the 1/7th power law velocity profile are small. Figure 7.10 also shows that for no reaction the calculated mean radial concentrations at the various axial positions vary by up to ± 5% of their true value. This fluctuation seems to be due to random errors, and although the measured concentrations at differing radii (for any one probe) lie on reasonably smooth curves, they are subject to errors. These errors arise from small random fluctuations of the gas phase concentrations of reactant in the turbulent air stream and errors in concentration measurement with the gas chromatograph. They are largest for the lower concentrations which occur near the reactor walls, and it is these portions of the radial concentration profile which are most important since they make the largest contribution to the total flowrate of reactant along the reactor by virtue of the large proportion of the total cross-sectional area of the reactor which they occupy.

Examining the results for the cases where a reaction was occurring, it is immediately obvious that the largest conversion of reactant was occurring for the case where no catalyst was flowing. The radial concentration profiles for this case show a steep concentration gradient at the reactor walls suggesting that the reaction was occurring on the

reactor walls. It has been found (section 7.2.1) that the stainless steel walls have no catalytic activity and so a layer of catalyst particles must have been attached to the reactor wall.

With flowing catalyst there was also a large concentration gradient near the reactor walls (Figure 7.7), again suggesting catalyst particles adhering to the walls. That the reaction was occurring on the walls of the reactor is supported by the shape of the axial concentration profiles, showing an initially high reaction rate decreasing to a minimum and then increasing again (Figure 7.10). This effect was to be expected for a negative order reaction together with a wall concentration of reactant which increased to a maximum, as the reactant diffused to the wall, and then decreased again, as the reactant reacted along the reactor length. Thus the rate of reaction, being inversely proportional to the CO concentration decreased to a minimum and then increased.

The higher conversions obtained for no catalyst flow may have been due to a layer of particles (on the walls of the reactor) consisting of both small and large diameter particles. When catalyst was flowing, the scouring effect of the flowing particles might have removed, or prevented the attachment of, the larger particles. The larger particles would be held comparatively weakly since the attractive force was likely to have been a surface force. Electrostatic charging was probably the cause of the adhesion of particles to the walls. Electrostatic effects have already been noted in this chapter (7.2.4) and have been found by many workers in the field of suspension flow, (Mehta, Smith and Comings, 1957; Soo, 1964; Soo, Trezek, Dimick and Hohnstreiter, 1964; Soo and Trezek, 1966; Doig and Roper, 1968;

Arundel, Bibb and Boothroyd, 1970/71; Mason and Boothroyd, 1971; Duckworth and Kakka, 1971; Soo, 1971; Duckworth and Chan, 1973).

Several other effects were noted that point to a layer of particles on the reactor walls:

With the reactor at steady state, turning on the carbon monoxide feed to the reactor caused the reactor wall temperatures to increase for about 20 minutes until a steady state was reached. During this time the conversion of reactant also showed an increase. A reaction occurring in the flowing catalyst particles would depend on the air stream temperature only, whereas a reaction occurring on the reactor wall would increase in rate as the reactor wall temperature increased, (i.e. at a much slower rate than the air stream). Similarly, when the air stream temperature was reduced, high conversions could be achieved for several minutes until the wall temperatures had fallen.

The conversions obtained in the reactor decreased slowly over a period of several weeks, but measurements (in the fixed bed reactor) of the activity of samples of the catalyst taken from the transport reactor showed that the catalyst activity was unchanged. Addition of fresh catalyst was accompanied by extremely high (100%) conversions at relatively low temperatures (325°C) for about one hour during which period pronounced electrostatic effects were observed in the solids flowing from the cyclone.

The following observations may be made:

(i) Catalytic activity was due to a layer of catalyst particles on the reactor walls.

(ii) These particles were held by electrostatic forces which appeared to be strongest in fresh catalyst, decaying in strength as the catalyst aged (so that fewer particles were held on the wall).

(iii) There was no loss in activity in the circulating catalyst over the period of this work.

7.5 Conclusions

The problem of catalytic reaction on a layer of particles on the reactor walls may only be overcome by increasing greatly the solids to gas mass flow ratio. This will have two effects; one of causing more scouring of the walls and the other of providing so high a catalyst loading in the gas stream that any effect of reaction on the walls will be small in comparison.

To make this possible several modifications to the system described in Chapter 5 would be necessary. The blower would be replaced by a compressor to deal with the resulting high pressure drop through the system. The suspension would be brought to reaction temperature by heating of the solid instead of, or in addition to, the gas. The reason for this is that the total heat capacity of the solids would be high in comparison to that of the gas. Heating the solids would be best carried out in a fluidized bed by a heating element immersed in the bed.

Other than in the above respect the system performed adequately:

(i) The reaction was convenient to study, having easily characterised kinetics. The reactant was readily available in cylinders and analysis by gas chromatography was simple and reliable.

(ii) The sampling system operated well at high flowrates and would have done so at low flowrates if catalyst particles could have been prevented from entering the probes.

(iii) The injector used gave complete mixing in $L / d_t < 20$.

(iv) The validity of the theoretical models of Chapter 4 could not be tested in the system used because of the problem of reaction at the reactor wall.

(v) Any model developed to explain the experimental results obtained would require a measure of the loading of catalyst on the reactor walls. This was impossible to obtain and varied with time so no modifications of the theoretical models of Chapter 4 have been attempted. Some modification of the models is desirable to take account of the non-uniform radial concentration near the reactor entrance.

8. CONCLUSIONS

8.1 Summary

The evaluation of the transport reactor has been divided into two sections. An experimental study of a laboratory reactor examined the performance of the reactor at very low solids loadings. A theoretical study was made to interpret the results of the experimental work, and by choice of suitable values for the parameters employed, the expressions developed were used to predict the performance of commercial systems operating at much higher solids loadings than the laboratory reactor.

The experimental investigation of the transport reactor has made clear the particular practical difficulties of operating a laboratory reactor at a solids to gas mass flow ratio of much less than unity. Electrostatic charging of the catalyst particles seriously affected the performance of the reactor under these conditions in two ways. Firstly, adhesion of particles to the reactor wall was such that a higher solids loading was indicated on the walls than in the gas stream, causing a higher reaction rate at the wall and thus preventing the uniform radial conditions which ideally would be achieved in the transport reactor. Secondly, erratic flow of solids fed to the conveying gas stream can result in considerable variation in the solids loading and hence fluctuations of the reactant conversion with time.

Charging of the catalyst particles cannot be prevented, or its effects alleviated, by earthing and only the careful selection of materials of construction for the reactor and catalyst carrier using

substances of similar Fermi levels can avoid or minimize electrostatic effects. If this is impossible, use of high solids to gas mass flow ratios will mean that particle adhesion to the reactor walls is small in relation to solids flow, and a positive (screw) feed for the solids will lessen fluctuations in solids flowrate.

Operation of a transport reactor at a solids to gas mass flow ratio of less than 0.2 has highlighted the problems involved in achieving sufficient conversion of reactant at the low solids loadings sometimes employed in laboratory transport reactors. High conversions of reactant may be achieved by three basic policies, corresponding to the three parameters ϕ^2, M and P, which may be thought of as dimensionless forms of the reaction rate function, the residence time and the catalyst loading respectively. In the system used, by far the largest increase in conversion could be attained by increasing the reaction rate function, since the exponential dependence of this function on reaction temperature allowed a considerable increase in reaction rate for a relatively small temperature increase. Physical limitations of the reactor prevented much variation in the reactor residence time, the problem of obtaining a high enough air velocity for good heat transfer to the gas stream from a heating element being the critical factor in the system used. For high solids loadings, heating of the solids would prove necessary, whilst for solids to gas mass flow ratios of about one, heating of both solids and gas streams would be desirable in order to eliminate the use of high temperatures for one of the two streams. (Injection of catalyst particles into a very hot gas stream may cause sintering, as may heating the catalyst to a very high temperature before injecting it into a cold gas stream.)

Increase of catalyst loading was again limited by the physical characteristics of the experimental system, particularly the problem of achieving reaction temperatures by heating the airstream alone. At higher solids to gas mass flow ratios, a change from a blower to a compressor would be necessary to deal with the higher pressure drops encountered.

The theoretical examination of the transport reactor, directed towards the prediction of the behaviour of commercial systems, pointed to the desirability of using small particles, a choice which would not only decrease the value of the parameter ϕ^2 (and thus increase the particle effectiveness factor), but also reduce the particle film heat and mass transfer resistance per unit volume of catalyst. A high solids to gas mass flow ratio was also indicated for it allows a high overall conversion of reactant to be obtained using a relatively low reaction rate per particle, hence a high effectiveness factor and low film resistance to heat and mass transfer is possible.

The above experimental and theoretical conclusions suggesting the use of small particles (for good film transfer), high solids to gas mass flow ratios (for high conversions and low film heat and mass transfer resistance), and high gas flowrates (for good heat transfer from heater element to gas stream) are similar to those obtained from the literature survey of the transfer processes (Chapter 3) for attaining good wall to suspension heat transfer. They are therefore important factors in attaining the most efficient operation of a transport reactor and are necessary for the existence of uniform radial conditions in the reactor.

Using small particles has two disadvantages however: (i) The effects of electrostatic charging are most serious for smaller particles. (ii) Efficient operation of the cyclone may be difficult for small particles. Thus the particle size must be chosen to be as small as these two constraints will allow. This recommendation of small particles is a direct result of the consideration of film heat and mass transfer effects. If these were ignored, an optimum particle size would be expected where the effects of increased particle residence time (as a result of higher slip velocities) on reactant conversion are balanced by lower effectiveness factors as particle size increases. By examining a limited range of parameters Varghese and Varma (1977) showed that increasing particle size increased conversion, i.e. the optimum particle size is not reached under normal operating conditions for a commercial reactor. Their result is in direct contradiction to the one reached here; had film mass transfer resistance been considered by the above authors, a smaller particle size may have been suggested.

The literature survey of Chapter 3 has suggested a 1/7th power law for the gas velocity profiles in a transport reactor. The assumption of this velocity profile in the calculation of results for the experimental work has shown that it is a reasonable approximation to the true situation in the laboratory reactor.

The theoretical examination of the reactor has shown that in a real (industrial) system the rate of diffusion of reactant within the catalyst particles is fast relative to reaction rate and so a steady state approximation for the particles can be made under normal conditions of operation. This allows considerable simplification of

the reactor equations for a first order reaction. Consistent with this conclusion are the results of previous transport reactor studies referred to in Chapter 2 which generally show good agreement with the steady state models which were used.

The study of the optimization of the transport reactor for two consecutive first order reactions by imposition of an axial profile on the wall heat flux concluded that no advantage over the optimum isothermal temperature could be found for the reactions studied and that the suspension to wall heat transfer coefficient was sufficiently high to permit the removal of the heat of reaction through the reactor wall. For two consecutive first order reactions where the relatively unstable intermediate is the desired product, and where the heat of reaction is large, the plug flow and good wall heat transfer of the transport reactor make it the most suitable reactor for commercial production of the intermediate providing a sufficiently active catalyst can be found.

8.2 Discussion

8.2.1 Comparison of the Transport Reactor with Conventional Reactors

In evaluating the performance of the transport reactor, a comparison with conventional types of reactor is necessary if any justification is to be provided for the use of a novel type of reactor. The fixed bed reactor and the fluidized bed reactor are two common reactors providing widely differing conditions for reaction, and it is with these reactors that a comparison has been made.

(i) Fixed Bed Reactor

The fixed bed reactor and the transport reactor have in common the plug flow conditions which are necessary for accurate residence time control and good selectivity. The fixed bed reactor is simpler than the transport reactor, having no need for a solids feed system or a cyclone to remove particles from the gas stream. There is no erosion of the reactor by flowing particles and so generally construction will be simpler and thus cheaper than a transport reactor.

For rapidly fouling catalyst which requires frequent regeneration or for highly exothermic reactions requiring rapid removal of heat (and thus good heat transfer), the fixed bed reactor is inadequate and so a fluidized bed reactor is often used.

(ii) Fluidized Bed Reactor

The transport reactor has the same advantages of good wall heat transfer and the possibility of continuous regeneration of catalyst as does the fluidized bed reactor.

The fluidized bed reactor has poor selectivity because of by-passing and a large amount of backmixing and so is inferior to the transport reactor in this respect. In terms of construction, a method of removal of fines from the gas stream will be required for a fluidized bed, but with a much lighter duty than for the transport reactor. The fluidized bed is not able to cope with as wide a variation in feedstock flowrate (or composition) as is the transport reactor since the range of fluidizing velocities is smaller than the range of velocities for solids transport. The solids loading of the transport reactor can also be varied at will.

Thus the transport reactor combines the advantages of the fixed and fluidized bed reactors but requires a more active catalyst and an efficient cyclone. These factors may limit the advantages and use of the transport reactor.

8.2.2 Optimum Operating Conditions for the Transport Reactor

The optimum operating conditions for a transport reactor are:-

(i) Small Particle Diameter (d_p)

Particle diameters should be small to give good particle film heat and mass transfer rates (per unit volume of catalyst), good suspension to wall heat transfer and high particle effectiveness factors. The size of the catalyst particles will be limited however, by: the need to achieve sufficient slip velocity to ensure adequate particle residence time; electrostatic effects, which are of greatest relative importance for small particles; and by the ability of the cyclone to remove the particles efficiently. The latter factor will be the limiting one.

(ii) High Solids to Gas Mass Flowrate Ratio (W_s/W_g)

This will give good suspension to wall heat transfer rates, high conversions and supress electrostatic effects to some extent. The limiting factors here will be high pressure drops and high rates of erosion of the system internals.

(iii) High Tube Reynolds Number (Re_t)

High tube Reynolds Numbers will give improved suspension to wall heat transfer and ensure turbulent, uniform conditions within the reactor. Pressure drop may limit the Reynolds Number in practice

as a small pipe diameter (d_t) is necessary to obtain good heat removal per unit volume of suspension. A further limiting factor is the need for a high enough residence time to allow reasonable reactant conversion.

The transport reactor is most efficient for high reaction rates requiring short residence times. Highly active catalysts on high reaction temperatures are particularly suitable for transport reactors, and where equilibrium considerations (R. King, 1977) or the need for a shift in relative reaction rates dictate a high reaction temperature, the transport reactor may become economically attractive. For fast reactions (e.g. cracking and oxidation) I believe the transport reactor should be generally suitable even though it is more complicated than conventional reactors.

8.3 Recommendations for Further Work

The experimental work has indicated that the measurement of axial and radial concentration profiles in a transport reactor can lead to an improved understanding of the reactor and in the work undertaken allowed the effect of electrostatic charging to be detected. Electrostatic effects are unlikely to be so important industrially at the higher solids loadings utilized in commercial reactors and an extension of the experimental work to the higher values of W_s/W_g which would be used in an industrial reactor is desirable. This would necessitate heating of the solids instead of (or in addition to) the gas, replacing the blower by a compressor and possibly modifying the solids feed system. These modifications would also allow a wider range of the system parameters to be studied than was possible with the present system, and so allow better comparison with the theoretical predictions.

The effect of the reactant injector configuration on the shape of the radial concentration profiles could be examined with a view to finding the injector which gives the most efficient mixing of the reactant with the flowing suspension.

Analysis for carbon monoxide by gas chromatography allowed one measurement every four minutes; thus three measurements (to obtain a mean value) at each of the 16 radial positions of the 10 probes involved a total time of up to 32 hours for any single set of conditions. A more rapid method of analysis would therefore be advantageous. For carbon monoxide, infra-red analysis could be used although the equipment is costly.

A study of a more complex reaction system should allow a more rigorous test of the theoretical predictions. In particular, a reaction system of the type $A \rightarrow B \rightarrow C$ will allow the predictions of the optimization model to be tested.

Further development of the theoretical work of Chapter 4 to allow for the effect of the non-uniform reactant concentration profile at the reactor entrance on the reaction rate is required. Prediction of the concentration profile from the injector configuration, the velocity profile of the gas and the radial dispersion coefficient would be extremely difficult so measurement of the concentration profile is necessary for the development of this theory.

APPENDIX 1

SOLUTION OF THE REACTOR EQUATIONS FOR THE CASE OF NO REACTION

Making assumptions (i), (ii), (iv) and (v) of section 4.2 leads to the following equations for the system:-

$$\frac{1}{M}\frac{\partial Y}{\partial z} = \frac{\partial^2 Y}{\partial x^2} + \frac{2}{x}\frac{\partial Y}{\partial x} \qquad \text{A1.1}$$

$$\frac{1}{M}\frac{dy}{dz} = -3P \left.\frac{\partial Y}{\partial x}\right|_{x=1} \qquad \text{A1.2}$$

$$Y(x,0) = 0 \qquad 0 \leqslant x < 1 \qquad \text{A1.3}$$

$$Y(1,0) = 1 \qquad \text{A1.4}$$

$$Y(1,z) = y(z) \qquad \text{A1.5}$$

$$\frac{\partial Y}{\partial x}(0,z) = 0 \qquad \text{A1.6}$$

Solution of the above equations and boundary conditions by Laplace Transformation gives:-

$$Y = \frac{1}{(1+P)} + \sum_{n=2}^{\infty} \frac{\sin(\sqrt{\beta_{Dn}}\, x)}{x.\sin(\sqrt{\beta_{Dn}}).F_{Dn}} \exp(\gamma_{Dn} M z) \qquad \text{A1.7}$$

where $$F_{Dn} = \frac{3}{2}(1+P) + \frac{\beta_{Dn}}{6P} \qquad \text{A1.8}$$

and the β_{Dn}'s and γ_{Dn}'s are given by the solution of:

$$\beta_{Dn} = -\gamma_{Dn} \qquad \text{A1.9}$$

and $$\frac{\gamma_{Dn}}{3P} = 1 - \sqrt{\beta_{Dn}} \cot \sqrt{\beta_{Dn}} \qquad \text{A1.10}$$

NB (i) The above solution may also be obtained from the first order reaction solution by putting $\phi \to 0$ and from the zero order reaction solution by putting $x_e = 0$ and $\phi_o \to 0$.

NB (ii) The term (1/1 + P) of equation A1.7 is the term for n = 1 which has been taken outside the summation.

APPENDIX 2

SOLUTION OF THE REACTOR EQUATIONS FOR A ZERO ORDER REACTION

Making assumptions (i), (ii), (iv) and (v) of section 4.2 leads to the following equation:-

$$\frac{1}{M}\frac{\partial Y}{\partial z} = \frac{\partial^2 Y}{\partial x^2} + \frac{2}{x}\frac{\partial Y}{\partial x} - \phi_o^2 \qquad \text{A2.1}$$

Boundary conditions equations A1.2 to A1.5 are still valid. In obtaining the final boundary condition, however, a distinction must be made between two physical situations; exhaustion and non-exhaustion of reactant. In the former case the concentration of reactant is reduced to zero at some distance into the particle, whereas, in the latter case, the concentration of reactant is non-zero at all points within the particle. The limiting situation in each case is where the reactant concentration is zero at the particle centre.

For non-exhaustion of reactant boundary condition equation A1.6 holds.

For exhaustion of reactant the following boundary conditions apply:

$$Y(x_e, z) = 0 \qquad \text{A2.2}$$

and

$$\frac{\partial Y}{\partial x}(x_e, z) = 0 \qquad \text{A2.3}$$

where $x_e = x_e(z)$ is the point at which the reactant is exhausted.

Munro and Amundson (1950) presented a solution for a zero order reaction occurring in a moving bed where similar equations apply. Their solution is only valid for non-exhaustion of reactant.

The solution of the problem with reactant exhaustion may be made by use of Laplace Transformations on equations A2.1, A1.2 to A1.5, A2.2 and A2.3.

The result is as follows:

$$Y = \frac{-M\phi_o^2 zP(1-x_e^3)}{1+P(1-x_e^3)} + \frac{6+[\phi_o^2(x-x_e)^2(2x_e+x)]/x}{6[1+P(1-x_e^3)]} -$$

$$\frac{\{5[(1-x_e)^3+3x_e(1-x_e)^2]+3P[(1-x_e)^5+5x_e(1-x_e)^3]\}\phi_o^2}{30[1+P(1-x_e^3)]^2} +$$

$$\sum_{n=2}^{\infty} \frac{(\gamma_{on}+\phi_o^2)\{x_e\sqrt{\beta_{on}}\cos[\sqrt{\beta_{on}}(x-x_e)]+\sin[\sqrt{\beta_{on}}(x-x_e)]\}.\ \exp(\gamma_{on}Mz)}{\gamma_{on}x\{F_{01n}\cos[\sqrt{\beta_{on}}(1-x_e)]+F_{02n}\sin[\sqrt{\beta_{on}}(1-x_e)]\}} \qquad \text{A2.4}$$

where $$F_{01n} = \sqrt{\beta_{on}}[3x_e+(1-x_e)(1+3Px_e)]/2 \qquad \text{A2.5}$$

and $$F_{02n} = 1+\frac{3P}{2}(1+x_e^2) - \frac{\beta_{on}\, x_e(1-x_e)}{2} \qquad \text{A2.6}$$

and x_e, β_{on}'s and γ_{on}'s are the roots of:-

$$\beta_{on} = -\gamma_{on} \qquad \text{A2.7}$$

$$\frac{\gamma_{on}}{3P} = \frac{(1+x_e\beta_{on})-(1-x_e)\sqrt{\beta_{on}}\cot[\sqrt{\beta_{on}}(1-x_e)]}{1+x_e\sqrt{\beta_{on}}\cot[\sqrt{\beta_{on}}(1-x_e)]} \qquad \text{A2.8}$$

and

$$\frac{\{5[(1-x_e)^3+3x_e(1-x_e)^2]+3P[(1-x_e)^5+5x_e(1-x_e)^3]\}\phi_o^2}{30[1+P(1-x_e^3)]^2} +$$

$$\frac{M\phi_o^2P(1-x_e^3)z}{1+P(1-x_e^3)} - \frac{1}{1+P(1-x_e^3)} =$$

$$\sum_{n=2}^{\infty} \frac{(\gamma_{on}+\phi_o^2)\cdot\sqrt{\beta_{on}}\cdot\exp(\gamma_{on}Mz)}{\gamma_{on}\{F_{01n}\cos[\sqrt{\beta_{on}}(1-x_e)]+F_{02n}\sin[\sqrt{\beta_{on}}(1-x_e)]\}} \qquad \text{A2.9}$$

NB. $\beta_{01} = \gamma_{01} = 0$ and these terms are given outside the summations of equations A2.4 and A2.9.

β_{on}, γ_{on} and x_e are thus determined from the implicit equations A2.7 to A2.9. They may be seen to be functions of z and so must be found at every point along the reactor for which a value of Y is required.

For non-exhaustion of reactant the solution may be obtained by setting $x_e = 0$ in equations A2.4 to A2.8. Equation A2.9 does not hold in this case since it is derived from boundary condition equation A2.3. Hence the dependence of β_{on} and γ_{on} on z is removed and a considerably simpler solution results.

APPENDIX 3

SOLUTION OF THE REACTOR EQUATIONS FOR TWO CONSECUTIVE FIRST ORDER REACTIONS

Making assumptions (i), (ii), (iv) and (v) of section 4.2 leads to the following equations for the reaction system:

$$A \xrightarrow{k_A} B \xrightarrow{k_B} C$$

$$\frac{1}{M_A}\frac{\partial Y_A}{\partial z} = \frac{\partial^2 Y_A}{\partial x^2} + \frac{2}{x}\frac{\partial Y_A}{\partial x} - \phi_A^2 Y_A \qquad \text{A3.1}$$

$$\frac{1}{M_A}\frac{dy_A}{dz} = -3P \left.\frac{\partial Y_A}{\partial x}\right|_{x=1} \qquad \text{A3.2}$$

$$\frac{1}{M_B}\frac{\partial Y_B}{\partial z} = \frac{\partial^2 Y_B}{\partial x^2} + \frac{2}{x}\frac{\partial Y_B}{\partial x} - \phi_B^2 Y_B + D_N \phi_A^2 Y_A \qquad \text{A3.3}$$

$$\frac{1}{M_B}\frac{dy_B}{dz} = -3P \left.\frac{\partial Y_B}{\partial x}\right|_{x=1} \qquad \text{A3.4}$$

$x \neq 1$, $Y_A(x,0) = 0$ A3.5 $\qquad$ $x \neq 1$, $Y_B(x,0) = 0$ A3.6

$Y_A(1,0) = 1$ A3.7 $\qquad$ $Y_B(1,0) = 0$ A3.8

$Y_A(1,z) = y_A(z)$ A3.9 $\qquad$ $Y_B(1,z) = y_B(z)$ A3.10

$\frac{\partial Y_A}{\partial x}(0,z) = 0$ A3.11 $\qquad$ $\frac{\partial Y_B}{\partial x}(0,z) = 0$ A3.12

A solution for y_B is found by Laplace Transformation:

$$y_B = 3P\phi_A^2 \left\{ D_N \sum_{n=1}^{\infty} \frac{\sqrt{\delta_{An}}\cot\sqrt{\delta_{An}} - \sqrt{\beta_{An}}\cot\sqrt{\beta_{An}} \cdot \exp(\gamma_{An}M_{Az})}{(\beta_{An}-\delta_{An})[D_N\gamma_{An} - 3P(1-\sqrt{\delta_{An}}\cdot\cot\sqrt{\delta_{An}})] \cdot F_{An}} + \right.$$

$$\left. \sum_{n=1}^{\infty} \frac{\sqrt{\beta_{Bn}}\cot\sqrt{\beta_{Bn}} - \sqrt{\delta_{Bn}}\cot\sqrt{\delta_{Bn}} \cdot \exp(\gamma_{Bn}M_B z)}{(\delta_{Bn}-\beta_{Bn})[\gamma_{Bn}/D_N - 3P(1-\sqrt{\delta_{Bn}}\cdot\cot\sqrt{\delta_{Bn}})] \cdot F_{Bn}} \right\} \quad \text{A3.13}$$

where $F_{An} = 1 + \frac{3P}{2} - \frac{\gamma_{An}}{2\beta_{An}} + \frac{\gamma_{An}^2}{6P\beta_{An}}$ A3.14

and $F_{Bn} = 1 + \frac{3P}{2} - \frac{\gamma_{Bn}}{2\beta_{Bn}} + \frac{\gamma_{Bn}^2}{6P\beta_{Bn}}$ A3.15

and β_{An}, γ_{An} and δ_{An} are the roots of:-

$$\beta_{An} = -\gamma_{An} - \phi_A^2 \quad \text{A3.16}$$

$$\frac{\gamma_{An}}{3P} = 1 - \sqrt{\beta_{An}}\cot\sqrt{\beta_{An}} \quad \text{A3.17}$$

$$\delta_{An} = -D_N\gamma_{An} - \phi_B^2 \quad \text{A3.18}$$

and β_{Bn}, γ_{Bn} and δ_{Bn} are the roots of:-

$$\beta_{Bn} = -\gamma_{Bn} - \phi_B^2 \quad \text{A3.19}$$

$$\frac{\gamma_{Bn}}{3P} = 1 - \sqrt{\beta_{Bn}}\cot\sqrt{\beta_{Bn}} \quad \text{A3.20}$$

$$\delta_{Bn} = -\frac{\gamma_{Bn}}{D_N} - \phi_A^2 \quad \text{A3.21}$$

APPENDIX 4

EFFECTIVENESS FACTORS FOR A FIRST ORDER REACTION IN THE TRANSPORT REACTOR

The two definitions for effectiveness factor made in Section 4.4 lead to the expressions for η_f and η_i given in Equations 4.28 and 4.29. These two equations are reproduced below as equations A4.1 and A4.2.

$$\eta_f = \frac{-1}{\phi^2 P}\left[\frac{\sum_{n=1}^{\infty} \frac{\gamma_n \exp(\gamma_n Mz)}{F_n}}{\sum_{n=1}^{\infty} \frac{\exp(\gamma_n Mz)}{F_n}}\right] \qquad \text{A4.1}$$

$$\eta_i = \frac{1}{P}\left[\frac{\sum_{n=1}^{\infty} \frac{\gamma_n \exp(\gamma_n Mz)}{\beta_n F_n}}{\sum_{n=1}^{\infty} \frac{\exp(\gamma_n Mz)}{F_n}}\right] \qquad \text{A4.2}$$

β_n, γ_n and F_n are defined by equations 4.21 to 4.23.

As $Mz \to \infty$, η_f and η_i tend to the asymptotic values η_f^{∞} and η_i^{∞} respectively. Implicit expressions for η_f^{∞} and η_i^{∞} may be obtained from equations A4.1 and A4.2 (cf Lewis and Paynter, 1971):

$$\eta_f^{\infty} = \frac{3}{\phi}\left[\frac{\sqrt{(1-\eta_f^{\infty} P)}}{\tanh[\phi\sqrt{(1-\eta_f^{\infty} P)}]} - \frac{1}{\phi}\right] \qquad \text{A4.3}$$

and

$$\eta_i^{\infty} = \frac{3(1+\eta_i^{\infty}P)}{\phi} \left[\frac{1/\sqrt{(1+\eta_i^{\infty}P)}}{\tanh[\phi/\sqrt{(1+\eta_i^{\infty}P)}]} - \frac{1}{\phi} \right] \qquad \text{A4.4}$$

It is interesting to note the similarity between equations A4.3, A4.4 and A4.5, the steady state effectiveness factor for a first order reaction in a sphere.

$$\eta_{ss} = \frac{3}{\phi} \left[\frac{1}{\tanh \phi} - \frac{1}{\phi} \right] \qquad \text{A4.5}$$

The following relationships may be found from equations A4.3 and A4.4.

$P \to 0$ $\quad \eta_f^{\infty}$ and $\eta_i^{\infty} \to \eta_{ss}$ A4.6

$\phi \to \infty$ $\quad \eta_f^{\infty}$ and $\eta_i^{\infty} \to 0$ A4.7

$\phi \to 0$ $\quad \eta_f^{\infty} \to 1/(1+P)$ A4.8

$\phi \to 0$ $\quad \eta_i^{\infty} \to 1$ A4.9

The following relation may be observed from equation A4.4:

$$\eta_i^{\infty}(\phi) = \eta_{ss} \left(\frac{\phi}{\sqrt{1+\eta_i^{\infty}P}} \right) \qquad \text{A4.10}$$

Since, at large ϕ, $\eta_{ss} = 3/\phi$ (Petersen, 1965) A4.11

$$\eta_i^{\infty} = \frac{3}{\phi} \sqrt{1+\eta_i^{\infty}P} \quad \text{at large } \phi \text{ (i.e. } \phi \geq 3) \qquad \text{A4.12}$$

The above equation may be solved for η_i^{∞} giving:

$$\frac{\eta_i^{\infty}}{\eta_{ss}} \simeq 1 + \frac{3P}{2\phi} \qquad (\text{for } \phi \geq 3) \qquad \text{A4.13}$$

The corresponding result for η_f^{∞} is:

$$\frac{\eta_f^{\infty}}{\eta_{ss}} \simeq 1 - \frac{3P}{2\phi} \qquad (\text{for } \phi \geq 3) \qquad \text{A4.14}$$

Equation A4.13 suggests that the maximum difference between η_i^{∞} and η_{ss} occurs for $\phi = 3$ and, for $P = 0.1$, is about 5%. In fact, the computer studies mentioned in section 4.4 show that the maximum difference between η_i^{∞} and η_{ss} occurs at $\phi \simeq 3$, but for $P = 0.1$ is only about 2%.

Using equations A4.13 and A4.14 together with observations from Figure 4.2 (and Figure 3 of Robertson and Pratt, 1975) the conclusion can be drawn that at some point in the reactor $\eta_i = \eta_{ss}$ and $\eta_f = \eta_{ss}$.

Thus: $\eta_i(z=0) = 0 < \eta_{ss}$ (from figure 2) A4.15

$\eta_i^{\infty} > \eta_{ss}$ (from equation A4.13) A4.16

$\therefore$ $\eta_i(z=z_a) = \eta_{ss}$ A4.17

and similarly

$\eta_f(z=0) = \infty > \eta_{ss}$ A4.18

$\eta_f^{\infty} < \eta_{ss}$ A4.19

$\therefore$ $\eta_f(z=z_a) = \eta_{ss}$ A4.20

The physical significance of the above relations and their use in defining the entrance length are discussed in Appendix 5.

APPENDIX 5

ASYMPTOTIC SOLUTIONS

Equations 4.11 and 4.12 may be written in an alternative integral form, also obtained by a mass balance on the reactor:

$$\varepsilon u_s (1-\alpha)\frac{d(c\eta_*)}{dl} + \alpha u_g \frac{dc}{dl} = -(1-\alpha)\eta_g S(c) \qquad \text{A5.1}$$

where

$$\eta_* = \frac{\int_0^R 4\pi r^2 \varepsilon C dr}{\frac{4}{3}\pi R^3 \varepsilon c_s} \qquad \text{A5.2}$$

and

$$\eta_g = \frac{\int_0^R 4\pi r^2 S(C) dr}{\frac{4}{3}\pi R^3 S(c_s)} \qquad \text{A5.3}$$

The second term of equation A5.1 corresponds to the rate of change of gas phase reactant concentration. The first term corresponds to the rate of change of mean reactant concentration within the catalyst particles. The term on the right of equation A5.1 represents the mean rate of reaction within the particles.

The equations above may be written in the following dimensionless forms:

$$P\frac{d(\eta_* y)}{dz} + \frac{dy}{dz} = -PM\phi_g^2 \eta_g \Psi_{x=1} \qquad \text{A5.4}$$

where $$\eta_* = \frac{3}{y_s} \int_0^1 x^2 Y dx = \frac{\bar{Y}}{y_s} \qquad \text{A5.5}$$

and $$\eta_g = \frac{3}{\Psi_{x=1}} \int_0^1 x^2 \Psi dx \qquad \text{A5.6}$$

Entrance Length

The results of the effectiveness factor studies Section 4.4 give rise to the concept of an entrance length in which catalyst concentration profiles are becoming established. For the purpose of this work the entrance length is defined by equation A5.7.

$$\left.\frac{d(\eta_* y)}{dz}\right|_{z=z_a} = 0 \qquad \text{A5.7}$$

Subscript 'a' refers to conditions existing at the end of the entrance length.

Equation A5.7 thus refers to the point in the reactor at which the mean concentration of reactant within the catalyst particle is a maximum and is where diffusion into the particle is equal to the total reaction rate in the particle.

Hence $$\eta_* = \eta_{*ss} \quad \text{at} \quad z = z_a \qquad \text{A5.8}$$

and η_* is slightly less than η_*^{∞}, the final asymptotic value.

It may be assumed that in the entrance region of the reactor the amount of reaction occurring is small and hence equation A5.4 may be reduced to:

$$P\frac{d(\eta_* y)}{dz} + \frac{dy}{dz} = 0 \qquad \text{A5.9}$$

The reaction term has been ignored, a step which is further justified in section A5.1.

Solving equation A5.9 produces:

$$y_a = \frac{1}{(1+\eta_{*a}P)} \qquad \text{A5.10}$$

having used the boundary conditions;

$$z = 0 \qquad y = \eta_* = 0 \qquad \text{A5.11}$$

$$z = z_a \qquad y = y_a \qquad \eta_* = \eta_{*a} \qquad \text{A5.12}$$

but from equation A5.8 $\eta_{*a} = \eta_{*ss}$

$$\therefore \quad y_a = \frac{1}{(1+\eta_{*ss}P)} \qquad \text{A5.13}$$

This equation gives an approximate value of the gas phase concentration of reactant at the end of the entrance region.

The entrance region of the reactor may be represented by the solution of the equation for no reaction, to be found in Appendix 1.

A5.1 First Order Reaction

The foregoing discussion has been of general validity but attention is now focussed on the case of first order reactions where the results of the effectiveness factor investigations (Appendix 6) allows further developments.

For the first order rate law $\Psi_{x=1} = y$ equation A5.4 may be rearranged to give:

$$\frac{dy}{dz} = \frac{-P}{(1+\eta P)} \left(\frac{d\eta}{dz} + M\phi^2\eta \right) . y \qquad \text{A5.14}$$

having put $$\eta_* = \eta_g = \eta = \frac{3}{Y} \int_0^1 x^2 Y dx \qquad \text{A5.15}$$

for first order case.

For Small Mz

The assumption that the reaction term of equation A5.14 may be ignored at small Mz can be seen to be true from Figure 4.2 where, for Mz small;

$$\frac{d\eta}{M\, dz} \gg \phi^2\eta \qquad \text{A5.16}$$

This leads to $$y_a = \frac{1}{(1+\eta_{ss}P)} \qquad \text{A5.17}$$

For $Mz \to \infty$

Appendix 4 shows $\eta \to \eta^{\infty}$ (a constant) $\therefore \quad \frac{d\eta}{dz} \to 0$

so for large Mz equation A5.14 becomes:

$$\frac{dy}{dz} = \frac{-PM\phi^2\eta^{\infty}y}{(1+\eta^{\infty}P)} \qquad \text{A5.18}$$

Integrating this with the boundary conditions at $z = z_a$, $y = y_a$ and substituting from Equation A5.17 results in:

$$y = \frac{1}{(1+\eta_{ss}P)} \quad \exp\left\{\frac{-PM\phi^2\eta^{\infty}(z-z_a)}{(1+\eta^{\infty}P)}\right\} \qquad \text{A5.19}$$

but from Appendix 4 $\qquad \eta^{\infty} \approx \eta_{ss}$ $\qquad$ A5.20

so this may be substituted into Equation A5.19.

Equation A5.19 may also be used to obtain an estimate of z_a, the entrance length.

Using the boundary condition $y = 1$ at $z = 0$ in equation A5.19

$$1 = \frac{1}{(1+\eta_{ss}P)} \quad \exp\left\{\frac{PM\phi^2\eta_{ss}z_a}{1+\eta_{ss}P}\right\} \qquad \text{A5.21}$$

giving $\qquad Mz_a = \frac{(1+\eta_{ss}P)\ln(1+\eta_{ss}P)}{\phi^2\eta_{ss}P}$ $\qquad$ A5.22

Since $\eta_{ss} < 1$ and $P < 0.1$ in general, the logarithm may be expanded. Neglecting higher order terms:-

$$Mz_a \simeq \frac{1+\eta_{ss}P/2}{\phi^2} \qquad \text{A5.23}$$

or, for small P

$$\boxed{Mz_a \simeq 1/\phi^2} \qquad \text{A5.24}$$

which gives good agreement with Figure 4.2.

In summary the reactor may be divided into two sections:-

$z < 1/M\phi^2$ Equation A1.7 applies

$1 \geqslant z \geqslant 1/M\phi^2$ Equation A5.19 applies

It has been found, however, that for the range of parameters: M, 5 to 1000; P, 0.005 to 0.1 and ϕ^2, 0.01 to 1000 the equation below gives the reactant concentration to better than $\pm$ 1% of the entrance concentration, for $z > 0.1$.

$$\boxed{y = \frac{1}{(1+\eta_{ss}P)} \quad \exp\left\{\frac{-PM\phi^2\eta_{ss}z}{(1+\eta_{ss}P)}\right\}} \qquad \text{A5.25}$$

A5.2 Consecutive First Order Reactions

The system of equations described in Appendix 3 may also be written in integral form as:-

$$\frac{dy_A}{dz} = \frac{-P}{(1+\eta_A P)} \left[\frac{d\eta_A}{dz} \quad y_A + M_A\phi_A^2\eta_A y_A\right] \qquad \text{A5.26}$$

and $$\frac{dy_B}{dz} = \frac{-P}{(1+\eta_B P)} \left[\frac{d\eta_B}{dz} y_B + M_B\phi_B^2\eta_B y_B - M_A\phi_A^2\eta_A y_A\right] \quad \text{A5.27}$$

where $$\eta_A = \frac{3}{y_A}\int_0^1 x^2 Y_A dx \quad \text{A5.28} \qquad \text{and} \quad \eta_B = \frac{3}{y_B}\int_0^1 x^2 Y_B dx \quad \text{A5.29}$$

The following solution may be obtained in a similar manner to Equation A5.25:

$$y_B = \frac{M_A\phi_A^2\eta_{Ass}}{[(1+\eta_{Ass}P)M_B\phi_B^2\eta_{Bss} - (1+\eta_{Bss}P)M_A\phi_A^2\eta_{Ass}]} \left\{\exp\left[\frac{-PM_A\phi_A^2\eta_{Ass}z}{(1+\eta_{Ass}P)}\right] - \exp\left[\frac{-PM_B\phi_B^2\eta_{Bss}z}{(1+\eta_{Bss}P)}\right]\right\} \quad (z > 0.1) \quad \text{A5.30}$$

With

$$\eta_{Ass} = \left[\frac{3}{\phi_A}\right]\left[\frac{1}{\tanh\ \phi_A} - \frac{1}{\phi_A}\right] \quad \text{A5.31}$$

and

$$\eta_{Bss} = \left[\frac{3}{\phi_B}\right]\left[\frac{1}{\tanh\ \phi_B} - \frac{1}{\phi_B}\right] \quad \text{A5.32}$$

A5.3 General Rate Law Reactions

For any rate law the effectiveness factor at steady state is given by:-

$$\eta_{gss} = \eta_{gss}(\phi_s) \quad \text{A5.33}$$

where

$$\phi_s = R\sqrt{\frac{S(c_s)}{D_{eff} \cdot c_s}} \qquad \text{A5.34}$$

$$\therefore \quad \phi_s^2 = \phi_g^2 \cdot \frac{S(c_s).c_o}{S(c_o).c_s} = \phi_g^2 \cdot \frac{\Psi_{x=1}}{y_s} \qquad \text{A5.35}$$

Thus ϕ_s and hence η_{gss} are functions of y_s, the reactant concentration at the particle surface for any rate law other than first order (where $\Psi_{x=1} = y_s$).

Similarly $\eta_{*ss} = \eta_*(\phi_s)$ - also a function of y.

Thus for rate laws other than first order, both η_{*ss} and η_{gss} are functions of z, the reactor length coordinate, and so they do not reach asymptotic values.

Solution of the reactor equations must therefore be by numerical methods as described in Section 4.3.2.

APPENDIX 6

FILM MASS TRANSFER RESISTANCE

In dealing with mass transfer across surface films it is common to represent the flux of reactant across the film by the product of a mass transfer coefficient with the concentration difference of reactant between the surface and the bulk of the fluid. Thus a mass balance at the particle surface gives:-

$$4\pi R^2 D_{eff} \left.\frac{\partial C}{\partial r}\right|_{r=R} = 4\pi R^2 k_f (c-c_s) \qquad \text{A6.1}$$

or, in dimensionless form:

$$\left.\frac{\partial Y}{\partial x}\right|_{x=1} = D_m \frac{Sh}{2}(y-y_s) \qquad \text{A6.2}$$

where $$D_m = D_{12}/D_{eff} \qquad \text{A6.3}$$

An equation of this form was used by Munro and Amundson (1950) to describe film mass transfer in a moving bed reactor. Using the equation, together with equations of the form of Equations 4.11 to 4.14 and 4.16, they obtained a solution for Y by Laplace Transformation.

Equation A6.2 is valid only for an established film concentration profile; it gives no information as to the time dependence of the mass flux across the film. To represent the time dependence of the film mass flux, a partial differential equation together with detailed knowledge of the fluid mechanics of the gas around the particle is necessary. In the

unsteady-state conditions of the transport reactor, equation A6.2 may only be used if it can be assumed that the film concentration profile is established, and changes, rapidly in comparison to the concentration profile within the catalyst particles. This assumption may generally be made since the relative rate of change of the film and particle concentration profiles is approximately proportional to the ratio of the bulk and effective diffusivities (i.e. D_{12}/D_{eff}). This ratio is normally of the order of 25 or more.

Equations 4.12 and A6.2 may be combined to give:

$$\frac{dy}{dz} = \frac{-3}{2} PMD_m Sh(y-y_s) = -N(y-y_s) \qquad A6.4$$

where $N = 3PMD_m Sh/2$ A6.5

For total film mass transfer control $y_s = 0$ and the reactor equation becomes:

$$\frac{dy}{dz} = -Ny \qquad A6.6$$

which may be solved to give:

$$y = \exp(-Nz) \qquad A6.7$$

A6.1 Importance of Film Mass Transfer Resistance

Defining a non-steady state effectiveness factor based on the surface mass flux (cf. Equation 4.26):

$$\eta_{gf} = \frac{3}{\phi_g^2 \Psi_{x=1}} \left.\frac{\partial Y}{\partial x}\right|_{x=1} \qquad A6.8$$

and combining equations A6.2 and A6.8 gives:

$$y-y_s = \frac{2\eta_{gf}\phi_g^2\Psi_{x=1}}{3D_m Sh} \qquad A6.9$$

Thus the fractional drop in concentration across the film is given by:

$$\frac{y-y_s}{y} = \frac{2\eta_{gf}\phi_g^2\Psi_{x=1}}{3D_m Shy} \qquad A6.10$$

This may be best examined by consideration of the first order case where $\Psi_{x=1} = y_s$. A6.11

Outside the entrance region $\eta_{gf} = \eta_f^{\infty}$ A6.12

Thus

$$\frac{y-y_s}{y} = \frac{2\eta_f^{\infty}\phi^2/3D_m Sh}{[1+2\eta_f^{\infty}\phi^2/3D_m Sh]} \qquad A6.13$$

Taking the asymptotic value of η_{ss} as $\phi \to \infty$ ($\eta_{ss} = 3/\phi$) since the film resistance is of greatest importance at large ϕ, and assuming that $\eta_f^{\infty} \simeq \eta_{ss}$ (Equation A4.17), equation A6.13 may be evaluated.

Using $D_m = 25$ and $Sh = 4$ as typical values:

$$\frac{y-y_s}{y} = \frac{\phi/50}{[1+\phi/50]} \qquad \text{for } \phi > 3 \qquad A6.14$$

The following regimes may be suggested:

$\phi^2 \ll 1$ film mass transfer resistance may be neglected - equation A5.25 applies for first order case.

$1 < \phi^2 \leq 6.25 \times 10^6$ film mass transfer resistance is important, equation A6.29 applies for first order case ($z \geq z_a$).

$6.25 \times 10^6 < \phi^2$ film mass transfer is controlling and equation A6.7 applies.

From equation A6.10 it may be seen that, for rate laws other than first order, the fractional drop in reactant concentration across the film is dependent on y_s, and hence on z, so that film mass transfer resistance may be important or controlling for <u>part</u> of the length of the reactor. This is not the case for a first order system.

Equation A6.10 also shows that in the case of power law kinetics ($\Psi_{x=1} = y_s^n$) film mass transfer resistance increases as the power 'n' decreases for a given value of ϕ_g^2, D_m and Sh.

A6.2 <u>Asymptotic Solution for First Order Kinetics</u>

For first order kinetics with film mass transfer resistance, the following equation (cf Equation A5.4) may be written:

$$P\frac{d(\eta y_s)}{dz} + \frac{dy}{dz} = -PM\phi^2\eta y_s \qquad \text{A6.15}$$

Substituting for y_s in equation A6.15 from equation A6.4:

$$\left(\frac{\eta P}{N}\right)\cdot\frac{d^2y}{dz^2} + (1+\eta P)\frac{dy}{dz} + P\left(y+\frac{1}{N}\frac{dy}{dz}\right)\frac{d\eta}{dz} = -PM\phi^2\eta y_s \qquad \text{A6.16}$$

Outside the entrance region (i.e. $Mz \to \infty$) $\quad \eta \to \eta^{\infty}$ (a constant)

$$\therefore \quad \frac{d\eta}{dz} \to 0 \qquad \text{as} \qquad z \to \infty$$

So equation A6.16 reduces to:

$$\left(\frac{\eta^{\infty}P}{N}\right).\frac{d^2y}{dz^2} + (1+\eta^{\infty}P)\frac{dy}{dz} + PM\phi^2\eta^{\infty}y_s = 0 \qquad \text{A6.17}$$

This equation may be solved for y; however it may be further simplified without great loss of accuracy.

Differentiating equation A6.4:

$$\frac{dy_s}{dz} = \frac{dy}{dz} + \frac{1}{N}\frac{d^2y}{dz^2} \qquad \text{A6.18}$$

The term d^2y/dz^2 is zero for no mass transfer resistance and increases as mass transfer resistance increases.

For total film control $y_s = 0$ and $\frac{dy_s}{dz} = 0$

$$\therefore \quad \frac{dy}{dz} = \frac{-1}{N}\frac{d^2y}{dz^2} \qquad \text{A6.19}$$

But for $y_s = 0$, ϕ is large $\therefore$ η^{∞} is small

$$\therefore \quad \eta^{\infty}P \ll (1+\eta^{\infty}P) \qquad \text{A6.20}$$

So from equations A6.19 and A6.20

$$\left(\frac{\eta^{\infty}P}{N}\right) \cdot \frac{d^2y}{dz^2} \ll (1+\eta^{\infty}P)\frac{dy}{dz} \qquad \text{A6.21}$$

The above equation represents the worst case of total film control so generally the first term of equation A6.17 may be neglected giving (for $z > z_a$):

$$\boxed{\frac{dy}{dz} = \frac{-PM\phi^2\eta^{\infty}y_s}{(1+\eta^{\infty}P)}} \qquad \text{A6.22}$$

For $Mz \to 0$

The right-hand side of equation A6.15 may be neglected since diffusion is the major process.

$$P\frac{d(\eta y_s)}{dz} + \frac{dy}{dz} = 0 \qquad \text{A6.23}$$

Integrating from $z = 0$ to $z = z_a$ and using $\eta(z_a) = \eta_{ss}$

$$[1-\eta_{ss}Py_s-y]_{z=z_a} = 0 \qquad \text{A6.24}$$

But at $z = z_a$ $\quad \frac{d(\eta y_s)}{dz} = 0$ by definition.

$\therefore$ equation A6.15 becomes:

$$\frac{dy}{dz} = -PM\phi^2\eta_{ss}y_s \qquad \text{A6.25}$$

Combining equations A6.4 and A6.25:

$$[\phi^2\eta_{ss}y_s = \frac{3}{2}D_m Sh(y-y_s)]_{z=z_a} \qquad \text{A6.26}$$

Solving equations A6.24 and A6.26 for y and y_s:

$$y(z_a) = \frac{1}{[1+\eta_{ss}P/(1+2\eta_{ss}\phi^2/3D_mSh)]} \qquad \text{A6.27}$$

$$y_s(z_a) = \frac{y(z_a)}{[1+2\eta_{ss}\phi^2/3D_mSh]} \qquad \text{A6.28}$$

Putting $\eta^\infty = \eta_{ss}$ in equation A6.22 and integrating using equations A6.27 and A6.28 as boundary conditions:

for $z \geq z_a$

$$y = \left[\frac{1}{1+\dfrac{\eta_{ss}P}{[1+2\eta_{ss}\phi^2/3D_mSh]}}\right] \exp\left\{\frac{-PM\phi^2\eta_{ss}(z-z_a)}{\dfrac{1+2\eta_{ss}\phi^2}{3D_mSh}}\right\} \qquad \text{A6.29}$$

Substituting y = 1 at z = 0 in the above equation allows an estimate of the entrance length to be made. It is found that $z_a \simeq 1/M\phi^2$ as for no film resistance. This is to be expected since in deriving the above equation it has been assumed that the film concentration profile is established rapidly in comparison to the particle concentration profile. The model used would therefore not show any effect of film resistance lengthening the entry region.

For the entry region ($z < 1/M\phi^2$) a solution for y may be found from equations A1.1 to A1.4 and A1.6 with equation A6.30 replacing equation A1.5.

$$\frac{\partial Y(1,z)}{\partial x} = \frac{D_mSh}{2}[y(z)-Y(1,z)] \qquad \text{A6.30}$$

By Laplace Transformation:

for $z < z_a$

$$\boxed{y(z) = \frac{1}{(1+P)} + \sum_{n=2}^{\infty} \frac{N}{(\gamma_{fn}+N)} \cdot \frac{\exp(\gamma_{fn} Mz)}{F_{fn}}} \qquad \text{A6.31}$$

where: $$F_{fn} = \frac{3}{2} + \frac{1}{ShD_m} \cdot (\gamma_{fn}+N) - \frac{\gamma_{fn}}{\gamma_{fn}+N} \cdot (1+D_m Sh/4) \qquad \text{A6.32}$$

and the γ_{fn}'s are given by the solution of:

$$\gamma_{fn} = \frac{2}{D_m Sh} (\gamma_{fn}+N)(1-\sqrt{-\gamma_{fn}} \cot\sqrt{-\gamma_{fn}}) \qquad \text{A6.33}$$

The assumptions which have been made in deriving equations A6.29 and A6.31 are as follows:-

(i) The film concentration profile is established rapidly in comparison to the particle concentration profile.

(ii) The volume of the film is negligible compared to the volume of the bulk gas phase.

A6.3 General Rate Laws

Numerical solution of equations 4.11 to 4.14, 4.16 and A6.30 is necessary for rate laws other than first order.

APPENDIX 7

FILM HEAT TRANSFER RESISTANCE

A7.1 Importance of Film Heat Transfer Resistance

In contrast to film mass transfer, film heat transfer is generally worse than heat transfer within the catalyst particle since the ratio of the conductivities (κ_g/κ_{eff}) is of the order of 0.1 or less. The result of this is that it cannot be assumed that film temperature profile changes are faster than particle temperature profile changes. Thus the equation A7.1, equivalent to the mass transfer equation A6.2, is not generally true. However, for situations where the rate of temperature change along the reactor is small, a steady state approximation may be made.

$$\left.\frac{\partial \tau}{\partial x}\right|_{x=1} = \kappa_m \frac{Nu_p}{2} (\tau_g - \tau_s) \qquad \text{A7.1}$$

Writing the heat transfer equivalent of equation 4.12

$$\frac{d\tau_g}{dz} = -3P_T M_T \left.\frac{\partial \tau}{\partial x}\right|_{x=1} \qquad \text{A7.2}$$

and, combining equations A7.1 and A7.2:

$$\frac{d\tau_g}{dz} = -\frac{3}{2} P_T M_T \kappa_m Nu_p (\tau_g - \tau_s) = N_T (\tau_s - \tau_g) \qquad \text{A7.3}$$

where $$N_T = 3P_T M_T \kappa_m Nu_p / 2 \qquad \text{A7.4}$$

A heat balance on the reactor gives:

$$(1-\varepsilon)(1-\alpha)u_s\rho_s C_{ps}T_{go}+\alpha u_g\rho_g C_{pg}T_{go}+\alpha u_g(c_o-c)(-\Delta H)$$

$$-\varepsilon u_s\eta_* c_s(1-\alpha)(-\Delta H)=(1-\varepsilon)(1-\alpha)u_s\rho_s C_{ps}\eta_T T_s+\alpha u_g\rho_g C_{pg}T_g \qquad \text{A7.5}$$

which in dimensionless form is:

$$\boxed{P_T(\eta_T\tau_s-1)+(\tau_g-1)= -\frac{P_T M_T\chi[(1-y)-\eta_* P y_s]}{PM}} \qquad \text{A7.6}$$

where

$$\eta_T = \frac{3}{\tau_s}\int_0^1 x^2\tau dx = \frac{\bar{\tau}}{\tau_s} \qquad \text{A7.7}$$

$$\chi = \frac{\sigma_g^2}{\phi_g^2} = \frac{D_{eff}c_o\Delta H}{\kappa_{eff}T_{go}} \qquad \text{A7.8}$$

and η_* is given by equation A5.5.

Differentiating equation 7.6 with respect to z and substituting from equation A5.4 gives the reactor heat balance equation:

$$P_T\frac{d(\eta_T\tau_s)}{dz} + \frac{d\tau_g}{dz} = -P_T M_T\sigma_g^2\eta_g\Psi_{x=1} \qquad \text{A7.9}$$

Assuming that the catalyst particles may be considered to be in a pseudo steady state, equation 3.6 may be used to give:

$$T_{max} - T_s = \frac{(-\Delta H)D_{eff}c_s}{\kappa_{eff}} \qquad \text{A7.10}$$

i.e.

$$\boxed{\tau_{max} - \tau_s = -\chi y_s} \qquad \text{A7.11}$$

An estimate of the temperature rise within the particles may be obtained from the above equation using values of the parameters from the example given in section 4.8.

$D_{eff} = 5 \times 10^{-7}\ m^2/s$; $\kappa_{eff} = 0.17\ J/sm°K$;
$c_o = 2.04 \times 10^{-1}\ moles/m^3$; $\Delta H = -1.881 \times 10^6\ J/mole$;
$T_{go} = 762°K$ (Catalyst 2, optimum isothermal temperature)

These give $\chi = -0.001481$ A7.12

Since the maximum rise will be for $y_s = 1$

$$T_{max} - T_s = 0.001481 \times 762 = 1.13°K \qquad \text{A7.13}$$

This is in agreement with the conclusions of section 3.3.1 that the particles in a transport reactor are essentially isothermal.

The assumption that $\eta_T \simeq 1$ can be made in the light of the above result and equation A7.9 re-written as:

$$P_T \frac{d\tau_s}{dz} + \frac{d\tau_g}{dz} = -P_T M_T \sigma_g^2 \eta_g \Psi_{x=1} \qquad \text{A7.14}$$

The maximum surface heat flux and hence film temperature drop may be found using equation A7.3.

Differentiating and setting equal to zero for the maximum:

$$\frac{d^2\tau_g}{dz^2} = N_T \left[\frac{d\tau_s}{dz} - \frac{d\tau_g}{dz} \right] = 0 \qquad \text{A7.15}$$

Thus the maximum particle film temperature drop occurs when:

$$\frac{d\tau_s}{dz} = \frac{d\tau_g}{dz} \qquad \text{A7.16}$$

This is true only at one position in the reactor i.e. at $z = z_m$. (It also holds at $z = \infty$ where $d\tau_s/dz = 0$ for an adiabatic reactor).

Substituting equation A7.16 in equation A7.14.

$$\left[\frac{d\tau_g}{dz}\right]_{z_m} = \frac{-P_T M_T \sigma_g^2 [\eta_g \Psi_{x=1}]}{(1+P_T)} \quad z=z_m \qquad \text{A7.17}$$

Combining equations A7.3 and A7.17:

$$\boxed{[\tau_s - \tau_g]_{max} = \frac{-2\sigma_g^2 [\eta_g \Psi_{x=1}]}{3(1+P_T)\kappa_m Nu_p} \quad z=z_m} \qquad \text{A7.18}$$

Using equations A7.18 and A7.11:

$$[\tau_s - \tau_g]_{max} = \frac{[\tau_{max} - \tau_s]_{z_m}}{y_s(z_m)} \times \frac{2\phi_g^2 [\eta_g \Psi_{x=1}]_{z_m}}{3(1+P_T)\kappa_m Nu_p} \qquad \text{A7.19}$$

This equation enables the temperature difference across the particle film to be compared with the temperature rise within the particle.

For a first order case equation A7.19 may be simplified considerably since $[\Psi_{x=1} = y_s]_{z_m}$ and η_g is constant outside the entry region. For large ϕ, $\eta_g = 3/\phi$ thus:

($\phi > 3$)

$$[\tau_s-\tau_g]_{max} = [\tau_{max}-\tau_s]_{z_m} \cdot \frac{2\phi}{(1+P_T)\kappa_m Nu_p} \qquad A7.20$$

Taking values of $\kappa_m = 0.1$ and $Nu_p = 4$ as typical and taking $(1+P_T) = 30$ (from section 4.8) as typical:

$$[\tau_s-\tau_g]_{max} = [\tau_{max}-\tau_s]_{z_m} \cdot \phi/6 \qquad A7.21$$

$[\tau_{max}-\tau_s]$ evaluated at z_m can only be found if $y_s(z_m)$ is known, however the maximum value of $[\tau_{max}-\tau_s]$ (which occurs for $y_s=1$) has been determined (equation A7.13) and this may be used to place an upper limit on the film temperature rise.

Using $[\tau_{max}-\tau_s] = 0.001481$ a value of ϕ^2 of 11305 is required to produce a film temperature rise of 20°K which roughly corresponds to an increase of 50% in the reaction rate for the example in Appendix 8.

The following may be taken as a guide to the importance of film heat transfer resistance for reactions of order one and above:

for $\phi^2 \leqslant 1000$	film heat transfer may be neglected,
for $\phi^2 > 1000$	equation 7.18 should be used to estimate the importance of film heat transfer resistance.

A7.2 Temperature Rise Along Reactor

The temperature rise along the reactor for adiabatic operation may be calculated by use of equation A7.6 making the following assumptions:-

$$P \text{ is small} \quad \therefore \quad \eta_* P y_s << (1-y)$$

$$\eta_\tau \simeq 1 \quad ; \quad \tau_g \simeq \tau_s \quad \text{at exit}$$

$$\therefore \quad [\tau_s]_{exit} = \frac{-P_T M_T \chi [1-y_{exit}] + 1}{(1+P_T)\ PM} \qquad \text{A7.22}$$

Using the parameters of the system in section 4.8 and assuming total conversion (i.e. $y_{ex} = 0$):

$$[\tau_s]_{exit} = 1 + \frac{28.9 \times 17.7 \times 0.001481}{29.9 \times 0.01 \times 93.8}$$

$$= 1 + 0.027 = 1.027$$

$$\therefore \text{ For } T_{go} = 762°K \quad \underline{T_{exit} - T_{go} = 20.6°K}$$

NB For adiabatic conditions in a fixed bed reactor, the temperature rise of the gas stream for the same conversion of reactant would be about P_T times the above amount or $\simeq 600°K$.

The results obtained in this Appendix showing almost isothermal catalyst particles and small film temperature drops suggest that the original steady state approximation is reasonable. At high values of ϕ however, where appreciable film temperature differences exist, these assumptions may break down and equation A7.18 should be used with caution.

APPENDIX 8

OPTIMIZATION

For the reaction system A → B → C consisting of two consecutive first order reactions the system equations and boundary conditions are:

$$\frac{1}{M_A}\frac{\partial Y_A}{\partial z} = \frac{\partial^2 Y_A}{\partial x^2} + \frac{2}{x}\frac{\partial Y_A}{\partial x} - \phi_{\infty A}^2 \exp(-G_A/\tau)\, Y_A \qquad \text{A8.1}$$

$$\frac{1}{M_B}\frac{\partial Y_B}{\partial z} = \frac{\partial^2 Y_B}{\partial x^2} + \frac{2}{x}\frac{\partial Y_B}{\partial x} - \phi_{\infty B}^2 \exp(-G_B/\tau) Y_B + D_N \phi_{\infty A}^2 \exp(-G_A/\tau) Y_A \qquad \text{A8.2}$$

$$\frac{1}{M_T}\frac{\partial \tau}{\partial z} = \frac{\partial^2 \tau}{\partial x^2} + \frac{2}{x}\frac{\partial \tau}{\partial x} - \sigma_{\infty B}^2 \exp(-G_B/\tau) Y_B - \sigma_{\infty A}^2 \exp(-G_A/\tau) Y_A \qquad \text{A8.3}$$

$$Y_A(x,0) = Y_B(x,0) = 0 \;;\; \tau(x,0) = 1 \quad 0 \leq x < 1 \qquad \text{A8.4}$$

$$Y_A(1,0) = 1 \;;\; Y_B(1,0) = 0 \;;\; \tau(1,0) = 1 \qquad \text{A8.5}$$

$$Y_A(1,z) = y_A(z) \;;\; Y_B(1,z) = y_B(z) \qquad \text{A8.6}$$

$$\frac{\partial Y_A}{\partial x}(0,z) = \frac{\partial Y_B}{\partial x}(0,z) = \frac{\partial \tau}{\partial x}(0,z) = 0 \qquad \text{A8.7}$$

$$\left[\frac{\partial Y_A}{\partial z} = -3PM_A \frac{\partial Y_A}{\partial x}\right]_{x=1} \qquad \text{A8.8} \qquad \left[\frac{\partial Y_B}{\partial z} = -3PM_B \frac{\partial Y_B}{\partial x}\right]_{x=1} \qquad \text{A8.9}$$

$$\left[\frac{\partial \tau}{\partial z} = -3P_T M_T \frac{\partial \tau}{\partial x} + Q\right]_{x=1} \qquad \text{A8.10} \qquad Q = \frac{2L}{a_o}\left(\frac{Nu_s}{Re_t \,.\, Pr}\right).(\tau_w - \tau_{x=1}) \qquad \text{A8.11}$$

The assumptions made in the derivation of these equations are given in section 4.8.

Using the method of Denn, Gray and Ferron (1966) the following adjoint equations and boundary conditions result:

$$\frac{\partial \lambda_A}{\partial z} = \exp(-G_A/\tau)\left[(\phi^2_{\infty A} M_A)\lambda_A - (D_N \phi^2_{\infty A} M_B)\lambda_B + (\sigma^2_{\infty A} M_T)\lambda_T\right] + M_A\left[\frac{\partial}{\partial x}\left(\frac{2\lambda_A}{x}\right) - \frac{\partial^2 \lambda_A}{\partial x^2}\right] \quad \text{A8.12}$$

$$\frac{\partial \lambda_B}{\partial z} = \exp(-G_B/\tau)\left[(\phi^2_{\infty B} M_B)\lambda_B + (\sigma^2_{\infty B} M_T)\lambda_T\right] + M_B\left[\frac{\partial}{\partial x}\left(\frac{2\lambda_B}{x}\right) - \frac{\partial^2 \lambda_B}{\partial x^2}\right] \quad \text{A8.13}$$

$$\frac{\partial \lambda_T}{\partial z} = \exp(-G_A/\tau)\,\frac{Y_A G_A}{\tau^2}\left[(\phi^2_{\infty A} M_A)\lambda_A - (D_N \phi^2_{\infty A} M_B)\lambda_B + (\sigma^2_{\infty A} M_T)\lambda_T\right] +$$

$$\exp(-G_B/\tau)\frac{Y_B G_B}{\tau^2}\left[(\phi^2_{\infty B} M_B)\lambda_B + (\sigma^2_{\infty B} M_T)\lambda_T\right] + M_T\left[\frac{\partial}{\partial x}\left(\frac{2\lambda_T}{x}\right)\frac{-\partial^2 \lambda_T}{\partial x^2}\right] \quad \text{A8.14}$$

$$\lambda_A(x,1) = \lambda_B(x,1) = \lambda_T(x,1) = 0 \qquad 0 \leq x < 1 \quad \text{A8.15}$$

$$\lambda_A(1,1) = \lambda_T(1,1) = 0 \;;\; \lambda_B(1,1) = 1 \quad \text{A8.16}$$

$$\lambda_A(0,z) = \lambda_B(0,z) = \lambda_T(0,z) = 0 \quad \text{A8.17}$$

$$\left[3PM_A\left(2\lambda_A - \frac{\partial \lambda_A}{\partial x}\right) + \frac{\partial \lambda_A}{\partial z} = 0\right]_{x=1} \quad \text{A8.18}$$

$$\left[3PM_B\left(2\lambda_B - \frac{\partial \lambda_B}{\partial x}\right) + \frac{\partial \lambda_B}{\partial z} = 0\right]_{x=1} \quad \text{A8.19}$$

$$\left[3P_T M_T \left(2\lambda_T - \frac{\partial \lambda_T}{\partial x} \right) + \frac{\partial \lambda_T}{\partial z} = 0 \right]_{x=1} \qquad \text{A8.20}$$

Equations A8.1 to A8.11 were solved from z = 0 to z = 1 using a Crank-Nicholson method. Equations A8.12 to A8.20 were then solved from z = 1 to z = 0 by the same method. A new function Q(z) was then chosen according to the relation:

$$Q^{n+1} = Q^n + \delta Q \qquad \text{A8.21}$$

where

$$\delta Q = \frac{s[\lambda_T]^{x=1}}{\left[\int_0^1 [\lambda_T]^2 dz \right]^{\frac{1}{2}}} \qquad \text{A8.22}$$

s is a scaling factor.

This procedure was repeated until no further improvement in $Y_B(1,1)$ could be obtained.

The computer programme used for numerical solution of the above equations is given as programme 3 of Appendix 9.

APPENDIX 9

COMPUTER PROGRAMMES

Programme 1 - Numerical solution of reactor equations for a single irreversible reaction.

Programme 2 - Evaluation of optimum isothermal temperature for two consecutive first order reactions. ($A \rightarrow B \rightarrow C$).

Programme 3 - Determination of optimum axial heat flux profile for two consecutive first order reactions. ($A \rightarrow B \rightarrow C$).

PROGRAMME 1

```
      PROGRAM CATAL(INPUT,OUTPUT,TAPE5=INPUT,TAPE6=OUTPUT)
C
C     THIS PROGRAM SOLVES  THE TRANSPORT REACTOR EQUATIONS NUMERICALLY
C     BY A CRANK NICHOLSON METHOD FOR GENERAL RATE LAWS WITH NON-
C     EXHAUSTION OF REACTANT.  THE RATE LAW AND ITS DERIVATIVE ARE
C     SUPPLIED AS FUNCTIONS.
C
C     IMAX IS THE NUMBER OF RADIAL INCREMENTS
C     THETA, ANU, AND GAMMA ARE CONSTANTS IN THE CRANK NICHOLSON METHOD
C          THEY USUALLY HAVE THE VALUES 0.5, 0.5, AND 1.0 RESPECTIVELY
C     P IS DIMENSIONLESS GROUP P
C     EM IS DIMENSIONLESS GROUP M
C     PHISQ IS THE SQUARE OF THE THIELE MODULUS
C     OX IS THE RATIO OF CO/O2 AT THE REACTOR INLET
C     COI IS THE CONCENTRATION OF CO AT THE REACTOR INLET
C     A, B, AND C ARE ELEMENTS OF THE MATRIX EQUATIONS
C
      DIMENSION A0(102),A1(102),B0(102),B1(102),C0(102),C1(102),D(102),
     1V(102),X(102),Y(102),Z(102),DZ(200)
C
      COMMON COI,OX
C
C       READ IN SYSTEM PARAMETERS,WEIGHTING FACTORS AND STEP SIZES
C
      READ(5,1000) IMAX,THETA,ANU,GAMMA,P,EM,PHISQ
 1000 FORMAT(I3/5(F10.4/),E10.4)
      READ(5,1001) OX,COI
 1001 FORMAT(F10.4/F10.4)
      WRITE(6,2000) EM,P,PHISQ,THETA,ANU,GAMMA,IMAX
 2000 FORMAT(@1M = @,F10.4,5X,@P = @,F10.4,5X,@PHISQ = @,F10.4//X,
     1@THETA = @,F5.3,5X,@MU = @,F5.3,5X,@GAMMA = @,F5.3//X,@I = @,I3//)
      WRITE(6,2004) OX,COI
 2004 FORMAT(X,@OX = @,F10.4,5X,@COI = @,E10.4//)
C
C       READ IN INITIAL CONDITIONS
C
      IP = IMAX-1
      IQ = IMAX+1
      ID = IMAX/10
      DO 9 I=1,IMAX
    9 Y(I) = 0.0
      Y(IQ) = 1.0
      WRITE(6,2001) (Y(I),I=1,IQ,ID)
 2001 FORMAT(@0INITIAL PROFILE@/2(16F8.3/))
C
      PI = 3.14159
      AI = IMAX
      DELX = 1./AI
      DIST = 0.0
      CK = 0.0
C
      NN = 200
      DO 93 NS = 1,3
      DO 93 NQ = 1,20
      NR = NQ+(NS-1)*20
      AS = NS
   93 DZ(NR) = (5. E-7)*(10.**AS)
      DO 94 NR = 61,140
   94 DZ(NR) = 0.0025
      DO 95 NR = 141,162
   95 DZ(NR) = 0.01
      DO 96 NR = 163,199
   96 DZ(NR) = 0.015
      DZ(200) = 0.0139
C
C       BEGIN NUMERICAL INTEGRATION
C
      DO 17 N=1,NN
      DIST = DIST+DZ(N)
      RHO = (EM*DZ(N))/(DELX*DELX)
      ANU = EM*DZ(N)*PHISQ
C
C       CALCULATE COEFFICIENTS IN SIMULTANEOUS EQUATIONS
C
      IF(Y(1).LE.0.0) Y(1) = 1.0 E-6
      B1(1) = 1.+6.*RHO*THETA+ANU*AMU*DRT(Y(1))
      C1(1) = -6.*RHO*THETA
      B0(1) = 1.-6.*RHO*(1.-THETA)-ANU*(RATE(Y(1))/Y(1)-AMU*DRT(Y(1)))
      C0(1) = 6.*RHO*(1.-THETA)
C
      DO 11 I=2,IMAX
      RI = I
      IF(Y(I).LE.0.0) Y(I) = 1.0 E-6
      A1(I) = -RHO*THETA*(1.-1./RI)
```

```
      B1(I) = 1.+2.*RHO*THETA+AMU*AMU*DRT(Y(I))
      C1(I) = -RHO*THETA*(1.+1./RI)
      A0(I) = RHO*(1.-THETA)*(1.-1./RI)
      B0(I) = 1.-2.*RHO*(1.-THETA)-AMU*(RATE(Y(I))/Y(I)-AMU*DRT(Y(I)))
   11 C0(I) = RHO*(1.-THETA)*(1.+1./RI)
C
      R11 = A1(IMAX)
      S11 = B1(IMAX)
      T11 = C1(IMAX)
      R01 = A0(IMAX)
      S01 = B0(IMAX)
      T01 = C0(IMAX)
C
      PP = P*DELX*RHO
C
      R12 = 1.5*PP*THETA*GAMMA
      S12 = -3.*PP*THETA*(1.+GAMMA)
      T12 = 1.+1.5*PP*THETA*(2.+GAMMA)
      R02 = -1.5*PP*(1.-THETA)*GAMMA
      S02 = 3.*PP*(1.-THETA)*(1.+GAMMA)
      T02 = 1.-1.5*PP*(1.-THETA)*(2.+GAMMA)
C
      A1(IMAX) = R11*T12-R12*T11
      B1(IMAX) = S11*T12-S12*T11
      A0(IMAX) = R01*T12-R02*T11
      B0(IMAX) = S01*T12-S02*T11
      H = (T01*T12-T02*T11)*Y(IQ)
C
C       CALCULATE VECTOR @V@ FOR USE IN THOMAS ALGORITHM
C
      V(1) = B1(1)
      DO 12 K=2,IMAX
   12 V(K) = B1(K)-A1(K)*C1(K-1)/V(K-1)
C
C       CALCULATE VECTOR @D@ ,R.H.S. OF MATRIX EQUATIONS
C
      D(1) = B0(1)*Y(1)+C0(1)*Y(2)
      DO 13 J=2,IP
   13 D(J) = A0(J)*Y(J-1)+B0(J)*Y(J)+C0(J)*Y(J+1)
      D(IMAX) = A0(IMAX)*Y(IP)+B0(IMAX)*Y(IMAX)+H
C
C       CALCULATE VECTOR @W@ FOR USE IN THOMAS ALGORITHM
C
      W(1) = D(1)/V(1)
      DO 14 K=2,IMAX
   14 W(K) = (D(K)-A1(K)*W(K-1))/V(K)
C
C       SOLUTION FOR @Y@
C
      Z(IMAX) = W(IMAX)
      DO 15 K=1,IP
      KK = IMAX-K
   15 Z(KK) = W(KK)-C1(KK)*Z(KK+1)/V(KK)
      Z(IQ) = (R02*Y(IP)+S02*Y(IMAX)+T02*Y(IQ)-R12*Z(IP)-S12*Z(IMAX))/
     1T12
      DO 16 M=1,IQ
      Y(M) = Z(M)
   16 IF(Y(M).LT.0.0) Y(M) = 0.0
C
C       WRITE OUT PROFILES
C
      IF(((DIST-CK)*10.0).LT.1.0) GO TO 17
      WRITE(6,2002)  N,DIST,(Y(I),I=1,IQ,ID)
 2002 FORMAT(30PROFILE AT STEP  @,I5,3X,@AND DISTANCE @,E14.4/2(16F8.3/
     1))
      CK = CK + 0.1
      IF(DIST.GE.1.0) GO TO 18
   17 CONTINUE
   18 WRITE(6,2003)
 2003 FORMAT(1H1)
      STOP
      END



      FUNCTION RATE(Y)
      COMMON COI,OX
      RK1 = 1. E4
      B = RK1*COI
      RATE =(Y*(1.+B)*(1.+B)/((1.+B*Y)*(1.+B*Y)))*(1.-OX*(1.-Y)/2.)
      RETURN
      END
```

```
      FUNCTION DRT(Y)
C
C     THIS FUNCTION PROVIDES THE DERIVATIVE OF THE RATE FUNCTION
C
      COMMON CO1,OX
      RK1 = 1.E4
      B = RK1*CO1
      DRT = ((1.+B)*(1.+B)/((1.+B*Y)**3))*((1.-B*Y)*(1.-OX*(1.-Y)/2.)
     1          +(1.+B*Y)*OX*Y*Y/2.)
      RETURN
      END
```

PROGRAMME 2

```
      PROGRAM ISOPT(INPUT,OUTPUT,TAPE5=INPUT,TAPE6=OUTPUT)
C
C         THIS PROGRAM FINDS THE OPTIMUM ISOTHERMAL TEMPERATURE FOR
C         PRODUCTION OF THE INTERMEDIATE IN A SET OF CONSECUTIVE FIRST
C         ORDER REACTIONS OCCURING IN A TRANSPORT REACTOR
C
C         P,EM,PHISQ ARE THE DIMENSIONLESS GROUPS P,M AND THE SQUARE OF
C         THIELE MODULUS RESPECTIVELY
C         G IS THE DIMENSIONLESS ACTIVATION ENERGY
C         DLEN IS THE DIMENSIONLESS DISTANCE ALONG THE REACTOR
C         PHI0 IS THE THIELE MODULUS AT INFINITE TEMPERATURE
C         X,Y,ZJ ARE THE ROOTS OF THE EQUATIONS AND ARE USED IN THE
C         THE TERMS OF THE SUMMATION TERM
C         C IS THE DIMENSIONLESS CONCENTRATION OF B AT THE REACTOR EXIT
C
      DIMENSION X(2,50),Y(2,50),ZJ(2,50),TTERM(2,50),PHISQ(2),PHI0(2),
     1          EM(2),G(2),DLEN(10),C(2)
      READ(5,1100) P,EM,PHI0,G
 1100 FORMAT(7E10.4)
C
      DO 10 JD=1,10
      DINC = 0.1
      AJD = JD
   10 DLEN(JD) = DINC*AJD
C
      WRITE(6,2100) P,EM,PHI0,G
 2100 FORMAT(X////@ P = @,F8.3/X,@MA = @,F12.2,5X,@MB = @,F12.2/X
     1       ,@PHI0A = @,E14.4,5X,@PHI0B = @,E14.4/X,@GA = @,F6.2,5X,
     2       @GB = @,F6.2////)
C
      T = 1.
      DELT = 0.1
      DN = EM(1)/EM(2)
      CPRES = 0.
C
   40 DO 45 I=1,2
   45 PHISQ(I) = PHI0(I)*EXP(-G(I)/T)
C
      DO 60 JD=1,10
      SIGAB = 0.
C
      DO 30 IZ=1,2
      SIGMA = 0.
C
      DO 70 JX=1,50
      IF(JD.NE.1) GO TO 100
      X(IZ,JX) = XVAL(JX,P,PHISQ(IZ))
      Y(IZ,JX) = -X(IZ,JX)-PHISQ(IZ)
      IF(IZ.EQ.1) ZJ(1,JX) = -DN*Y(1,JX)-PHISQ(2)
      IF(IZ.EQ.2) ZJ(2,JX) = -Y(2,JX)/DN-PHISQ(1)
      TTERM(IZ,JX) = TERM(X(IZ,JX),Y(IZ,JX),ZJ(IZ,JX),P,EM(IZ),EM(3-IZ))
  100 FTERM = TTERM(IZ,JX)*EXP(EM(IZ)*Y(IZ,JX)*DLEN(JD))
      SIGMA = SIGMA+FTERM
      IF(ABS(FTERM).GT.(1. E-10)*ABS(SIGMA)) GO TO 70
      GO TO 85
C
   70 CONTINUE
C
   85 SIGAB = SIGAB+SIGMA
C
   30 CONTINUE
C
      C(2) = SIGAB**3.*P*EM(1)*PHISQ(1)
      WRITE(6,2110) DLEN(JD),C(2)
 2110 FORMAT(X,@L = @,F6.3,10X,@CB = @,F8.5)
C
   60 CONTINUE
C
C         TEST FOR CONVRGENCE
C
      IF(C(2).LT.CPRES) DELT = -DELT/2.
      IF(ABS((C(2)-CPRES)/C(2)).LT.1. E-6) STOP
      CPRES = C(2)
      T = T+DELT
      WRITE(6,2120) T
 2120 FORMAT(X//@ T = @,F9.5/)
      GO TO 40
      END
```

```
      FUNCTION XVAL(JX,P,PHISQ)
C
C         THIS FUNCTION  EVALUATES THE COEFFICIENTS X(N) AND Y(N)
C
C         GUESSES ARE MADE FOR THE VALUES OF X AND Y AND THEN BY COMPARING
C         THE TWO SIMULTANEOUS EQUATIONS FOR XAND Y RESIDUALS ARE
C         DETERMINED. BY EXAMINING THE SIGN OF THESE RESIDUALS A CONVERGENCE
C         TO THE TRUE VALUES OF X AND Y IS OBTAINED BY TAKING INCREASINGLY
C         SMALLER STEPS.
C
      IF(JX.NE.1) GO TO 1
      X=-PHISQ
      GO TO 2
    1 RJX=JX-1
      PI =3.141592
      PISQ=PI*PI
      X=RJX*RJX*PISQ
    2 DO 3 JACC=1,100
      AMULT=(0.1)**JACC
      DO 4 KSTEP=1,1000
      X=X+AMULT
      IF(JX.NE.1) GO TO 5
      IF(X.LT.0.0) GO TO 5
      X=X-AMULT
      GO TO 3
    5 IF(RESID(X,P,PHISQ)) 4,7,8
    4 CONTINUE
      WRITE(6,1000)
 1000 FORMAT(8 'ERROR - X HAS NOT BEEN FOUND. 8)
    8 X=X-AMULT
C
C         TEST FOR ACCURACY OF DETERMINED ROOT
C
      IF(ABS(X/AMULT).GT.(10.0 E+10)) GO TO 7
    3 CONTINUE
    7 XVAL=X
      RETURN
      END



      FUNCTION RESID(X,P,PHISQ)
C
C         THIS FUNCTION EVALUATES THE RESIDUALS USED IN DETERMINING  THE
C         QUANTITIES X(N) AND Y(N) FOR N GREATER THAN 0   IN THE FUNCTION  XVAL
C
      D=(X+PHISQ)/(3.0*P)+1.0
      E = RTCT(X)
      RESID=D-E
      RETURN
      END



      FUNCTION TERM(X,Y,ZJ,P,EM1,EM2)
      F = 1.+1.5*P-Y/(2.*X)+Y*Y/(6.*P*X)
      BOT = (X-ZJ)*F*(EM1*Y-3.*P*EM2*(1.-RTCT(ZJ)))
      TOP = RTCT(ZJ)-RTCT(X)
      TERM = TOP/BOT
      RETURN
      END



      FUNCTION RTCT(X)
      IF(X.LT.0.0.AND.(-X).LT.100.) RTCT = SQRT(-X)/TANH(SQRT(-X))
      IF(X.LT.0.0.AND.(-X).GE.100.) RTCT = SQRT(-X)
      IF(X.GE.0.0) RTCT = SQRT(X)*(COS(SQRT(X))/SIN(SQRT(X)))
      RETURN
      END
```

PROGRAMME 3

```
      PROGRAM OPTTEM(INPUT,OUTPUT,TAPE5 = INPUT,TAPE6 = OUTPUT)
C
C     THIS PROGRAM FINDS THE OPTIMUM HEAT FLUX TO MAXIMIZE THE YIELD
C     OF THE INTERMEDIATE IN A SET OF TWO CONSECUTIVE REACTIONS OCCURING
C     IN A TRANSPORT REACTOR
C
C     A AND B ARE DIMENSIONLESS CONCENTRATIONS OF COMPONENTS A AND B
C     T IS DIMENSIONLESS TEMPERATURE
C     D IS ELEMENT OF MATRIX EQUATION
C     GA,GB AND GT ARE ADJOINT VARIABLES
C     GTN IS VALUE OF GT AT PARTICLE SURFACE
C     Q IS DIMENSIONLESS HEAT FLUX
C     DZ IS DIMENSIONLESS LENGTH INCREMENT
C
C     NA1  IS ONE FOR WRITING OUT OF A,B,T AT REACTOR ENTRANCE
C     NANN IS ONE FOR WRITING OUT OF A,B,T AT REACTOR EXIT
C     NGT  IS ONE FOR WRITING OUT OF GTN ONLY AT EVERY 0.1 OF REAC. LEN.
C     NANY IS ONE FOR WRITING OUT OF A,B,T    AT EVERY 0.1 OF REAC. LEN.
C     NGNM IS ONE FOR WRITING OUT OF ADJOINT VARIABLES AT REACTOR EXIT
C     NGNY IS ONE FOR WRITING OUT OF ADJOINT VARIABLES AT EVERY .1 OF L.
C     CONST IS SCALE FACTOR IN CHOOSING NEW HEAT FLUX
C     IN IS NUMBER OF RADIAL INCREMENTS
C     AM IS DIMENSIONLESS GROUP MA
C     BM IS DIMENSIONLESS GROUP MB
C     TM IS DIMENSIONLESS GROUP MT
C     PH1 IS THIELE MODULUS AT INFINITE TEMPERATURE FOR REACTION ONE
C     PH2 IS THIELE MODULUS AT INFINITE TEMPERATURE FOR REACTION TWO
C     PS1 AND PS2 ARE EQUIVALENTS OF PH1 AND PH2 IN TEMPERATURE EQUATION
C     G1 AND G2 ARE DIMENSIONLESS ACTIVATION ENERGIES FOR REACTIONS
C     P AND PT ARE DIMENSIONLESS GROUPS
C
      DIMENSION A(11,201),B(11,201),T(11,201),D(33,8),GA(11),GB(11),
     1          GT(11),GTN(201),LJ(6),Q(201),DZ(200)
      COMMON /ONE/ A,B,T,D,GA,GB,GT,GTN,LJ
      COMMON /TWO/ N,NN,NM,NY,NGT,NGNY,NANY,NANN,SUMZ,IM3,IM32,JM3,JM32,
     1     IM,M
      DOUBLE PRECISION D
C
      READ(5,1000) NA1,NANN,NGT,NANY,NGNM,NGNY,CONST,IN,AM,BM,TM,
     1             PH1,PH2,PS1,PS2,G1,G2,PT,P
 1000 FORMAT(6(I2/),E10.2/I2/11(E10.2/))
      WRITE(6,2006) NA1,NANN,NGT,NANY,NGNM,NGNY,CONST,IN,AM,BM,TM,PH1,
     1              PH2,PS1,PS2,G1,G2,PT,P
 2006 FORMAT(@1NA1 = @,I2/@ NANN = @,I2/@ NGT = @,I2/@ NANY = @,I2/
     1       @ NGNM = @,I2/@ NGNY = @,I2/@ CONST = @,E10.2/@ IN = @,I2/
     2       @ AM = @,E10.2/@ BM = @,E10.2/@ TM = @,E10.2/@ PH1 = @
     3       ,E10.2/@ PH2 = @,E10.2/@ PS1 = @,E10.2/@ PS2 = @,E10.2/
     4       @ G1 = @,E10.2/@ G2 = @,E10.2/@ PT = @,F10.2/@ P = @,
     5       E10.2//)
      TH = 0.5
      CN = 0.5
      AL = 0.5
      BE = 0.5
      RIN = IN
      DX = 1./RIN
      IM = IN+1
      IM3 = 3*IM
      IM31 = IM3-1
      IM32 = IM3-2
      IM33 = IM3-3
      IM34 = IM3-4
      IM35 = IM3-5
      IM38 = IM3-8
C
C     DEFINE LENGTH INCREMENTS
C
      SUMZ = 0.0
      NN = 200
      DO 93 NS = 1,3
      DO 93 NQ = 1,20
      NR = NQ+(NS-1)*20
   93 DZ(NR) = (5. E-7)*(10**NS)
      DO 94 NR = 61,140
   94 DZ(NR) = 0.0025
      DO 95 NR = 141,162
   95 DZ(NR) = 0.01
      DO 96 NR = 163,199
   96 DZ(NR) = 0.015
      DZ(200) = 0.0139
C
      RNN = NN
      RY = RNN/10.
      NY = RY+1.
      IF(MOD(NN,10).EQ.0) NY = RY
```

```
      WRITE(6,7000) NY
 7000 FORMAT(' NY = ',I3//)
      NM = NN+1
      NM1 = NM+1
C
C     EVALUATE COMMONLY OCCURING GROUPS OF SYMBOLS
C
      PDX = 3.*P*DX
      PDXT = 3.*PT*DX
      PDT = PDX*TH
      PDTT = PDXT*TH
      PDT1 = PDX*(1.-TH)
      PDTT1 = PDXT*(1.-TH)
      PDR = PDX*RE
      PDRT = PDXT*RE
      PDR1 = PDX*(1.-RE)
      PDRT1 = PDXT*(1.-RE)
C
      RNEW = 0.
      SUMZ = 0.
      COLD = CONST
C
C     READ IN INITIAL HEAT FLUX PROFILE
C
      READ(5,1001) (Q(N),N = 1,NM)
 1001 FORMAT (16F4.0)
      WRITE(6,2003) (Q(N),N = 1,NM,NY)
C
  103 ROLD = RNEW
C
C     READ IN BOUNDARY CONDITIONS FOR A,B,T
C
      DO 101 I = 1,IN
      A(I,1) = 0.
      B(I,1) = 0.
  101 T(I,1) = 1.
      A(IM,1) = 1.
      B(IM,1) = 0.
      T(IM,1) = 1.
C
C     READ IN BOUNDARY CONDITIONS FOR ADJOINT VARIABLES
C
      GTN(NM) = 0.
      DO 201 I = 1,IN
      GA(I) = 0.
      GB(I) = 0.
  201 GT(I) = 0.
      GA(IM) = 0.
      GB(IM) = 1.
      GT(IM) = 0.
C
      NLM = NN*2
C
      DO 330 N = 1,NLM
C
      IF(N.EQ.1.AND.NA1.EQ.1)WRITE(6,2002) N,SUMZ,(A(I,1),I = 1,IM),
     1      (B(I,1),I = 1,IM),(T(I,1),I = 1,IM)
 2002 FORMAT('0N = ',I4,5X,'DIST = ',F8.5/' A = ',11F9.5/' B = '11F9.5/
     1          ' T = ',11F9.5//)
      IF(N.EQ.NM.AND.NGM.EQ.1) WRITE(6,2001) N,SUMZ,(GA(I),I = 1,IM),
     1      (GB(I),I = 1,IM),(GT(I),I = 1,IM)
 2001 FORMAT('0N = ',I4,5X,'DIST = ',F8.5/' GA = ',11E9.2/' GB = ',
     1       11E9.2/' GT = ',11F9.2//)
C
C     EVALUATE COMMONLY OCCURING GROUPS OF SYMBOLS
C
      IF(N.GE.NM) GO TO 97
      NL = N
      SUMZ = SUMZ+DZ(NL)
      GO TO 98
   97 NL = NLM-N+1
      SUMZ = SUMZ-DZ(NL)
   98 RA = AM*DZ(NL)/(DX*DX)
      RB = BM*DZ(NL)/(DX*DX)
      RT = TM*DZ(NL)/(DX*DX)
      AN = AM*DZ(NL)*PH1
      BN = BM*DZ(NL)*PH2
      TN1 = TM*DZ(NL)*PS1
      TN2 = TM*DZ(NL)*PS2
      RATH = RA*TH
      RBTH = RB*TH
      RTTH = RT*TH
      RA1TH = RA*(1.-TH)
      RB1TH = RB*(1.-TH)
```

```
      RT1TH = RT*(1.-TH)
      RABE = RA*BE
      RBBE = RB*BE
      RTBE = RT*BE
      RA1BE = RA*(1.-BE)
      RB1BE = RB*(1.-BE)
      RT1BE = RT*(1.-BE)
      IF(N.GE.NM) GO TO 300
C
C     EVALUATE ELEMENTS OF A,B,T MATRIX
C
      DO 105 J = 1,IM3S,3
      K = (J+2)/3
      RK = K
      RK1 = 1.-1./RK
      RK2 = 1.+1./RK
      TG1 = G1/T(K,N)
      TG2 = G2/T(K,N)
      E1 = EXP(-TG1)
      E2 = EXP(-TG2)
      AE = AN*E1
      BE2 = BN*E2
      T1E = TN1*E1
      T2E = TN2*E2
      GAT = TG1*A(K,N)/T(K,N)
      GBT = TG2*B(K,N)/T(K,N)
      CNA = CN*AE
      CNB = CN*BE2
      CNT1 = CN*T1E
      CNT2 = CN*T2E
      CNTG1 = 1.-CN*TG1-CN
      CNTG2 = 1.-CN*TG2-CN
C
      IF(K.EQ.1) GO TO 106
C
      D(J,1) = -RATH*RK1
      D(J+1,1) = -RBTH*RK1
      D(J+2,1) = -RTTH*RK1
      D(J,2) = 0.
      D(J+1,2) = 0.
      D(J+2,2) = CNT1
      D(J,3) = 0.
      D(J+1,3) = -CNA
      D(J+2,3) = CNT2
      D(J,4) = 1.+2.*RATH+CNA
      D(J+1,4) = 1.+2.*RBTH+CNB
      D(J+2,4) = 1.+2.*RTTH+GAT*CNT1+GBT*CNT2
      D(J,5) = 0.
      D(J+1,5) = -GAT*CNA+GBT*CNB
      D(J+2,5) = 0.
      D(J,6) = GAT*CNA
      D(J+1,6) = 0.
      D(J+2,6) = 0.
      D(J,7) = -RATH*RK2
      D(J+1,7) = -RBTH*RK2
      D(J+2,7) = -RTTH*RK2
      D(J,8) = A(K-1,N)*RA1TH*RK1+A(K,N)*(1.-2.*RA1TH-AE*CNTG1)
     1+A(K+1,N)*RA1TH*RK2
      D(J+1,8) = B(K-1,N)*RB1TH*RK1+A(K,N)*AE*CNTG1+B(K,N)*(1.-2.*
     1          RB1TH-BE2*CNTG2)+B(K+1,N)*RB1TH*RK2
      D(J+2,8) = T(K-1,N)*RT1TH*RK1+A(K,N)*(-T1E)*CNTG1+B(K,N)*
     1          (-T2E)*CNTG2+T(K,N)*(1.-2.*RT1TH)+T(K+1,N)*RT1TH*
     2          RK2
C
      GO TO 105
C
  106 D(3,2) = CNT1
      D(2,3) = -CNA
      D(3,3) = CNT2
      D(1,4) = 1.+6.*RATH+CNA
      D(2,4) = 1.+6.*RBTH+CNB
      D(3,4) = 1.+6.*RTTH+GAT*CNT1+GBT*CNT2
      D(1,5) = 0.
      D(2,5) = -CNA*GAT+CNB*GBT
      D(3,5) = 0.
      D(1,6) = CNA*GAT
      D(2,6) = 0.
      D(3,6) = 0.
      D(1,7) = -6.*RATH
      D(2,7) = -6.*RBTH
      D(3,7) = -6.*RTTH
      D(1,8) = A(1,N)*(1.-6.*RA1TH-AE*CNTG1)+A(2,N)*6.*RA1TH
      D(2,8) = A(1,N)*AE*CNTG1+B(1,N)*(1.-6.*RB1TH-BE2*CNTG2)
     1+B(2,N)*6.*RB1TH
```

```
      D(3,8) = A(1,N)*T1E*CNTG1+B(1,N)*(-T2E*CNTG2)+T(1,N)*
     1        (1.-6.*RT1TH)+T(2,N)*6.*RT1TH
C
  105 CONTINUE
C
      D(IM32,1) = -RA*PDT
      D(IM31,1) = -RB*PDT
      D(IM3,1) = -RT*PDTT
      D(IM32,2) = 0.
      D(IM31,2) = 0.
      D(IM3,2) = 0.
      D(IM32,3) = 0.
      D(IM31,3) = 0.
      D(IM3,3) = 0.
      D(IM32,4) = 1.+RA*PDT
      D(IM31,4) = 1.+RB*PDT
      D(IM3,4) = 1.+RT*PDTT
      D(IM32,5) = 0.
      D(IM31,5) = 0.
      D(IM32,6) = 0.
      D(IM32,8) = A(IM,N)*RA*PDT1+A(IM,N)*(1.-PDT1*RA)
      D(IM31,8) = B(IM,N)*RB*PDT1+B(IM,N)*(1.-PDT1*RB)
      D(IM3,8) = T(IM,N)*RT*PDTT1+T(IM,N)*(1.-PDTT1*RT)+(Q(N)*(1.-TH)+
     1           Q(N+1)*TH)*DZ(NL)
C
      JM3 = IM3
      CALL HEPSOL
      GO TO 330
C
  300 M = NLM-N+2
      DO 20 I = 1,IM3
      DO 20 J = 1,8
   20 D(I,J) = 0.
C
C     EVALUATE COMMONLY OCCURING GROUPS OF SYMBOLS
C
      DO 109 J = 1,IM38,3
      K = (J+2)/3
      RK = K+1
      RK1 = 1.-1./RK
      RK2 = 1.+1./RK
      RK3 = 1.-1./(RK*RK)
      TG1 = G1/T(K+1,M-1)
      TG2 = G2/T(K+1,M-1)
      E1 = EXP(-TG1)
      E2 = EXP(-TG2)
      AE = AN*E1
      BE2 = BN*E2
      T1E = TN1*E1
      T2E = TN2*E2
      GAT = TG1*A(K+1,M-1)/T(K+1,M-1)
      GBT = TG2*B(K+1,M-1)/T(K+1,M-1)
      TG12 = G1/T(K+1,M)
      TG22 = G2/T(K+1,M)
      E12 = EXP(-TG12)
      E22 = EXP(-TG22)
      AE2 = AN*E12
      BE22 = BN*E22
      T1E2 = TN1*E12
      T2E2 = TN2*E22
      GAT2 = TG12*A(K+1,M)/T(K+1,M)
      GBT2 = TG22*B(K+1,M)/T(K+1,M)
      ALA = AL*AE2
      ALB = AL*BE22
      ALT1 = AL*T1E2
      ALT2 = AL*T2E2
      AL1A = (1.-AL)*AE
      AL1B = (1.-AL)*BE2
      AL1T1 = (1.-AL)*T1E
      AL1T2 = (1.-AL)*T2E
C
C     EVALUATE ELEMENTS OF ADJOINT MATRIX
C
      IF(K.EQ.1) GO TO 109
C
      D(J,1) = -RA1BE*RK2
      D(J+1,1) = -RB1BE*RK2
      D(J+2,1) = -RT1BE*RK2
      D(J,2) = 0.
      D(J+1,2) = 0.
      D(J,3) = 0.
  109 D(J+2,2) = +AL1A*GAT
      D(J+1,3) = 0.
      D(J+2,3) = -AL1A*GAT+AL1B*GBT
```

```
      D(J,4) = 1.+2.*RA1BE*RK3+AL1A
      D(J+1,4) = 1.+2.*RB1BE*RK3+AL1B
      D(J+2,4) = 1.+2.*RT1BE*RK3+AL1T1*GAT+AL1T2*GBT
      D(J,5) = -AL1A
      D(J+1,5) = AL1T2
      D(J+2,5) = 0.
      D(J,6) = AL1T1
      D(J+1,6) = 0.
      D(J+2,6) = 0.
      D(J,7) = -RA1BE*RK1
      D(J+1,7) = -RB1BE*RK1
      D(J+2,7) = -RT1BE*RK1
      D(J,8) = GA(K)*RABE*RK2+GA(K+1)*(1.-2.*RABE*RK3-ALA)+GB(K+1)*ALA
     1+GT(K+1)*ALT1+GA(K+2)*RABE*RK1
      D(J+1,8) = GB(K)*RBBE*RK2+GB(K+1)*(1.-2.*RBBE*RK3-ALB)+GT(K+1)*
     1       ALT1+GB(K+2)*RBBE*RK1
  108 D(J+2,8) = GT(K)*RTBE*RK2-GA(K+1)*ALA*GAT2+GB(K+1)*(+ALA*GAT2-ALB*
     1          GBT2)+GT(K+1)*(1.-2.*RTBE*RK3-ALT1*GAT2-ALT2*GBT2)
     2+GT(K+2)*RTBE*RK1
C
      D(IM35,1) = -PDR1*RA
      D(IM34,1) = -PDR1*RB
      D(IM33,1) = -PDRT1*RT
      D(IM35,2) = 0.
      D(IM34,2) = 0.
      D(IM33,2) = 0.
      D(IM35,3) = 0.
      D(IM34,3) = 0.
      D(IM33,3) = 0.
      D(IM35,4) = -PDR1*RA*(2.*DX-1.)+1.
      D(IM34,4) = -PDR1*RB*(2.*DX-1.)+1.
      D(IM33,4) = -PDRT1*RT*(2.*DX-1.)+1.
      D(IM35,5) = 0.
      D(IM35,6) = 0.
      D(IM34,5) = 0.
      D(IM35,8) = GA(IN)*PDR*RA+GA(IM)*(PDR*RA*(2.*DX-1.)+1.)
      D(IM34,8) = GB(IN)*PDR*RB+GB(IM)*(PDR*RB*(2.*DX-1.)+1.)
      D(IM33,8) = GT(IN)*PDRT*RT+GT(IM)*(PDRT*RT*(2.*DX-1.)+1.)
C
      JM3 = IM3-3
      JM32 = IM32-3
C
      CALL HEPSOL
C
  330 CONTINUE
C
C     TEST FOR IMPROVEMENT IN YIELD OF B
C
      BNEW = B(IM,NM)
      IF(BOLD.EQ.0.0) GO TO 335
      IF(((BNEW-BOLD)/BOLD).LT.1.0 E-2) CONST = CONST/2.
  335 WRITE(6,2004) CONST
 2004 FORMAT(@ CONST = @,F8.4)
      IF(CONST.LT.(0.01*COLD))STOP
C
C     CHOOSE NEW HEAT FLUX PROFILE
C
      SINT = 0.0
      DO 212 N = 1,NN
  212 SINT = 0.5*(GTN(N)*GTN(N)+GTN(N+1)*GTN(N+1))*DZ(N)+SINT
      DO 211 N = 1,NM
  211 G(N) = G(N)+CONST*GTN(N)/SQRT(SINT)
      WRITE(6,2003) (G(N),N = 1,NM,NY)
 2003 FORMAT(@0G = @,11F8.3//)
C
      GO TO 103
C
      END




      SUBROUTINE HEPSOL
C
C     THIS SUBROUTINE SOLVES THE HEPTADIAGONAL MATRIX EQUATIONS
C
      DIMENSION A(11,201),B(11,201),T(11,201),D(33,8),GA(11),GB(11),
     1          GT(11),GTN(201),LJ(6)
      COMMON /ONE/ A,B,T,D,GA,GB,GT,GTN,LJ
      COMMON /TWO/ N,NN,NM,NY,NGT,NGNY,NANY,NANN,SUMZ,IM3,IM32,JM3,JM32,
     1     IM,M
      DOUBLE PRECISION D,DUM
      LM = 7
```

```
      LD = JM3
      LW = LM-1
      LV = LM-2
      LO = (LM+1)/2
      LT = LO-2
C
      DO 6 I = 1,LO
    6 D(LD-LT,I+LT) = D(LD-LT,I+LT)+D(LD,I)
      D(LD-LT,LM+1) = D(LD-LT,LM+1)+D(LD,LM+1)
      DO 9 I = 1,LO
    9 D(1+LT,I+1) = D(1+LT,I+1)+D(1,I+1+LT)
      D(1+LT,LM+1) = D(1+LT,LM+1)+D(1,LM+1)
C
      DO 1 LA = 1,LV
      LB = (LA+1)/2
      LC = LV-LB
      LK = LW-LA
      IF(MOD(LA,2).NE.0) GO TO 2
C
      LE = LM+1-LB
      K = -1
      GO TO 3
C
    2 LE = LB
      K = 1
C
    3 DO 4 I = 1,LW
    4 LJ(I) = LE+I*K
C
C
      DO 5 LZ = LC,LD
      IF(MOD(LA,2).NE.0) LY = LZ
      IF(MOD(LA,2).EQ.0) LY = LD+1-LZ
C
      IF(D(LY,LE).EQ.0.000) GO TO 5
      IF(D(LY-K,LE+K).EQ.0.000) WRITE(6,3000) LY,LE,K
 3000 FORMAT(' ERROR,ELEMENT = ',3(5X,I3))
      DUM = D(LY,LE)/D(LY-K,LE+K)
C
      DO 14 I = 1,LK
      DO 7 J = 1,LT
      IF(LZ.EQ.(LD+1-J).AND.I.GT.(LO-LB-1+J))GO TO 11
    7 CONTINUE
      D(LY,LJ(I)) = D(LY,LJ(I))-DUM*D(LY-K,LJ(I)+K)
   14 CONTINUE
C
   11 D(LY,LM+1) = D(LY,LM+1)-DUM*D(LY-K,LM+1)
C
    5 CONTINUE
C
    1 CONTINUE
C
      IF(N.GE.NM) GO TO 320
C
      T(IM,N+1) = D(IM3,8)/D(IM3,4)
      DO 16 K = 1,IM32,3
      J = IM3-K
      L = (J+1)/3
      B(L,N+1) = (D(J,8)-D(J,5)*T(L,N+1))/D(J,4)
      A(L,N+1) = (D(J-1,8)-D(J-1,5)*B(L,N+1))/D(J-1,4)
      IF(L.EQ.1) GO TO 16
      T(L-1,N+1) = (D(J-2,8)-D(J-2,5)*A(L,N+1))/D(J-2,4)
C
   16 CONTINUE
C
      N1 = N+1
      IF(MOD(N,NY).EQ.0.AND.MANY.EQ.1) WRITE(6,2000) N1,SUMZ,(A(I,N+1),
     1    I = 1,IM),(B(I,N+1),I = 1,IM),(T(I,N+1),I = 1,IM)
      IF(N.EQ.NN.AND.MANY.EQ.1) WRITE(6,2000) N1,SUMZ,(A(I,N+1),I = 1,IM
     1          ),(B(I,N+1),I = 1,IM),(T(I,N+1),I = 1,IM)
 2000 FORMAT('0N = ',14,5X,'DIST = ',F8.5/' A = ',11F9.5/' B = '11F9.5/
     1         ' T = ',11F9.5//)
C
      GO TO 330
C
  320 GT(IM) = D(JM3,8)/D(JM3,4)
      DO 17 K = 1,JM32,3
      J = JM3-K
      L = (J+4)/3
      GB(L) = (D(J,8)-D(J,5)*GT(L))/D(J,4)
      GA(L) = (D(J-1,8)-D(J-1,5)*GB(L))/D(J-1,4)
      IF(L.EQ.2) GO TO 17
      GT(L-1) = (D(J-2,8)-D(J-2,5)*GA(L))/D(J-2,4)
      GTN(N-1) = GT(IM)
```

```
C
   17 CONTINUE
C
C
      M1 = Y-1
      NP = N-2*MOD(NN,NY)
      IF(MOD(NP,NY).EQ.0.AND.NGNY.EQ.1) WRITE(6,2001)M1,SUM7,(GA(I),
     1         I = 1,IM),(GB(I),I = 1,IM),(GT(I),I = 1,IM)
 2001 FORMAT(@0N = @,I4,5X,@DIST = @,F8.5/@ GA = @,11E9.2/@ GB = @,
     1       11E9.2/@ GT = @,11E9.2//)
      IF(MOD(NP,NY).EQ.0.AND.NGT.EQ.1)WRITE(6,2005) M1,SUM7,GT(IM)
 2005 FORMAT(@ N = @,I4,5X,@DIST = @,F8.5/@ GT(IM) = @,E12.4)
C
  330 RETURN
      END
-
```

APPENDIX 10

EQUIPMENT AND INSTRUMENTATION

ITEM	DESCRIPTION
1. Blower	Air Control Installations 9MS8. 9 stage centrifugal blower providing up to 50 cfm. air at up to 23 in. water gauge. 6μm inlet filter.
2. Heater	4 kW total power of which 2 kW were switched and 2 kW controlled by a Eurotherm controller. Two 25.5 ft. lengths of coiled 0.024 in. diameter Nichrome wire were wound on a 2 in. square former made of four 16.5 in. lengths of quartz glass tubing - see Figure 5.3
3. Temperature Controller	Eurotherm 070 P.I.D. controller. Input: from a chromel-alumel thermocouple at the reactor entrance. Output: up to 15 amps (phase angle).
4. Hoppers (2)	Stainless steel (Grade 58E, 18 s.w.g.). 12 in. square by 18 in. deep. Connected by a 2 in. diameter stainless tube with a slide valve.

5. Solids Feed Valve	Modified 1 in. brass gate valve with the upper surface of the gate machined away to accommodate a sintered bronze disc 1/16 in. thick with $2\frac{1}{2}$ μm pores through which air was fed. See Figure 5.4.
6. Air Pump for Solids Feed Valve	Hy-Flo reciprocating pump giving up to 1.4 1/min. of air at 0.4 kg/cm^2.
7. Flow Straightener	Bundle of 12 thin-walled stainless-steel tubes 6 in. long.
8. Carbon Monoxide Injector	1/8 in. stainless steel tube through which CO was injected radially from 6 equally spaced 1/32 in. diameter holes around the tube circumference. See Figure 5.5.
9. Reactor	7 ft. of 1 1/8 in. O.D. by 0.064 in. stainless steel tubing, grade 304. See Figure 5.7.
10. Cyclone	6 in. diameter stainless steel high efficiency cyclone to specifications of Stairmand (1951b).
11. Sample Pump	Diaphragm pump giving up to 5 1/min., 350 torr.

12.	Gas Chromatograph	Taylor-Servomex. Column consisted of 2 ft. of 1/16 in. stainless steel tubing containing Poropak QS 80 → 100 # followed by 6 ft. of the same tubing containing Molecular Sieve MS13X 60 → 80 # (partially activated). Carrier gas: Helium at 15 psig. Column temperature 45°C. Katharometer voltage 7 v. Sample size 25 µl.
13.	Integrater Recorder	Fisons Vitatron UR406M recorder.
14.	Multi-Channel Recorder	Pye-Unicam PM8235 12 channel recorder with event marker. Input: iron-constantin (type J) thermocouples.
15.	Rotameters (i)	Air, 50 to 500 l/min. Calibrated (Series 2000).
	(ii)	CO, 3 to 30 l/min. Calibrated (Series 2000).
	(iii)	CO, 0.4 to 4 l/min. Calibrated (Series 1100).
	(iv) & (v)	2 x Air, 60 to 500 cc/min. Calibrated (Series 1100) - for catalyst test equipment.
16.	Manometers	Connected to pressure tapping with 1/8 in. Cu tubing.
	(i) Single Fluid	Paraffin with red dye - s.g. = 0.784.
	(ii) Two Fluid	Paraffin as above + distilled water.
17.	Globe Valve	$1\frac{1}{2}$ in. brass globe valve for air flowrate control.

18.	Pipework and Fittings	
	(i) Before Heater	1½ in. O.D. copper tubing with Simplifix compression fittings.
	(ii) After Heater	1 1/8 in. O.D. by 0.064 in. stainless steel tubing grade 304 with 4 in. diameter bolted weld-on flanges and 1/16 in. asbestos gaskets.
	(iii) From Cyclone	3½ in. diameter 'Aliduct' flexible corrugated steel tubing.
19.	Insulation	
	(i) Pipework	Bell's preformed glass fibre insulation. 3 ft. by 1 in. thick sections with canvas backing.
	(ii) Cyclone and Hoppers	Bell's woven mats, 40 mm thick, wire backed.
	(iii) Heater	Triton bulk wool - ceramic wool.
	(iv) Additional	1/4 in. asbestos yarn.
20.	Sampling Probes	0.8 mm O.D. (0.45 mm I.D.) hypodermic tubing fitted to threaded rods (40 threads/in.). See Figure 5.8.
21.	Sample Lines and Valves	1/8 in. stainless steel tubing grade 316. 10 by 1/8 in. brass globe valves with compression fittings. See Figure 5.6. Glass wool and sintered stainless steel filters.

LIST OF SYMBOLS

		UNITS
a	radial pipe coordinate	m
a_o	internal radius of reactor	m
a_1	constant in equation 3.5	-
a_2	constant in equation 3.7	-
A_1	constant in equation 3.1	-
b	defined by equation 7.4 (= $K[CO]_I$)	-
b_1	constant in equation 3.5	-
b_2	constant in equation 3.7	-
c	concentration of reactant in gas phase	moles/m^3
c_A	concentration of component A in gas phase	moles/m^3
c_{AO}	concentration of A in gas phase at reactor entrance	moles/m^3
c_B	concentration of component B in gas phase	moles/m^3
c_s	concentration of reactant at particle surface	moles/m^3
c_o	concentration of reactant in gas phase at reactor entrance	moles/m^3
c_1	constant in equation 3.5	-
c_2	constant in equation 3.7	-
C	concentration of reactant in catalyst particle	moles/m^3
C_A	concentration of component A in catalyst particle	moles/m^3
C_B	concentration of component B in catalyst particle	moles/m^3
C_{Dp}	particle drag coefficient (= $2F_p/\rho_g u_{sl}^2$)	-
$[CO]$	carbon monoxide concentration	moles/m^3
$[CO]_{ex}$	CO concentration at exit of fixed bed reactor	moles/m^3
$[CO]_{in}$	CO concentration at entrance of fixed bed reactor	moles/m^3
$[CO]_I$	CO concentration at entrance of transport reactor	moles/m^3
C_{pg}	specific heat of gas at constant pressure	J/kg.°K
C_{ps}	specific heat of solid	J/kg.°K

		UNITS
d_p	particle diameter	m
d_t	internal tube diameter	m
d_2	constant in equation 3.7	-
D_{Aeff}	effective diffusivity of component A in particles	m^2/s
D_{Beff}	effective diffusivity of component B in particles	m^2/s
D_{eff}	effective diffusivity of reactant in catalyst particles	m^2/s
D_m	defined by equation A6.3 (= D_{12}/D_{eff})	-
D_N	ratio of effective diffusivities (= D_{Aeff}/D_{Beff})	-
D_{12}	diffusivity of reactant in bulk gas phase	m^2/s
e_2	constant in equation 3.7	-
E	activation energy	J/mole
E_{ax}	axial diffusion coefficient for fixed bed reactor	m^2/s
E_A	activation energy for reaction A → B	J/mole
E_B	activation energy for reaction B → C	J/mole
E_{rad}	radial diffusion coefficient for fixed bed reactor	m^2/s
F_{An}	defined by equation A3.14	-
F_{Bn}	defined by equation A3.15	-
F_{Dn}	defined by equation A1.8	-
F_{fn}	defined by equation A6.32	-
F_n	defined by equation 4.21	-
F_p	drag force per unit area acting on particle	N/m^2
Fr	tube Froude number (= $u_g/\sqrt{g\ d_t}$)	-
F_{01n}	defined by equation A2.5	-
F_{02n}	defined by equation A2.5	-
g	gravitational acceleration	m^2/s
G	dimensionless activation energy (= $E/\mathcal{R}T_{go}$)	-
G_A	dimensionless activation energy for reaction A → B	-
G_B	dimensionless activation energy for reaction B → C	-

		UNITS
h_p	particle/gas heat transfer coefficient	$J/m^2s°K$
h_s	suspension/wall heat transfer coefficient	$J/m^2s°K$
h_o	gas/wall heat transfer coefficient for gas flowing alone	$J/m^2s°K$
j_D	'j' factor given by equation 3.7	-
k	first order rate constant per unit volume of catalyst particle	1/s
k^1	constant in Langmuir - Hinshelwood expression equation 6.15	m^3/mole s
k_A	first order rate constant per unit volume of catalyst particle for reaction A → B	1/s
k_B	first order rate constant per unit volume of catalyst particle for reaction B → C	1/s
k_{co}	rate constant per unit volume of catalyst for CO oxidation	moles/m^3s
k_f	mass transfer coefficient (particle/gas)	m/s
k_o	zero order rate constant per unit volume of catalyst	moles/m^3s
$k_{\infty A}$	pre-exponential factor for k_A $[k_A=k_{\infty A}\exp(-G_A/\tau)]$	1/s
$k_{\infty B}$	pre-exponential factor for k_B $[k_B=k_{\infty B}\exp(-G_B/\tau)]$	1/s
$k_{\infty co}$	pre-exponential factor for k_{co} $[k_{co}=k_{\infty co}\exp(-G/\tau)]$	moles/m^3s
K	constant in Langmuir-Hinshelwood expression equation 6.15	m^3/mole
l	reactor length coordinate	m
L	transport reactor length	m
L_B	fixed bed reactor length	m
m	power law index in equation 3.3	-
m_f	total molar flowrate in fixed bed reactor	moles/s
M	dimensionless group $(= D_{eff}\, L/\varepsilon R^2 u_s)$	-
M_A	dimensionless group $(= D_{Aeff}\, L/\varepsilon R^2 u_s)$	-
M_B	dimensionless group $(= D_{Beff}\, L/\varepsilon R^2 u_s)$	-
M_T	dimensionless group $(= K_{eff}\, L/(1-\varepsilon)R^2 u_s \rho_s C_{ps})$	-

		UNITS
n	power index in rate law	-
n_s	power law index in equation 3.2	-
n_t	number of size groups of particles (equation 7.9)	-
n_ρ	power law index in equation 3.4	-
N	dimensionless group ($=3PMD_m\ Sh/2$) equation A6.5	-
N_{dis}	dispersion number ($= u\ L_B/2E_{ax}$)	-
N_n	number of particles of size R_n (equation 7.9)	-
N_t	defined by equation 7.10	-
N_T	dimensionless group ($= 3P_T M_T \kappa_m Nu_p/2$) equation A7.4	-
Nu_p	particle/gas Nusselt number ($= h_p\ d_p/\kappa_g$)	-
Nu_s	suspension/wall Nusselt number ($= h_s\ d_t/\kappa_g$)	-
Nu_o	gas/wall Nusselt number for gas flowing alone ($= h_o\ d_t/\kappa_g$)	-
$[O_2]$	oxygen concentration	moles/m^3
$[O_2]_{in}$	oxygen concentration at entrance of fixed bed reactor	moles/m^3
$[O_2]_I$	oxygen concentration at entrance of transport reactor	moles/m^3
p	pressure at transport reactor entrance	Pa
P	dimensionless group ($= \varepsilon u_s(1-\alpha)/u_g\alpha$)	-
Pr	Prandtl number ($= \mu C_{pg}/\kappa_g$)	-
Pe_{ax}	axial Peclet number ($= ud_p/E_{ax}$)	-
Pe_{rad}	radial Peclet number ($= ud_p/E_{rad}$)	-
P_T	dimensionless group ($= (1-\varepsilon)(1-\alpha)u_s\rho_s C_{ps}/\alpha u_g \rho_g C_{pg}$)	-
q	volumetric flowrate of gas in fixed bed reactor	m^3/s
q_{ex}	volumetric flowrate of gas at fixed bed exit	m^3/s
q_{in}	volumetric flowrate of gas at fixed bed entrance	m^3/s
Q	dimensionless heat flux	-
r	radial particle coordinate	m
R	particle radius	m
R_{Av}	mean particle radius defined by equation 7.14	m

		UNITS
R_{Avfilm}	mean particle radius defined by equation 7.15	m
R_n	radius of fraction 'n' of particles (equation 7.9)	m
$\mathcal{R}$	gas constant	J/mole°K
Re_p	particle Reynolds number ($=\rho_g d_p u_s \alpha/\mu$)	-
Re_t	tube Reynolds number ($=\rho_g d_t u_g \alpha/\mu$)	-
s	scaling factor	
S	general rate law [= S(C)] per unit volume of catalyst	moles/m^3s
Sc	Schmidt number ($= \mu/D_{12}\ \rho_g$)	-
Sh	Sherwood number ($= k_f\ d_p/D_{12}$)	-
t	time coordinate	s
T	temperature in catalyst particles	°K
T_{exit}	temperature at exit of transport reactor	°K
T_g	gas phase temperature	°K
T_{go}	gas phase temperature at reactor entrance	°K
T_{max}	maximum temperature within catalyst particle	°K
T_s	temperature at particle surface	°K
T_w	internal reactor wall temperature	°K
u	interstitial gas velocity in fixed bed	m/s
u_g	mean interstitial gas velocity in transport reactor	m/s
u_s	mean particle velocity	m/s
u_{sl}	mean particle slip velocity ($= u_g - u_s$)	m/s
v_g	interstitial gas velocity ($= v_g(a)$)	m/s
v_{go}	interstitial gas velocity at tube centre	m/s
v_s	particle velocity ($= v_s(a)$)	m/s
v_{so}	particle velocity at tube centre	m/s
v_{sw}	particle velocity at tube wall	m/s
V	fixed bed volume coordinate	m^3
V_B	fixed bed volume	m^3

		UNITS
W_g	mass flowrate of gas	kg/s
W_n	weight of particles of size R_n (equation 7.11)	kg
W_s	mass flowrate of solids	kg/s
x	dimensionless particle radial coordinate (= r/R)	-
x_e	point of reactant exhaustion defined by equations A2.7 to A2.9	-
X	ratio of CO to O_2 at reactor inlet (= $[CO]_I/[O_2]_I$)	-
y	dimensionless gas phase concentration of reactant (= c/c_o)	-
y_a	dimensionless gas phase concentration of reactant at end of entry region	-
y_A	dimensionless gas phase concentration at component A (= c_A/c_{AO})	-
y_B	dimensionless gas phase concentration of component B (= c_B/c_{AO})	-
y_{ex}	fractional conversion defined by equation 6.5	-
y_{exit}	dimensionless gas phase concentration of reactant at transport reactor exit	-
y_s	dimensionless concentration of reactant at catalyst surface (= c_s/c_o)	-
Y	dimensionless concentration of reactant in catalyst particle (= C/c_o)	-
Y_A	dimensionless concentration of component A in catalyst particle (= C_A/c_{AO})	-
Y_B	dimensionless concentration of component B in catalyst particle (= C_B/c_{AO})	-
$\overline{Y}$	dimensionless mean concentration of reactant in catalyst particle (=$\eta_* y_s$)	-
z	dimensionless reactor length coordinate (= l/L)	-
z_a	dimensionless distance to end of entry region	-
z_m	point in reactor where (τ_s-τ_g) is maximum (equation A7.17)	-

		UNITS
α	reactor voidage (transport reactor)	-
α_f	fixed bed reactor voidage	-
β_{An}	roots of equations A3.16 and A3.17	-
β_{Bn}	roots of equations A3.19 and A3.20	-
β_{Dn}	roots of equations A1.9 and A1.10	-
β_n	roots of equations 4.22 and 4.23	-
β_{on}	roots of equations A2.7, A2.8 and A2.9	-
γ_{An}	roots of equations A3.16 and A3.17	-
γ_{Bn}	roots of equations A3.19 and A3.20	-
γ_{Dn}	roots of equations A1.9 and A1.10	-
γ_{fn}	roots of equation A6.33	-
γ_n	roots of equations 4.22 and 4.23	-
γ_{on}	roots of equations A2.7, A2.8 and A2.9	-
δ_{An}	roots of equations A3.16, A3.17 and A3.18	-
δ_{Bn}	roots of equations A3.19, A3.20 and A3.21	-
δQ	dimensionless heat flux increment	-
ΔH	heat of reaction	J/mole
ΔH_A	heat of reaction for A → B	J/mole
ΔH_B	heat of reaction for B → C	J/mole
ΔH_{co}	heat of reaction for CO oxidation	J/mole
Δp_{fsg}	pressure drop in reactor due to combined friction of gas and solids	Pa
Δp_o	pressure drop in reactor for gas flowing alone	Pa
ΔT_B	temperature rise along fixed bed reactor	°K
ε	voidage of catalyst particles	-
η	first order effectiveness factor	-
η^∞	asymptotic value of η	-

		UNITS
η_A	first order effectiveness factor for A → B defined by equation A5.28	-
η_{Ass}	first order effectiveness factor for A → B at steady state (equation A5.31)	-
η_B	first order effectiveness factor for B → C defined by equation A5.29	-
η_{Bss}	first order effectiveness factor for B → C at steady state (equation A5.32)	-
η_f	first order effectiveness factor defined by equation 4.24	-
η_f^∞	asymptotic value of η_f	-
η_g	general rate law effectiveness factor defined by equation A5.3	-
η_{gss}	steady state value of η_g	-
η_{gf}	general rate law effectiveness factor defined by equation A6.8	-
η_i	first order effectiveness factor defined by equation 4.25	-
η_i^∞	asymptotic value of η_i	-
η_{ss}	steady state first order effectiveness factor (=[(1/tanhϕ)-(1/ϕ)]3/ϕ)	-
η_T	thermal 'effectiveness factor' defined by equation A7.7	-
η_*	mean concentration relative to surface (= $\bar{Y}/y_s$) equation A5.5	-
η_{*a}	value of η_* at the end of the entrance region	-
η_*^∞	asymptotic value of η_*	-
η_{*ss}	steady state value of η_*	-
κ_{eff}	effective thermal conductivity of catalyst particle	J/ms°K
κ_g	thermal conductivity of gas	J/ms°K
κ_m	ratio of thermal conductivities (= κ_g/κ_{eff})	-
λ_A	adjoint variable in equations A8.12 to A8.14	-
λ_B	adjoint variable in equations A8.12 to A8.14	-
λ_T	adjoint variable in equations A8.12 to A8.14	-

		UNITS
μ	viscosity of gas	kg/ms
ρ_g	density of gas	kg/m^3
ρ_p	dispersed solids density [mass of solids per unit volume of reactor, $\rho_p(a)$]	kg/m^3
ρ_{pw}	dispersed solids density at reactor wall	kg/m^3
ρ_{po}	dispersed solids density at reactor centre	kg/m^3
ρ_s	density of catalyst particles	kg/m^3
σ_g	dimensionless group ($= R\sqrt{S(c_o)\Delta H/\kappa_{eff}T_{go}}$)	-
$\sigma_{\infty A}$	dimensionless group ($= R\sqrt{k_{\infty A}c_{Ao}\Delta H_A/\kappa_{eff}T_{go}}$)	-
$\sigma_{\infty B}$	dimensionless group ($= R\sqrt{k_{\infty B}c_{Ao}\Delta H_B/\kappa_{eff}T_{go}}$)	-
τ	dimensionless temperature in catalyst particle ($= T/T_{go}$)	-
$\bar{\tau}$	mean dimensionless temperature of catalyst particle ($= \eta_T\tau_S$)	-
τ_g	dimensionless gas phase temperature ($= T_g/T_{go}$)	-
τ_{max}	maximum value of τ in catalyst particle	-
τ_s	dimensionless temperature at catalyst surface ($= T_s/T_{go}$)	-
τ_w	dimensionless reactor wall temperature ($= T_w/T_{go}$)	-
ϕ	Thiele modulus for first order reaction ($= R\sqrt{k/D_{eff}}$)	-
ϕ_A	Thiele modulus for component A - first order reaction ($= R\sqrt{k_A/D_{Aeff}}$)	-
ϕ_B	Thiele modulus for component B - first order reaction ($= R\sqrt{k_B/D_{Beff}}$)	-
ϕ_{co}	Thiele modulus for CO oxidation	-
ϕ_g	Thiele modulus, general rate law ($= R\sqrt{S(c_o)/D_{eff}c_o}$)	-
ϕ_s	Surface Thiele modulus, general rate law ($= R\sqrt{S(c_s)/D_{eff}c_s}$)	-
ϕ_o	Thiele modulus for zero order reaction ($= R\sqrt{k_o/D_{eff}c_o}$)	-
$\phi_{\infty A}$	Thiele modulus for component A at $T = \infty$ ($= R\sqrt{k_{\infty A}/D_{Aeff}}$)	-
$\phi_{\infty B}$	Thiele modulus for component B at $T = \infty$ ($= R\sqrt{k_{\infty B}/D_{Beff}}$)	-

UNITS

χ	dimensionless group ($=\sigma_g^2/\phi_g^2 = D_{eff}c_o\Delta H/\kappa_{eff}T_{go}$)	-
Ψ	dimensionless rate law [$= S(C)/S(c_o)$]	-

REFERENCES

ARIS, R. (1960). Studies in optimization - II. Optimum temperature gradients in tubular reactors. Chem. Eng. Sci., 13, pp. 18 - 29.

ARIS, R. (1975). The mathematical theory of diffusion and reaction in permeable catalysts. Vol. I. The theory of the steady state. Oxford, Clarendon Press.

ARUNDEL, P.A., BIBB, S.D. and BOOTHROYD, R.G. (1970/71). Dispersed density distribution and extent of agglomeration in a polydisperse fine particle suspension flowing turbulently upwards in a duct. Powder Technol., 4, pp. 302 - 312.

ARUNDEL, P.A. and BOOTHROYD, R.G. (1971). Measurement of local solids velocity in a pneumatic conveyor from correlated electrostatic signals. British Hydromechanics Research Association. Proc. 1st. Int. Conf. on Pneumatic Transport of Solids in Pipes. Cambridge, England. 6 - 8 Sept. 1971. Paper D1, pp. D1 - 23 and D84 - 85.

ARUNDEL, P.A., TAYLOR, I.A., DEAN, W., MASON, J.S. and DORAN, T.E. (1973). The rapid erosion of various pipe-wall materials by a stream of abrasive alumina particles. British Hydromechanics Research Association. Proc. 2nd. Int. Conf. on Pneumatic Transport of Solids in Pipes. Guildford, England. 5 - 7 Sept. 1973. Paper E1. pp. E1 - 15 and E38 - 41.

BADDOUR, R.F., MODELL, M. and HEUSSER, U.K. (1968). Simultaneous kinetic and infrared spectral studies of carbon monoxide oxidation on palladium under steady-state conditions. J. Phys. Chem., 72, pp. 3621 - 3629.

BECK, M.S. and WAINWRIGHT, N. (1968/69). Current industrial methods of solids flow detection and measurement. Powder Technol., 2, pp. 189 - 197.

BECK, M.S. PLASKOWSKI, A. and WAINWRIGHT, N. (1968/69). Particle velocity and mass flow measurement in pneumatic conveyors. Powder Technol., 2, pp. 269 - 277.

BECK, M.S., HOBSON, J.H. and MENDIES, P.J. (1971). Mass flow and solids velocity measurement in pneumatic conveyors. British Hydromechanics Research Association. Proc. 1st. Int. Conf. on Pneumatic Transport of Solids in Pipes. Cambridge, England. 6 - 8 Sept. 1971. Paper D3. pp. D37 - 48 and D87 - 88.

BELDEN, D.H. and KASSEL, L.S. (1949). Pressure drops encountered in conveying particles of large diameter in vertical transfer lines. Ind. Eng. Chem., 41, pp. 1174 - 1178.

BILOUS, O. and AMUNDSON, N.R. (1956). Optimum temperature gradients in tubular reactors - I. General theory and methods. Chem. Eng. Sci., 5, pp. 81 - 92.

BOOTHROYD, R.G. (1966). Pressure drop in duct flow of gaseous suspensions of fine particles. Trans. Inst. Chem. Eng., 44, pp. 306 - 313.

BOOTHROYD, R.G. (1967a). An anemometric isokinetic sampling probe for aerosols. J. Sci. Instrum., 44, pp. 249 - 253.

BOOTHROYD, R.G. (1967b). Turbulence characteristics of the gaseous phase in duct flow of a suspension of fine particles. Trans. Inst. Chem. Eng., 45, pp. 297 - 310.

BOOTHROYD, R.G. (1969a). Heat transfer in a gas borne suspension of fine particles in turbulent duct flow. Appl. Sci. Res., 21, pp. 98 - 112.

BOOTHROYD, R.G. (1969b). Heat transfer in flowing gaseous suspensions. Chem. Process. Eng., 50, (10), pp. 108 - 114.

BOOTHROYD, R.G. (1969c). Similarity in gas-borne flowing particulate suspensions. J. Eng. Ind., 91B, pp. 303 - 314.

BOOTHROYD, R.G. (1971). Flowing gas-solids suspensions. London, Chapman and Hall.

BOOTHROYD, R.G. and GOLDBERG, A.S. (1970a). Protecting seals and bearings of shafts which rotate fully immersed in abrasive powders. Br. Chem. Eng., 15, pp. 68 - 69.

BOOTHROYD, R.G. and GOLDBERG, A.S. (1970b). Measurements in flowing gas-solids suspensions II. Br. Chem. Eng., 15, pp. 357 - 362.

BOOTHROYD, R.G. and HAQUE, H. (1970a). Fully developed heat transfer to a gaseous suspension of particles flowing turbulently in ducts of different size. J. Mech. Eng. Sci., 12, pp. 191 - 200.

BOOTHROYD, R.G. and HAQUE, H. (1970b). Experimental investigation of heat transfer in the entrance region of a heated duct conveying fine particles. Trans. Inst. Chem. Eng., 48, pp. 109 - 120.

BOOTHROYD, R.G. and HAQUE, H. (1973). Improved convective heat transfer in a fluid with artificially modified turbulence. J. Mech. Eng. Sci., 15, pp. 61 - 72.

BOOTHROYD, R.G. and WALTON, P.J. (1971). Suppression of wall turbulence in dense flowing aerosols. Nature Phys. Sci., 231, pp. 129 - 130.

BOOTHROYD, R.G. and WALTON, P.J. (1973). Fully developed turbulent boundary-layer flow of a fine solid-particulate gaseous suspension. Ind. Eng. Chem. Fund., 12, pp. 75 - 82 (and 13, pp. 92 - 94).

BRILLER, R. and PESKIN, R.L. (1968). Gas solids suspension convective heat transfer at a Reynolds Number of 130,000. J. Heat. Transf., 90C, pp. 464 - 468 (and 91C, p. 203).

BRITISH HYDROMECHANICS RESEARCH ASSOCIATION, (1972). The pneumatic transport of solids in pipes - a bibliography. THORNTON, W.A. (Ed.). Cranfield, England.

BRITISH HYDROMECHANICS RESEARCH ASSOCIATION, (1976). Pneumotransport 3. Proc. 3rd. Int. Conf. on Pneumatic Transport of Solids in Pipes. Bath, England. 7 - 9 April, 1976.

BRUCE, G.H., PEACEMAN, D.W., RACHFORD, H.H. and RICE, J.D. (1953). Calculations of unsteady-state gas flow through porous media. Petrol. Trans., Trans. A.I.M.E., 198, pp. 79 - 92 or J. Petrol. Technol., 5, pp. 79 - 92.

BRYSON, M.C., HULING, G.P. and GLAUSSER, W.E. (1972). Gulf explores riser cracking. Hydrocarbon Process., 51, (5), pp. 85 - 89.

CAPES, C.E. and NAKAMURA, K. (1973). Vertical pneumatic conveying - An experimental study with particles in the intermediate and turbulent flow regimes. Can. J. Chem. Eng., 51, pp. 31 - 38.

CARBERRY, J.J. (1966). Yield in chemical reactor engineering. Ind. Eng. Chem., 58, (10), pp. 40 - 53.

CHAND, P. (1971). Response of particles under pneumatic conveyance. British Hydromechanics Research Association. Proc. 1st. Int. Conf. on Pneumatic Transport of Solids in Pipes. Cambridge, England. 6 - 8 Sept. 1971. Paper B6. pp. B69 - 91 and B121.

CHANDOK, S.S. and PEI, D.C.T. (1971). Particle dynamics in solids-gas flow in a vertical pipe. British Hydromechanics Research Association. Proc. 1st. Int. Conf. on Pneumatic Transport of Solids in Pipes. Cambridge, England. 6 - 8 Sept. 1971. Paper B5. pp. B53 - 69 and B120.

CLAMEN, A. and GAUVIN, W.H. (1968a). Drag coefficients of evaporating spheres in a turbulent air stream. Can. J. Chem. Eng., 46 , pp. 73 - 78.

CLAMEN, A. and GAUVIN, W.H. (1968b). Effects of turbulence on particulate heat and mass transfer. Can. J. Chem. Eng., 46, pp. 223 - 228.

CLIFT, R. and GAUVIN, W.H. (1971). Motion of entrained particles in gas streams. Can. J. Chem. Eng., 49, pp. 439 - 448.

CLOSE, J.S. and WHITE, J.M. (1975). On the oxidation of carbon monoxide catalyzed by Palladium. J. Catal., 36, pp. 185 - 198.

CORRSIN, S. and LUMLEY, J. (1957). On the equation of motion for a particle in turbulent fluid. Appl. Sci. Res., A6, pp. 114 - 116.

DALLA LANA, I.G. and AMUNDSON, N.R. (1961). A tubular reactor. Ind. Eng. Chem., 53, pp. 22 - 26.

DANZIGER, W.J. (1963). Heat transfer to fluidized gas-solids mixtures in vertical transport. Ind. Eng. Chem. Process Des. Dev., 2, pp. 269 - 276.

DAVIES, C.N. (1966). Deposition of aerosols from turbulent flow through pipes. Proc. R. Soc., A289, pp. 235 - 246.

DE LASA, H. and GAU, G. (1973). Influence of aggregates on the performance of a pneumatic transport reactor. Chem. Eng. Sci., 28, pp. 1875 - 1884.

DE MARIA, F., LONGFIELD, J.E. and BUTLER, G. (1961). Catalytic reactor design. Ind. Eng. Chem., 53, pp. 259 - 266.

DENN, M.M., GRAY, R.D. Jr. and FERRON, J.R. (1966). Optimization in a class of distributed-parameter systems. Ind. Eng. Chem. Fund., 5, pp. 59 - 66.

DENNIS, R., SAMPLES, W.R., AMUNDSON, D.M. and SILVERMAN, L. (1957). Isokinetic sampling probes. Ind. Eng. Chem., 49, pp. 294 - 302.

DEPEW, C.A. and FARBAR, L. (1963). Heat transfer to pneumatically conveyed glass particles of fixed size. J. Heat Transf., 85C, pp. 164 - 172.

DIXON, J.K. and LONGFIELD, J.E. (1960). Oxidation of ammonia, ammonia and methane, carbon monoxide and sulphur dioxide. Catalysis. EMMETT, P.H. (Ed.) New York, Reinhold, 7, pp. 281 - 345.

DOIG, I.D. and ROPER, G.H. (1963a). The minimum gas rate for dilute phase solids transportation in a gas stream. Aust. Chem. Eng., 4, (1), pp. 9 - 19.

DOIG, I.D. and ROPER, G.H. (1963b). Energy requirements in pneumatic conveying. Aust. Chem. Eng., 4, (2), pp. 9 - 23.

DOIG, I.D. and ROPER, G.H. (1963c). Fundamental aspects and electrostatic influences in gas-solids transportation systems. Aust. Chem. Eng., 4, (4), pp. 9 - 17.

DOIG, I.D. and ROPER, G.H. (1967). Air velocity profiles in the presence of cocurrently transport particles. Ind. Eng. Chem. Fund., 6, pp. 247 - 256.

DOIG, I.D. and ROPER, G.H. (1968). Contribution of the continuous and dispersed phases to the suspension of spheres by a bounded gas-solids stream. Ind. Eng. Chem. Fund., 7, pp. 459 - 471.

DUCKWORTH, R.A. (1971). Pressure gradient and velocity correlation and their application to design. British Hydromechanics Research Association. Proc. 1st. Int. Conf. on Pneumatic Transport of Solids

in Pipes. Cambridge, England. 6 - 8 Sept. 1971. Paper R2, pp. R25 - 47 and R49 - 52.

DUCKWORTH, R.A. and CHAN, T.K. (1973). The influence of electrostatic charges on the pressure gradient during pneumatic transport. British Hydromechanics Research Association. Proc. 2nd. Int. Conf. on Pneumatic Transport of Solids in Pipes. Guildford, England. 5 - 7 Sept. 1973. Paper A5, pp. A61 - 76 and A88 - 92.

DUCKWORTH, R.A. and KAKKA, R.S. (1971). The influence of particle size on the frictional pressure drop caused by the flow of a solid-gas suspension in a pipe. British Hydromechanics Research Association. Proc. 1st. Int. Conf. on Pneumatic Transport of Solids in Pipes. Cambridge, England. 6 - 8 Sept. 1971. Paper C3, pp. C29 - 44 and C89 - 90.

DWYER, F.G. (1972). Catalysis for control of automotive emissions. Catal. Rev., 6, pp. 261 - 291.

ECHIGOYA, E., YEN, S.H. and MORIKAWA, K. (1969). Investigation of gas-solid transport reactor. Kagaku Kōgaku, 33, pp. 1002 - 1007.

EDDINGER, R.T., FRIEDMAN, L.D. and RAU, E. (1966). Devolatilization of coal in a transport reactor. Fuel, Lond., 45, pp. 245 - 252.

FARBAR, L. (1949). Flow characteristics of solids-gas mixtures - in a horizontal and vertical circular conduit. Ind. Eng. Chem., 41, pp. 1184 - 1191.

FARBAR, L. (1952). Metering of powdered solids in gas solid mixtures. Ind. Eng. Chem., 44, pp. 2947 - 2955.

FARBAR, L. (1953). The venturi as a meter for gas-solids mixtures. Trans. Am. Soc. Mech. Eng., 75, pp. 943 - 951.

FARBAR, L. and DEPEW, C.A. (1963). Heat transfer effects to gas-solids mixtures using solid spherical particles of uniform size. Ind. Eng. Chem. Fund., 2, pp. 130 - 135.

FARBAR, L. and MORLEY, M.J. (1957). Heat transfer to flowing gas-solid mixtures in a circular tube. Ind. Eng. Chem., 49, pp. 1143 - 1150.

FRIEDLANDER, S.K. (1957). Behaviour of suspended particles in a turbulent fluid. A.I.Ch.E.J., 3, pp. 381 - 385.

FRIEDMAN, L.D., RAU, E. and EDDINGER, R.T. (1968). Maximizing the tar yields in transport reactors. Fuel, Lond., 47, pp. 149 - 157.

GAUVIN, W.H. and GRAVEL, J.J.O. (1962). Chemical reactions in solids gas conveyed systems. Inst. Chem. Eng. Symp. on The Interaction between Fluids and Particles. London. 20 - 22 June, 1962. pp. 250 - 259 and pp. 289 - 296.

GLUCK, S.E. (1971). Abrasion in pneumotransport conveying systems. British Hydromechanics Research Association. Proc. 1st. Int. Conf. on Pneumatic Transport of Solids in Pipes. Cambridge, England. 6 - 8 Sept. 1971. Paper D6, pp. D77 - 80, D82 - 83 and D90 - 92.

GOLDBERG, A.S. and BOOTHROYD, R.G. (1969). Measurements in flowing gas solids suspensions I. Br. Chem. Eng., 14, pp. 1705 - 1708.

GOTO, K. and IINOYA, K. (1963a). Pressure drops of steady solid-gas two-phase flow. Chem. Eng. Jap., 1, pp. 7 - 12.

GOTO, K. and IINOYA, K. (1963b). Solids-gas two-phase flowmeter. Chem. Eng. Jap., 1, pp. 34 - 38.

GOTO, K. and IINOYA, K. (1964a). Solid flow distribution of the solid-gas mixture in a horizontal pipeline. Chem. Eng. Jap., 2, pp. 144 - 145.

GOTO, K. and IINOYA, K. (1964b). Measurement and control of the solid gas mixture ratio in two phase flow. Chem. Eng. Jap., 2, pp. 190 - 191.

HAAG, A. (1967). Velocity losses in pneumatic conveyor pipe bends. Br. Chem. Eng., 12, pp. 65 - 66.

HARIU, O.H. and MOLSTAD, M.C. (1949). Pressure drop in vertical tubes in transport of solids by gases. Ind. Eng. Chem., 41, pp. 1148 - 1160.

HELLINCKX, L.J. (1962). Slip velocity in carrier lines - A direct measurement of particle velocity. Inst. Chem. Eng., Symp. on The Interaction between Fluids and Particles. London. 20 - 22 June, 1962. pp. 72 - 77.

HEYWOOD, H. (1962). Uniform and non-uniform motion of particles in fluids. Inst. Chem. Eng., Symp. on The Interaction between Fluids and Particles. London. 20 - 22 June, 1952. pp. 72 - 77.

HINZE, J.O. (1962). Momentum and mechanical energy balance equations for a flowing homogeneous suspension with slip between the two phases. Appl. Sci. Res., A11, pp. 33 - 46.

HUGHMARK, G.A. (1967). Mass and heat transfer from rigid spheres. A.I.Ch.E.J., 13, pp. 1219 - 1221.

IINOYA, K. and GOTO, K. (1965). Static and dynamic characteristics of a cyclone separator for flow of solid-gas mixtures. Chem. Eng. Jap., 3, pp. 203 - 206.

IKEMORI, K. and MUNAKATA H. (1973). A new method of expressing pressure drop in horizontal pipe bend in pneumatic transport of solids. British Hydromechanics Research Association. Proc. 2nd. Int. Conf. on Pneumatic Transport of Solids in Pipes. Guildford, England. 5 - 7 Sept. 1973. Paper A3, pp. A33 - 47 and A85 - 86.

JEPSON, G., POLL, A. and SMITH, W. (1963). Heat transfer from gas to wall in a gas/solids transport line. Trans. Inst. Chem. Eng., 41, pp. 207 - 211.

JEPSON, G., POLL, A. and SMITH, W. (1965). The properties and uses of transfer lines as gas/solids reactors. A.I.Ch.E. - Inst. Chem. Eng., Symp. on Reaction Kinetics in Product and Process Design. London. 13 - 17 June, 1965. pp. 42 - 48.

JONES, J.H., BRAUN, W.G., DAUBERT, T.E. and ALLENDORF, H.D. (1966). Slip velocity of particulate solids in vertical tubes. A.I.Ch.E.J., 12, pp. 1070 - 1074.

JONES, J.H., BRAUN, W.G., DAUBERT, T.E. and ALLENDORF, H.D. (1967). Estimation of pressure drop for vertical pneumatic transport of solids. A.I.Ch.E.J., 13, pp. 608 - 611.

JONES, S.J.R. and SMITH, W. (1962). Mass transfer from solids freely suspended in an air stream. Inst. Chem. Eng., Symp. on The Interaction between fluids and Particles. London. 20 - 22 June, 1962. pp. 190 - 196.

JOTAKI, T. and TOMITA, Y. (1971). Turbulent friction drag of a dusty gas. British Hydromechanics Research Association. Proc. 1st. Int. Conf. on Pneumatic Transport of Solids in Pipes. Cambridge, England. 6 - 8 Sept. 1971. Paper C5, pp. C57 - 67.

JULIAN, F.M. and DUKLER, A.E. (1965). An eddy viscosity model for friction in gas solids flow. A.I.Ch.E.J., 11, pp. 853 - 858.

KANE, R.S., WEINBAUM, S. and PFEFFER, R. (1973). Characteristics of dilute gas-solids suspensions in drag reducing flow. British Hydromechanics Research Association. Proc. 2nd. Int. Conf. on Pneumatic Transport of Solids in Pipes. Guildford, England. 5 - 7 Sept. 1973. Paper C3, pp. C29 - 44 and C100 - 103.

KATZ, M. (1953). The heterogeneous oxidation of carbon monoxide. Adv. Catal., 5, pp. 177 - 216.

KHAN, J.I. and PEI, D.C. (1973). Pressure drop in vertical solid-gas suspension flow. Ind. Eng. Chem. Process Des. Dev., 12, pp. 428 - 431.

KING, P.W. (1973). Mass flow measurement of conveyed solids by monitoring of intrinsic electrostatic noise levels. British Hydromechanics Research Association. Proc. 2nd. Int. Conf. on Pneumatic Transport of Solids in Pipes. Guildford, England. 5 - 7 Sept. 1973. Paper D2, pp. D9 - 20 and D60.

KING, R. (1977). Unsuccessful processes - how to avoid and improve them. Process Eng., __, (3), pp. 85 - 87.

KONNO, H. and SAITO, S. (1969). Pneumatic conveying of solids through straight pipes. J. Chem. Eng. Jap., 2, p. 211.

KOVACS, L. (1971a). Calculation of pressure drop in horizontal and vertical bends inserted in pneumatic conveying pipes. British Hydromechanics Research Association. Proc. 1st. Int. Conf. on Pneumatic Transport of Solids in Pipes. Cambridge, England. 6 - 8 Sept. 1971. Paper C4, pp. C45 - 55 and C90 - 92.

KOVACS, L. (1971b). Some similarity criteria of pneumatic conveying. British Hydromechanics Research Association. Proc. 1st. Int. Conf. on Pneumatic Transport of Solids in Pipes. Cambridge, England. 6 - 8 Sept. 1971. Paper B4, pp. B45 - 52 and B118 - 119.

LEUNG, L.S., WILES, R.J. and NICKLIN, D.J. (1971a). On the design of vertical pneumatic conveying systems. British Hydromechanics Research Association. Proc. 1st. Int. Conf. on Pneumatic Transport of Solids in Pipes. Cambridge, England. 6 - 8 Sept. 1971. Paper B7, pp. B93 - 104.

LEUNG, L.S., WILES, R.J. and NICKLIN, D.J. (1971b). Correlation for predicting choking flowrates in vertical pneumatic conveying. Ind. Eng. Chem. Process. Des. Dev., 10, pp. 183 - 189.

LEWIS, W.E. and PAYNTER, J.D. (1971). Effectiveness factors in batch reactors. Chem. Eng. Sci., 26, pp. 1357 - 1360.

LLOYD, W.A. and AMUNDSON, N.R. (1961). A vertical flow reactor. Ind. Eng. Chem., 53, pp. 19 - 22.

LODH, B.B., MURTHY, G.S.R.N. and MURTI, P.S. (1970). Turbulence promotion for improved heat transfer to gas-solids mixtures. Br. Chem. Eng., 15, pp. 73 - 75.

LOVETT, C.D. and MUSGROVE, P.J. (1973). An electrical method for measuring the particle deposition velocity from a turbulent gas flow. British Hydromechanics Research Association. Proc. 2nd. Int. Conf. on Pneumatic Transport of Solids in Pipes. Guildford, England. 5 - 7 Sept. 1973. Paper D5, pp. D47 - 54 and D65 - 72.

McCARTHY, H.E. and OLSON, J.H. (1968). Turbulent flow of gas-solids suspensions. Ind. Eng. Chem. Fund., 7, pp. 471 - 483.

McVEIGH, J.C. and CRAIG, R.W. (1971). Metering of solids/gas mixtures using an annular venturi meter. British Hydromechanics Research Association. Proc. 1st. Int. Conf. on Pneumatic Transport of Solids in Pipes. Cambridge, England. 6 - 8 Sept. 1971. Paper D2, pp. D25 - 36 and D85 - 86.

MASON, J.S. and BOOTHROYD, R.G. (1971). Comparison of friction factors in pneumatically conveyed suspensions using different-sized particles in pipes of varying size. British Hydromechanics Research Association. Proc. 1st. Int. Conf. on Pneumatic Transport of Solids in Pipes. Cambridge, England. Paper C1, pp. C1 - 16 and C87 - 88.

MASON, J.S. and SMITH, B.V. (1972). The erosion of bends by pneumatically conveyed suspensions of abrasive particles. Powder Technol., 6, pp. 323 - 335.

MASON, J.S. and SMITH, B.V. (1973). Pressure drop and flow behaviour for the pneumatic transport of fine particles around 90 degree bends. British Hydromechanics Research Association. Proc. 2nd. Int. Conf. on Pneumatic Transport of Solids in Pipes. Guildford, England. 5 - 7 Sept. 1973. Paper A2, pp. A17 - 32 and A83 - 84.

MASUDA, H., ITO, Y. and IINOYA, K. (1973). Error in measurement of gas flow rate in gas-solids two-phase flow by use of a horizontal diffuser. J. Chem. Eng. Jap., 6, pp. 278 - 282.

MATSUSHIMA, T. and WHITE, J.M. (1975). On the mechanism and kinetics of the CO - oxidation reaction on polycrystalline palladium. I - The reaction paths. J. Catal., 39, pp. 265 - 276.

MATSUSHIMA, T., ALMY, D.B., FOYT, D.C., CLOSE, J.S. and WHITE, J.M. (1975). On the mechanism and kinetics of the CO - oxidation reaction on polycrystalline palladium. II - The kinetics. J. Catal., 39, pp. 277 - 285.

MEHTA, N.C., SMITH, J.M. and COMINGS, E.W. (1957). Pressure drop in air-solid flow systems. Ind. Eng. Chem., 49, pp. 986 - 992.

MENDIES, P.J., WHEELDON, J.M. and WILLIAMS, J.C. (1973). The velocity of granular materials flowing in the acceleration region of a horizontal pneumatic conveyor. British Hydromechanics Research Association. Proc. 2nd. Int. Conf. on Pneumatic Transport of Solids in Pipes. Guildford, England. 5 - 7 Sept. 1973. Paper D1, pp. D1 - 8 and D56 - 59.

MORI, Y. and SUGANUMA, A. (1966a). Behaviour of solid particles in the air flow flowing through the horizontal straight duct. Chem. Eng. Jap., 4, pp. 61 - 65.

MORI, Y. and SUGANUMA, A. (1966b). On the residence time of solid particles in the gas cyclone. Chem. Eng. Jap., 4, pp. 201 - 203.

MORI, Y. and SUGANUMA, A. (1966c). Behaviour of solid particles in the air flowing through a horizontal curved duct. Chem. Eng. Jap., 4, pp. 344 - 348.

MUNRO, W.D. and AMUNDSON, N.R. (1950). Solid fluid heat exchange in moving beds. Ind. Eng. Chem., 42, pp. 1481 - 1488.

OWEN, P.R. (1969). Pneumatic transport. J. Fluid Mech., 39, pp. 407 - 432.

PARASKOS, J.A., SHAH, Y.T., McKINNEY, J.D. and CARR, N.L. (1976). A kinematic model for catalytic cracking in a transfer line reactor. Ind. Eng. Chem. Process. Des. Dev., 15, pp. 165 - 169.

PASTERNAK, I.S. and GAUVIN, W.H. (1960). Turbulent heat and mass transfer from stationary particles. Can. J. Chem. Eng., 38, pp. 35 - 42.

PASTERNAK, I.S. and GAUVIN, W.H. (1961). Turbulent convective heat and mass transfer from accelerating particles. A.I.Ch.E.J., 7, pp. 254 - 260.

PERRY, J.H. (Ed.) (1973). Chemical Engineers' Handbook. 5th Edition. New York, McGraw-Hill.

PETERSEN, E.E. (1965). Chemical reaction analysis. Eaglewood Cliffs, Prentice-Hall.

PIERCE, W.L., SOUTHER, R.P., KAUFMAN, T.G. and RYAN, D.F. (1972). Innovations in flexicracking. Hydrocarbon Process., 51, (5), pp. 92 - 97.

PINKUS, O. (1952). Pressure drops in the pneumatic conveyance of solids. J. Appl. Mech., 19, pp. 425 - 431.

PRATT, K.C. (1974). Catalytic reactions in transport reactors. Chem. Eng. Sci., 29, pp. 747 - 751.

PRATT, K.C. and BYRNE, B.J. (1973). Useful feeding device for experiments in gas-solids flow. Chem. Ind., 8, p. 386.

PRATT, K.C. and WAKEHAM, W.A. (1975). Effectiveness factors for a size dispersed catalyst. Chem. Eng. Sci., 30, pp. 444 - 447.

PRUDEN, B.B. and WEBER, M.E. (1970). Evaluation of the three phase transport reactor. Can. J. Chem. Eng., 48, pp. 162 - 167.

RANZ, W.E., TALANDIS, G.R. and GUTTERMAN, B. (1960). Mechanics of particle bounce. A.I.Ch.E.J., 6, pp. 124 - 127.

RAO, C.S. and DUKLER, A.E. (1971). The isokinetic - momentum probe. A new technique for measurement of local voids and velocities in flow of dispersions. Ind. Eng. Chem. Fund., 10, pp. 520 - 526.

RAZUMOV, I.M. (1962). Calculating pneumatic transport of solid catalysts. Int. Chem. Eng., 2, pp. 539 - 543.

REDDY, K.V.S. and PEI, D.C.T. (1969). Particle dynamics in solids-gas flow in a vertical pipe. Ind. Eng. Chem. Fund., 8, pp. 490 - 497.

REDDY, K.V.S., VAN WIJK, M.C. and PEI, D.C.T. (1969). Stereophotogrammetry in particle-flow investigations. Can. J. Chem. Eng., 47, pp. 85 - 88.

REITHMULLER, M.L. and GINOUX, J.J. (1973). The application of a laser doppler velocimeter to the velocity measurements of solid particles pneumatically transported. British Hydromechanics Research Association. Proc. 2nd. Int. Conf. on Pneumatic Transport of Solids in Pipes. Guildford, England. 5 - 7 Sept. 1973. Paper D3, pp. D21 - 32 and D61 - 63.

RICHARDS, P.C. and WIERSMA, S. (1973). Pressure drop in vertical pneumatic conveying. British Hydromechanics Research Association. Proc. 2nd. Int. Conf. on Pneumatic Transport of Solids in Pipes. Guildford, England. 5 - 7 Sept. 1973. Paper A1, pp. A1 - 15 and A78 - 83.

RICHARDSON, J.F. and McLEMAN, M. (1960). Pneumatic conveying - Part II. Solids velocities and pressure gradients in a one-inch horizontal pipe. Trans. Inst. Chem. Eng., 38, pp. 257 - 266.

ROBERTSON, A.D. and PRATT, K.C. (1975). Catalytic effectiveness factors in transport reactors. Chem. Eng. Sci., 30, pp. 1185 - 1187.

ROSE, H.E. and BARNACLE, H.E. (1957). Flow of suspensions of non-cohesive spherical particles in pipes. Engineer, Lond., 203, pp. 898 - 901 and 939 - 941.

ROSE, H.E. and DUCKWORTH, R.A. (1969). Transport of solid particles in liquids and gases. Engineer, Lond., 227, pp. 392 - 396, 430 - 433 and 478 - 483.

ROSSETTI, S.J. and PFEFFER, R. (1972). Drag reduction in dilute flowing gas-solid suspensions. A.I.Ch.E.J., 18, pp. 31 - 39.

SADEK, S.E. (1972). Heat transfer to air-solids suspensions in turbulent flow. Ind. Eng. Chem. Process. Des. Dev., 11, pp. 133 - 135, 634 - 638 and 12, (1973) pp. 396 - 398.

SATTERFIELD, C.N. (1970). Mass transfer in heterogeneous catalysis. Cambridge, Massachusetts, M.I.T. Press.

SAXTON, A.L. and WORLEY, A.C. (1970). Modern catalytic-cracking design. Oil and Gas J., 68, (20), pp. 82 - 99.

SCHIEMANN, G., FETTING, F., PRAUSNER, G. and STEINBACH, F. (1968). Heterogeneous reactions in a free-fall reactor. Chem. Ing. Tech., 40, pp. 1050 - 1056. Also Inst. Chem. Eng. - VTG/VDI. Symp. on The Engineering of Gas-Solid Reactions. Brighton, 24 - 26 April, 1968. pp. 153 - 160.

SCHUCHART, P. (1968). Resistance laws concerning pneumatic transport in tube bends. Chem. Ing. Tech., 40, pp. 1060 - 1067. Also Inst. Chem. Eng. - VTG/VDI. Symp. on The Engineering of Gas-Solid Reactions. Brighton, 24 - 26 April, 1968. pp. 65 - 72 and 118 - 119.

SOO, S.L. (1956). Statistical properties of momentum transfer in two phase flow. Chem. Eng. Sci., 5, pp. 57 - 67.

SOO, S.L. (1962a). Fully developed turbulent pipe flow of a gas solids suspension. Ind. Eng. Chem. Fund., 1, pp. 33 - 37.

SOO, S.L. (1962b). Boundary layer motion in a gas-solids suspension. Inst. Chem. Eng. Symp. on The Interaction between Fluids and Particles. London, 20 - 22 June, 1962. pp. 50 - 63.

SOO, S.L. (1964). Effect of electrification on the dynamics of a particulate system. Ind. Eng. Chem. Fund., 3, pp. 75 - 80.

SOO, S.L. (1965a). Laminar and separated flow of a particulate suspension. Astronaut. Acta., 11, pp. 422 - 431.

SOO, S.L. (1965b). Dynamics of multiphase flow systems. Ind. Eng. Chem. Fund., 4, pp. 426 - 433.

SOO, S.L. (1967). Fluid dynamics of multiphase systems. Waltham, Massachusetts, Blaisdell.

SOO, S.L. (1971). A review of electrical effects in pneumatic conveying. British Hydromechanics Research Association. Proc. 1st. Int. Conf. on Pneumatic Transport of Solids in Pipes. Cambridge, England. 6 - 8 Sept. 1971. Paper R1, pp. R1 - 20 and R21 - 23.

SOO, S.L. IHRIG, H.K. Jr. and EL KOUH, A.F. (1960). Experimental determination of statistical properties of two phase turbulent motion. J. Bas. Eng., 82D, pp. 609 - 621.

SOO, S.L. and REGALBUTO, J.A. (1960). Concentration distribution in two-phase pipe flow. Can. J. Chem. Eng., 38, pp. 160 - 166.

SOO, S.L. and TIEN, C.L. (1960). Effect of the wall on two-phase turbulent motion. J. Appl. Mech., 27E, pp. 5 - 15.

SOO, S.L. and TREZEK, G.J. (1966). Turbulent pipe flow of magnesia particles in air. Ind. Eng. Chem. Fund., 5, pp. 388 - 392.

SOO, S.L., TREZEK, G.J., DIMICK, R.C. and HOHNSTREITER, G.F. (1964). Concentration and mass flow distribution in a gas-solid suspension. Ind. Eng. Chem. Fund., 3, pp. 98 - 106.

STAIRMAND, C.J. (1951a). The sampling of dust-laden gases. Trans. Inst. Chem. Eng., 29, pp. 15 - 44.

STAIRMAND, C.J. (1951b). The design and performance of cyclone separators. Trans. Inst. Chem. Eng., 29, pp. 356 - 373.

STANNARD, B. (1961). A theoretical analysis of pneumatic conveying. Trans. Inst. Chem. Eng., 39, pp. 321 - 327.

STEMERDING, S. (1962). The pneumatic transport of cracking catalyst in vertical risers. Chem. Eng. Sci., 17, pp. 599 - 608.

STROTHER, C.W., VERMILLION, W.L. and CONNER, A.J. (1972). Riser cracking gives advantages. Hydrocarbon Process., 51, (5), pp. 89 - 92.

TAJBL, D.G., SIMONS, J.B. and CARBERRY, J.J. (1966). Heterogeneous catalysis in a continuous stirred tank reactor. Ind. Eng. Chem. Fund., 5, pp. 171 - 175.

THOMAS, J.M. and THOMAS, W.J. (1967). Introduction to the principles of heterogeneous catalysis. London, Academic Press.

TIEN, C.L. (1961). Heat transfer by a turbulently flowing fluid-solids mixture in a pipe. J. Heat Transf., 83C, pp. 183 - 188.

TOROBIN, L.B. and GAUVIN, W.H. (1959a). Fundamental aspects of solids-gas flow. Part I - Introductory concepts and idealized sphere motion in viscous regime. Can. J. Chem. Eng., 37, pp. 129 - 141.

TOROBIN, L.B. and GAUVIN, W.H. (1959b). Fundamental aspects of solids-gas flow. Part II - The sphere wake in steady laminar fluids. Can. J. Chem. Eng., 37, pp. 167 - 176.

TOROBIN, L.B. and GAUVIN, W.H. (1959c). Fundamental aspects of solids-gas flow. Part III - Accelerated motion of a particle in a fluid. Can. J. Chem. Eng., 37, pp. 224 - 236.

TOROBIN, L.B. and GAUVIN, W.H. (1960a). Fundamental aspects of solids-gas flow. Part IV - The effects of particle rotation, roughness and shape. Can. J. Chem. Eng., 38, pp. 142 - 153.

TOROBIN, L.B. and GAUVIN, W.H. (1960b). Fundamental aspects of solids-gas flow. Part V - The effects of fluid turbulence on the particle drag coefficient. Can. J. Chem. Eng., 38, pp. 189 - 200.

TOROBIN, L.B. and GAUVIN, W.H. (1961). Fundamental aspects of solids-gas flow. Part VI - Multiparticle behaviour in turbulent fluids. Can. J. Chem. Eng., 39, pp. 247 - 253.

VAN DEEMTER, J.J. and VAN DER LAAN, E.T. (1961). Momentum and energy balance for dispersed two-phase flow. Appl. Sci. Res., A10, pp. 102 - 108.

VAN ZOONEN, D. (1962). Measurement of diffusional phenomena and velocity profiles in a vertical riser. Inst. Chem. Eng., Symp. on The Interaction between Fluids and Particles. London, 20 - 22 June, 1962. pp. 64 - 71 and 112 - 113.

VAN ZUILLICHEM, D.J., BLEUMINK, G.H. and DE SWART, J.G. (1973). Slip velocity measurements by radio tracer techniques in vertical conveying systems of different pipe diameters. British Hydromechanics Research Association. Proc. 2nd. Int. Conf. on Pneumatic Transport

of Solids in Pipes. Guildford, England. 5 - 7 Sept. 1973. Paper D4, pp. D33 - 46 and D63 - 65.

VARGHESE, P. and VARMA, A. (1977). Catalytic reactions in transport-line reactors. (To be published in Chem. Eng. Sci.)

VOGT, E.G. and WHITE, R.R. (1948). Friction in the flow of suspensions. Ind. Eng. Chem., 40, pp. 1731 - 1738.

WAINWRIGHT, M.S. and HOFFMAN, T.W. (1974). The oxidation of o-Xylene in a transported bed reactor. Adv. Chem., 133, pp. 669 - 685.

WALTON, P.J., GAMMON, L.N. and BOOTHROYD, R.G. (1970/71). Equipment for circulating gas/solid-particle suspensions for process development studies. Powder Technol., 4, pp. 293 - 301.

WANG, P.Y. and HELDMAN, D.R. (1973). Heat transfer to dry milk powder during pneumatic transport through an entrance region. Ind. Eng. Chem. Process. Des. Dev., 12, pp. 424 - 427.

WEEKMAN, V.W. Jr. (1974). Laboratory reactors and their limitations. A.I.Ch.E.J., 20, pp. 833 - 840.

WEEKMAN, V.W. Jr. (1975). Industrial process models. Adv. Chem., 148, pp. 122 - 125.

WEI, J. (1975a). Catalysis for motor vehicle emissions. Adv. Catal., 24, pp. 57 - 129.

WEI, J. (1975b). The catalytic muffler. Adv. Chem., 148, pp. 1 - 25.

WEN, C.Y. and MILLER, E.N. (1961). Heat transfer in solids-gas transfer lines. Ind. Eng. Chem., 53, pp. 51 - 53.

WESTERTERP, K.R. (1962). Maximum allowable temperatures in chemical reactors. Chem. Eng. Sci., 17, pp. 423 - 433.

WILKINSON, G.T. and NORMAN, J.R. (1967). Heat transfer to a suspension of solids in a gas. Trans. Inst. Chem. Eng., 45, pp. 314 - 318.

YANG, W.C. (1973). Estimating the solid particle velocity in vertical pneumatic conveying lines. Ind. Eng. Chem. Fund., 12, pp. 349 - 352.

YANG, W.C. (1974). Correlations for solid friction factors in vertical and horizontal pneumatic conveying. A.I.Ch.E.J., 20, pp. 605 - 607.

YANNOPOULOS, J.C., THEMELIS, N.J. and GAUVIN, W.H. (1966). An evaluation of the pneumatic transport reactor. Can. J. Chem. Eng., 44, pp. 231 - 235.

YOUSFI, Y., GAU, G. and LE GOFF, P. (1973). Heat transfer between a flowing air-solid suspension and the wall of the tube. British Hydromechanics Research Association. Proc. 2nd. Int. Conf. on Pneumatic Transport of Solids in Pipes. Guildford, England. 5 - 7 Sept. 1973. Paper A4, pp. A49 - 59 and A87.

ZENZ, F.A. (1949). Two-phase fluid-solid flow. Ind. Eng. Chem., 41, pp. 2801 - 2806.

ZENZ, F.A. and OTHMER, D.F. (1960). Fluidisation and fluid-particle systems. New York, Reinhold.